UNIVERSITY OF CALIFORNIA
SANTA CRUZ

Microbial community structure from the surface ocean to deep sea sediments and linking deep sea microbes to organic matter degradation

A dissertation submitted in partial satisfaction
of the requirements for the degree of

DOCTOR OF PHILOSOPHY

in

OCEAN SCIENCES

By

Rachel C. Clark

September 2019

The Dissertation of Rachel C. Clark is approved:

_____
Professor Alexandra Z. Worden,
Chair

_____
Associate Professor Phoebe Lam

_____
Assistant Professor Marilou Sison-Mangus

_____
Professor Victoria Orphan

_____
Quentin Williams
Acting Vice Provost and Dean of Graduate Studies

Table of Contents

List of Figures

Abstract

Microbial community structure from the surface ocean to deep sea sediments and linking deep sea microbes to organic matter degradation

Rachel C. Clark

Patterns of marine microbial community composition are observable across ocean depths, with distinct ecological niches based on the environmental conditions at each depth. A fundamental biogeochemical role of microbes in the marine carbon cycle is the degradation of particulate organic matter. Identifying the microbes that are actively degrading organic matter in the deep sea is challenging. The main objective of this dissertation is to understand variations in vertical distributions of microbial communities and to develop methods that could allow us to understand which community members contribute actively to degradation of organic matter. Vertical gradients of marine bacterial diversity and overall abundances were characterized from the surface to the seafloor (Chapter 2), and the variability of deep sea sediment bacterial communities was identified through replicated sampling of sediments (Chapter 3). Flow cytometric cell enumeration showed that bacterial abundance decreased with increasing water depth regardless of the region studied or distance from shore. V1-V2 16S rRNA gene amplicon analyses at 100% nucleotide identity as amplicon sequence variants (ASVs) identified distinct bacterial communities in four defined zones: photic (0 – 200 m), mesopelagic (200 – 1000 m), bathypelagic (> 1000 m) and surface sediments (0 to 20 cmbsf). Bacterial communities of surface sediments >10 km apart were distinct from each other, while those sampled from

within 1 m were similar. Phylogenetic approaches focusing on the ubiquitous pelagic bacteria, Alphaproteobacteria Pelagibacterales (SAR11 clade) and Deltaproteobacteria SAR324, expanded our evolutionary understanding about the diversity of these groups while also distinguishing potential ecological niches based on vertical depth distributions. Building on characterization of bacterial diversity, deep water *in situ* incubation experiments were performed to identify bacterial groups activity involved in phytodetrital organic matter degradation (Chapter 4). The addition of phytodetritus led to an increase in relative abundance of taxa known to degrade polysaccharides. The results provided in this thesis provide high-resolution analyses of marine bacterial community composition throughout the water column and into the upper 20 cm of deep sea sediments in the eastern North Pacific Ocean. Collectively, these studies provide a baseline for assessment of future changes, as the influences of global climate change reshape ocean communities.

Acknowledgements

I would first like to thank my PhD advisor Alexandra Z, Worden for her support and guidance throughout my time in her lab. Additional thanks to my dissertation reading committee for your thoughtful feedback and advice: Phoebe Lam, Marilou Sison-Mangus, and Victoria Orphan. I would also like to express my gratitude to the members of the Worden lab during my PhD for your support at sea, in the lab, chatting about science and keeping me sane during the tough moments. Additional thanks and gratitude to the extra support and guidance provided by Sebastian Sudek and highly influencing my success. In addition, I'd like thank collaborators from the Orphan lab: Kat Dawson, Lizzy Wilbanks, Sujung Lim. The extensive field work and bioinformatics included in this dissertation was made possible through the efforts of various MBARI staff members, especially: Larry Bird, Brian Schlining, Erich Rienecker, ROV *Doc Ricketts* pilots (Knute Brekke, Marko Talkovic, Randy Prickett, Brian Tourayn-Schaefer, Ben Erwin), and R/V *Western Flyer* Captain and crew. Finally, special thanks to my husband David Clark and our parents, Mary and David Harbeitner and Alison and Jim Clark, for providing unyielding support and love.

I was financially supported by the Department of Defense National Defense Science and Engineering Graduate Fellowship, University of California Chancellors Fellowship, and NSF Dimensions Program. This research was financially support by grants from the Gordon and Betty Moore Foundation, the National Science Foundation and the David and Lucille Packard Foundation.

Chapter 1: Introduction

Marine microbial communities process about half of the global biogeochemical flux of important elements such as carbon, nitrogen, phosphorous and sulfur (Falkowski et al. 2008; Zehr and Kudela 2010). Microbes fulfill a variety of roles such as autotrophs, heterotrophs, mixotrophs, symbionts and parasites in order to interact with these elements. These roles are performed by a diverse suite of microbial community members throughout the water column. It is widely recognized that heterotrophic microbes are involved in elemental transformation and energy flow (Worden et al. 2015) by recycling dissolved organic carbon and nutrients through the microbial loop (Azam et al. 1983). The microbial loop formalizes the fundamental roles of microbes such as bacteria in both the trophic transfer of energy and in carbon remineralization. The flux of organic carbon from the surface ocean to the seafloor is mediated by diverse microbes vertically distributed in the ocean.

A fundamental biogeochemical role of microbes in the marine carbon cycle is the degradation of particulate organic matter (POM, > 0.5 μm). This degradation regulates oceanic carbon sequestration via the biological pump (Buesseler et al., 2008; Charette et al., 1999). A portion of organic carbon produced at the surface is exported to the deep sea where heterotrophic microbial respiration is supported by organic carbon availability (Arístegui et al., 2009). Microbes are critical in the degradation and remineralization of both sinking (Cho and Azam 1988; Steinberg et

al. 2008) and suspended POM (Giering et al., 2014; Karl et al., 1988), as well as metabolizing biochemically heterogeneous dissolved organic matter (DOM, < 0.5μm; Azam et al., 1983; Benner et al., 1992; Pomeroy et al., 2007). Once organic matter generated from the surface ocean reaches the deep sea, there is a gap in our understanding of the specific deep sea bacteria actively remineralizing sinking phytodetritus or other forms of organic matter.

The ability for microbes at a particular location in the ocean to process organic carbon depends on the specific community members present. Patterns in marine microbial community structure are observable across latitude, longitude, depth and temporally (Zinger et al. 2011). Depth has been found to be a major factor in observed differences in microbial community composition between the surface and the deep ocean (Bergauer et al. 2018; Brown et al. 2009), with the similarity in community composition decreasing over this gradient (Brown et al. 2009; Delong et al. 2006; Treusch et al. 2009; Walsh et al. 2016). While diversity has been well studied at select depths of the water column globally (Brown et al. 2009; Delong et al. 2006; Easson and Lopez 2019; Ghiglione et al. 2008; Jing et al. 2013; Signori et al. 2014; Walsh et al. 2016), there have been fewer studies with repeated sampling over surface to seafloor depth intervals (Cram et al. 2015). A multi-depth view vertically through the ocean (Fig. 1.1) provides the opportunity to identify differences in bacterial diversity and community, potentially highlighting distinct ecological niches based on the environmental conditions at each depth.

Additionally, surface sediment bacterial communities are influenced by organic matter flux from the surface ocean, as this is the interface between the water column and deeper subseafloor sediments. The availability of organic matter and its recalcitrance are significantly associated with differences in bacterial community structure of deep sea sediments (Bienhold et al. 2016; Danovaro et al. 2016). In locations with high sedimentation rates such as near the coast, the metabolism of sediment microbes depletes oxygen rapidly leading to a scarcity of optimal terminal electron acceptors (D'Hondt et al. 2004). A vertical zonation of sediment porewater geochemistry leads to peak concentrations of dissolved products from different redox processes with increasing depth into the sediment (Jørgensen 2000). The close coupling between geochemistry and microbiology provides insight into specific microbial activities when examined in parallel. In addition to the influence of surface derived organic matter on sediment communities, further organic matter may be supplied through biological and physical perturbations. Sediments located within a submarine canyon are affected by various physical disturbances (e.g. sediment slumps, dense water cascading events, tidal forcing and storm-induced gravity flows) and resource availability (De Leo et al. 2014; Pasqual et al. 2011; Tesi et al. 2008). These factors are thought to have a strong influence on prokaryotic activities in the sediments (Šimek et al. 2005). A biological perturbation may come from fast sinking blooms of particular algae, or ever the deposition of a dead whale. This latter results in a massive punctuated input of organic matter that potentially provides the equivalent of 2000 years of accumulated background particulate organic carbon flux

to the deep seafloor (Smith and Baco 2003). These types of perturbations influence deep sea surface sediment bacterial community composition and activities (Goffredi and Orphan 2010).

Recently, a wealth of new genomic data has been generated, in both the surface ocean and deep sea (e.g. Salazar et al. 2016; Sunagawa et al. 2015), and used to infer an expanded version of the tree of life (Hug et al. 2016). This tree underscores the importance of organisms that so far lack representative isolates, and highlights that major lineages are currently underrepresented in today's biogeochemical models.

The widely used ribosomal RNA (rRNA) amplicon sequencing method provides the opportunity to learn about environmental microbial communities without relying on cultivated representatives. This dissertation uses amplicon sequences of V1-V2 16S rRNA gene hypervariable region. The 16S rRNA gene product is essential (Acinas et al., 2004; Woese, 1987) for prokaryotic ribosomal structure, making the gene highly conserved with characteristic loops (V1 to V9) where mutation is not deleterious. Here, so-called universal primers for V1-V2 16S rRNA were used to amplify and sequence bacterial and phytoplankton rRNA genes. While these primers are excellent for capturing sequences from both bacteria and even plastids they do exclude archaea (Wear et al. 2018). Analyzing 16S rRNA gene amplicons at the 100% nucleotide identity level allows for the potential to probe strain-level variation (Callahan et al. 2017) and to discriminate distinct microbial populations of ecological importance (Eren et al. 2013).

In addition to analyzing microbial population structure based on 16S rRNA gene amplicons, phylogenetics can connect fine scale genetic variations with evolutionary relationships within taxa. We examined the vertical distribution of Alphaproteobacteria Pelagibacterales and Deltaproteobacteria SAR324 throughout the water column. These taxa were selected for more fine-scale analysis because they were abundant in our datasets. Moreover, Pelagibacterales is distributed globally, with the greatest relative abundances in the photic zone (Morris et al. 2002), and Deltaproteobacteria SAR324 are considered ubiquitous at depths below the photic zone (Swan et al. 2011).

The objectives of this dissertation were to:

1. Characterize the variation in bacterial community structure from the surface ocean to the seafloor, in and near Monterey Bay
2. Identify deep sea sedimentary bacteria from a submarine canyon and assess the heterogeneity from sediments sampled < 1m and > 10 km apart, including sediments that have received a massive input of organic carbon in past time (whalefall)
3. Identify deep sea bacteria that actively respond to fresh input of phytodetrital organic carbon

This dissertation aims to contribute to the understanding of microbial community connectivity over vertical gradients in the ocean and identifying the deep sea bacteria involved in organic matter remineralization. These studies are important for establishing a baseline of the current bacterial community composition in order to

understand both water column and sediment ecosystems in coastal and mesotrophic conditions. Replicated sampling of surface sediments was used to assess the variability of bacterial community composition at spatial scales: < 1 m and > 10 km apart. The study additionally compares sites known to have had massive episodic input of organic matter, in the form of a deposited dead whale. Building on the identification of deep sea bacterial community composition, deep sea *in situ* incubation experiments were conducted to identify the portion of the microbial communities that responds actively to organic matter input to the deep sea.

To address these objectives a variety of oceanographic research tools were employed. A conductivity-temperature-depth (CTD) Niskin rosette is a standard instrument used for identifying initial water conditions with depth and targeting collection of seawater at specific depths. A remotely operated vehicle (ROV) enables targeted sediment sampling and deployable *in situ* incubators. ROVs allow for a visual assessment of the seafloor in order to sample sediments < 1 m apart and to focus on sediments located at a previous whale fall and ~100 m away at the same seafloor depth. Additionally, ROVs are capable of manipulating the *in situ* incubators developed during this study to collect and incubate deep sea seawater for varying lengths of time freshly amended with phytodetrital organic matter.

Collectively, the research presented here provides insights into vertical distributions of bacteria in the water column from the surface to seafloor and into the upper 20 cm of deep sea sediments and links deep sea bacterial groups to organic matter remineralization. In the long term these studies should help to better inform

microbial oceanographers about the distributions, heterogeneity and activities of marine bacterial communities.

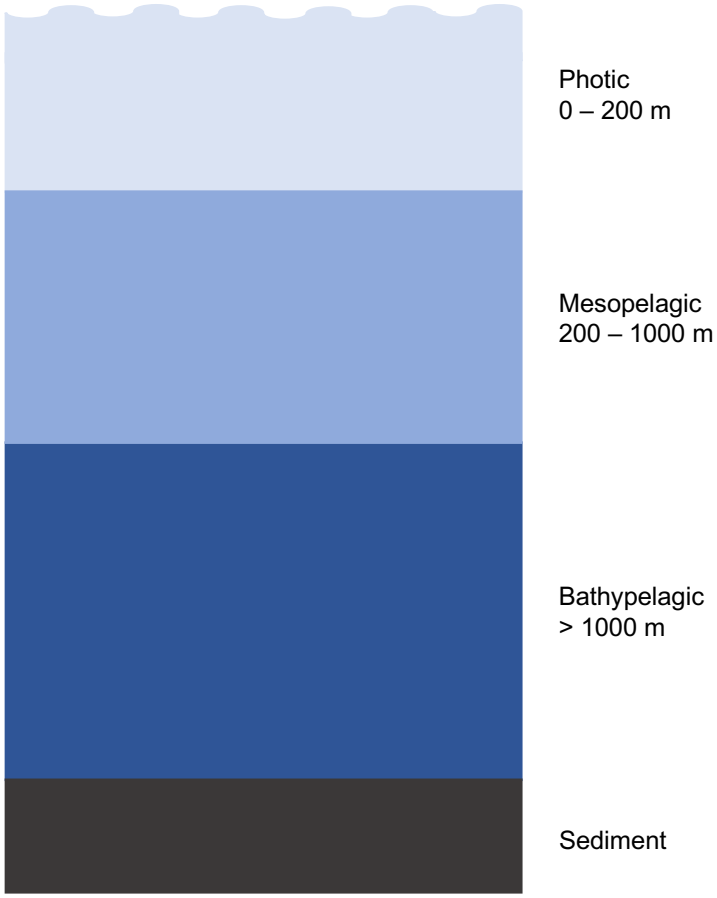

Figure 1.1

Schematic of the ocean zones and depths ranges from the surface to the seafloor.

Chapter 2: Vertical gradients of diversity and distributions of bacteria in the oceanic water column

Abstract

To examine the fate and degradation of organic carbon compounds in the ocean, it is important to understand variations in bacterial communities from the surface to the deep sea. We performed vertical diversity profiling at sites in a submarine canyon ecosystem, in or near Monterey Bay, CA, USA, with bottom depths ranging from 633 m to 1,978 m. Bacterial diversity was assessed using V1-V2 16S rRNA gene amplicons analyzed at 100% nucleotide identity as amplicon sequence variants (ASV). A sharp gradient of increased bacterial diversity (computed with cyanobacteria removed) was observed from photic to bathypelagic depths. Bacterial cell abundances determined by flow cytometry decreased by >1 order of magnitude from 1,215,206 ± 691,526 cells ml^{-1} in the seasonally variable photic zone (0 – 200 m) sampled during three expeditions, to 228,073 ± 143,227 and 67,106 ± 12,252 cells ml^{-1} in mesopelagic (200 – 1000 m) and bathypelagic (>1000 m) samples, respectively. Bacterial diversity as ASV relative abundances were much more variable between depth zones than between sites, resulting in reproducible distributions of community ASVs into photic, mesopelagic and bathypelagic zones. ASVs classified as Alphaproteobacterial groups Pelagibacterales (SAR11 clade) Ia and *Rhodobacteraceae* exhibited the highest relative amplicon abundances in the photic zone; Deltaproteobacteria SAR324 and Gammaproteobacteria

Oceanospirillales dominated mesopelagic and bathypelagic amplicons. We examined two of these top four lineages with phylogenetic methods to better distinguish biological groupings with ecological differences within these bacterial lineages. Amplicon placement on Pelagibacterales and SAR324 phylogenetic reconstructions based on near-full length 16S rRNA gene sequences showed that Pelagibacterales subclade dominants differed across depths, such that subclades Ib and Ic were the most abundant among the 12% ± 2 Pelagibacterales (out of total bacterial amplicons) in the bathypelagic. In contrast, the most dominant SAR324 clade is clade II, comprising 13.37% ± 2.93 of all bacterial amplicons in the mesopelagic and bathypelagic. These strong, highly resolved vertical gradients of bacterial diversity and distributions identify variations in dominants that likely connect to functional differences in gene content and physiology.

Introduction

Patterns in marine microbial community structure are observable across latitude, longitude, depth and temporally (Zinger et al. 2011). Depth has been found to be a major factor in observed differences in microbial community composition between the surface and the deep ocean (Bergauer et al. 2018; Brown et al. 2009), with the similarity in community composition decreasing over this gradient (Brown et al. 2009; Delong et al. 2006; Treusch et al. 2009; Walsh et al. 2016). While diversity has

been well studied at select depths of the water column globally (Brown et al. 2009; Delong et al. 2006; Easson and Lopez 2019; Ghiglione et al. 2008; Jing et al. 2013; Signori et al. 2014; Walsh et al. 2016), there are fewer studies from repeated sampling over surface to seafloor depth intervals (Cram et al. 2015).

A multi-depth view vertically through the ocean provides the opportunity to identify differences in bacterial diversity and community, potentially highlighting distinct ecological niches based on the environmental conditions at each depth. Analyzing 16S rRNA gene amplicons at the 100% nucleotide identity level allows for the potential to probe strain-level variation (Callahan et al. 2017) and to discriminate distinct microbial populations of ecological importance (Eren et al. 2013). A previous study focusing on the differences of the two most abundant Pelagibacterales sequences within a marsh ecosystem, found their V4 16S rRNA gene amplicon sequences to be 99.57% similar to each other. Nevertheless, these closely related sequences delineated according to temperature, such that the Pelagibacterales taxa represented seemingly occupy distinct ecological niches (Eren et al. 2013). This identification of microdiversity within a bacterial community allows for the inference of evolutionary forces with important ecological implications (Needham et al. 2017).

In addition to analyzing microbial population structure based on 16S rRNA gene amplicons, phylogenetics can connect fine scale nucleotide variations with evolutionary relationships between taxa. For the Alphaproteobacterial group Pelagibacterales there are currently five broad clades that further split into nine recognized subclades (Ia, Ib, Ic, IIa, IIb, IIIa, IIIb, IV, V) based on phylogenetic

analysis of the partial or near-full length 16S rRNA gene (Brown et al. 2012; Giovannoni 2017; Grote et al. 2012; Vergin et al. 2013). Collectively, Pelagibacterales are known for their high abundance in the ocean (Morris et al. 2002) and simple metabolic schemes for oxidizing a broad range of labile dissolved organic compounds (Giovannoni 2005; Schwalbach et al. 2010; Sowell et al. 2009; Sun et al. 2011; Tripp et al. 2008, 2009). Pelagibacterales subclades that have been connected to differences in relative abundance over geographical locations, depths and seasons (Brown et al. 2012; Carlson et al. 2009; Field et al. 1997; García-Martínez and Rodríguez-Valera 2000; Stingl, Tripp et al. 2007; Vergin et al. 2013). The original exploration of major clades of Pelagibacterales was performed using V1-V3 16S rRNA terminal restriction fragment length polymorphism (T-RFLP) data from the Bermuda Atlantic Time-Series (BATS), in the western Sargasso Sea, showing that subclade Ia is highly abundant in summer surface waters, subclade Ib is more common in spring throughout the photic zone, and subclade II is found in mesopelagic waters year-round (Carlson et al. 2009). Furthermore, metagenomic reads mapping to single-cell genomes of subclade Ic, isolated from 770 m at Station ALOHA, in the North Pacific Subtropical Gyre, are highly abundant in mesopelagic and bathypelagic waters (Thrash et al. 2014). Comparison of these subclade Ic single-cell genomes to previous surface Pelagibacterales genomes (Grote et al. 2012) found that subtle genome variation controls phenotypic characters connected to adaptation of various Pelagibacterales subclade members to their respective niches in the surface and deep ocean (Thrash et al. 2014). In other ocean regions where oxygen minimum

zones (OMZs) have been studied, specifically the Eastern Tropical North Pacific off Mexico, subclades IIa and IIb peaked at anoxic depths (Tsementzi et al. 2016). In the absence of oxygen, nitrate reduction to nitrite is the dominant process of organic matter oxidation. The high abundance of subclades IIa and IIb suggests they may contribute to nitrite production in OMZs (Tsementzi et al. 2016).

While Pelagibacterales is found globally, it has the greatest relative abundances in the photic zone (Morris et al. 2002), and Deltaproteobacteria SAR324 are considered ubiquitous at depths below the photic zone (Swan et al. 2011). There are not yet any cultivated representatives of SAR324, though genomes have been assembled from single cell genomes (SAGs) and metagenomes (Chitsaz et al. 2011; Haroon et al. 2016). The diversity of SAR324 has become a focus point more recently than the Pelagibacterales. However, several studies have addressed the variable metabolic capacity of members of this group via genomes and metatranscriptomes (Georges et al. 2014; Li et al. 2014; Sheik et al. 2014; Swan et al. 2011). The possible metabolic flexibility of SAR324 was reported based on the presence of carbon fixation genes (ribulose-1,5-bisphosphate carboxylase-oxygenase; RuBisCO) and sulfur oxidation genes (adenosine 5'-phosphosulfate reductase and reverse-type dissimilatory sulfite reductase), in single amplified genomes from the mesopelagic in the South Atlantic and North Pacific. These data suggest sulfur oxidation provides the energetic support for autotrophic carbon fixation (Swan et al. 2011). In contrast, a SAR324 SAG generated from a sample collected at 6 m near La Jolla, California, suggests an aerobic, motile, and heterotrophic lifestyle of SAR324 (Chitsaz et al. 2011). The idea

that members of SAR324 have a versatile metabolism that includes inorganic carbon fixation, sulfur oxidation, hydrocarbon utilization capabilities and heterotrophy, with genes for these pathways being present and actively expressed simultaneously, has been supported by metagenome and metatranscriptome analyses from a hydrothermal plume (1950 and 1963 m) and surrounding waters (1600 and 1900 m) in the Gulf of California. This versatility may explain the ubiquity of SAR324 in the deep ocean (Sheik et al. 2014) as the particulate organic matter at these depths is heterogenous in its quality and quantity, depending on changing surface productivity and other factors (Lima et al. 2014; Smith et al. 2013). Moreover, comparisons of these metagenomes to the surface coastal SAG from La Jolla, California found less than 100 proteins out of 3536 were shared and 16S rRNA gene sequence similarity was less than 90% (Sheik et al. 2014). The abundance of SAR324 throughout the global ocean has been found to be correlated with low-oxygen conditions associated with OMZs and microscale oxyclines forming on particles throughout the water column (Wright et al. 2012). A more complete (> 96%) draft genome (lautmerah 10) (Haroon et al. 2016) assembled from a metagenome sampled at 10 m in the Red Sea supports the metabolically diverse metabolisms identified with previous SAR324 genomes (Chitsaz et al. 2011; Sheik et al. 2014; Swan et al. 2011). Hence, it is clear that understanding the diversity within SAR324, paired with the known metabolic capacity, will allow us to better predict the ecological niches that SAR324 is occupying throughout the water column.

Here, we examine the distribution of bacterial taxa and transitions in diversity throughout the water column, using the V1-V2 region of the 16S rRNA gene and amplicon sequencing as well as flow cytometry. We focused on a dynamic submarine canyon ecosystem with a multi-depth sampling strategy implemented on three research expeditions. Our analysis applies a two part approach, sampling throughout the water column combined with an ASV analysis and phylogenetic analysis of two key groups. These analyses advanced our understanding of how different clades within key bacterial groups are distributed throughout the water column and aspects of community connectivity between the surface and deep ocean. Our studies reveal variations in marine microbial community composition over space and time, information that is necessary to understand a baseline of community structure against which future deviations resulting from climate change or other perturbations can be assessed.

Materials and Methods

Oceanographic sampling

Three research cruises were conducted onboard the R/V *Western Flyer* in September 2015, May 2016, and September 2016, in or near Monterey Bay, in the

eastern North Pacific Ocean (Fig. 2.1). Five stations were sampled: CY1978m, CY1833m, WF1820m, WF1018m, and WF633m. Station name letters indicate being at a location where a whale carcass existed on the sea floor (WF, whale fall) while "CY" corresponds to a submarine canyon site with no such known unusual attributes. Number values in names indicate the bottom depth at the station.

Seawater was collected at 12 to 16 depths from the surface to near the seafloor using Niskin bottles mounted on a conductivity-temperature-depth (CTD) rosette or on the remotely operated vehicle (ROV) *Doc Ricketts*. Samples for DNA extraction were collected by filtering 1 L of seawater onto a 0.2 μm 47 mm Supor filter (Pall Gelman, East Hills, NY, USA) in duplicate and immediately frozen at -80°C. Flow cytometry samples were preserved in glutaraldehyde (EM grade, 0.25% final concentration, Electron Microscopy Services, Hatfield, PA, USA) at room temperature in the dark for 20 min, flash frozen in liquid nitrogen and stored at -80°C (Marie et al. 2001). Corresponding nutrient samples were taken and analyzed as previously described (Pennington and Chavez 2000) (Table S2.1).

Flow cytometry

Bacterial cell counts were measured by analytical flow cytometry using a BD Influx flow cytometer (BD Biosciences, San Jose, CA, USA). After thawing, preserved seawater samples were stained with SYBR Green I (0.5X final

concentration; Molecular Probes, Inc., Eugene, OR, USA) for 15 min at room temperature in the dark (Marie et al. 2001). Two types of fluorescent polystyrene beads, 0.75 μm yellow-green and 0.5 μm green (Polysciences, Inc., Warrington, PA, USA), were added to the stained sample for reference. Samples were run at 25 μl min^{-1}, as measured with an inline flow meter (Sensirion SLG-1430), using a 200 mW 488 nm laser to interrogate cells. Each sample was pre-run 2 min, then bacterial populations were resolved by green fluorescence (520 nm±35nm filter, trigger) and Forward Angle Light Scatter (FALS). Events were collected for 2 min, and the volume analyzed was confirmed by weight measurements. Prior to determining bacterial counts, phototrophs were analyzed based on red chlorophyll autofluorescence (692/40 nm bp) vs FALS (trigger) or orange phycoerythrin autofluorescence (572/27 nm bp) vs FALS (trigger). Cyanobacteria and eukaryotic algae were subsequently gated out so that non-phototrophic bacteria could be enumerated. Flow cytometry data were analyzed in WinList 3D 8.0 (Verity Software House, Topsham, ME, USA).

DNA extraction, PCR and sequencing

DNA was extracted from filters using a modification of the QIAGEN DNeasy Plant kit (Qiagen, Valencia, CA, USA), including addition of a bead beating step (Demir-Hilton et al. 2011), and quantified with the QuBit dsDNA high-sensitivity

assay (Invitrogen, Carlsbad, CA, USA). Prior to PCR, templates were diluted to 5 ng μl^{-1} with TE pH 8 (Thermo Fisher Scientific, Waltham, MA, USA). Polymerase chain reactions (50 µl) were set up as previously described (Hamady et al. 2008) with 5 µl of 10x buffer, 1 U of HiFi-Taq, 1.6 mM $MgSO_4$ provided in the Platinum Taq kit (Invitrogen, Carlsbad, CA, USA), 5 ng of template DNA, 200 nM of the forward primer (27FB, 5′-AGRGTTYGATYMTGGCTCAG-3′) and of the reverse primer (338RPL, 5′- GCWGCCWCCCGTAGGWGT-3′) (Fortunato et al. 2012). The PCR cycling parameters were 94°C for 2 min; 30 × 94°C for 15 s, 55°C for 30 s, 68°C for 1 min and a final elongation at 68°C for 7 min. Following the PCR, an aliquot was run on a 1% Agarose gel to verify the desired V1-V2 16S rRNA gene product (~ 300 nt in length) had been amplified. Samples were sequenced using Illumina MiSeq 2x300 bp paired-end reads.

V1-V2 16S rRNA gene amplicon quality control

Amplicon sequence reads were processed with USEARCH v9 (Edgar 2010) for quality control and to merge paired-end reads. Low quality bases were trimmed from the sequences using a 10% read length window with a Q25 running-quality threshold. Paired-end sequences were merged with a ≥ 50-nucleotide overlap, minimum sequence length of 200 nucleotides, and maximum 5% mismatches. A filtering step was performed to discard low-quality merged sequences with a maximum expected

error >1. Primers were removed from the sequences with cutadapt (Martin 2011). For each sample, between 15,181 and 460,250 amplicons were generated (average = 181,368 ± 77,639, median = 178,316, n = 97; Table S2.2).

Amplicon sequence variant resolution

Merged amplicon sequences were resolved into amplicon sequence variants (ASVs) of 100% pairwise nucleotide identity with USEARCH v10.0.240 (Edgar 2010). The unoise3 algorithm (Edgar 2016) was used to infer exact ASVs from the sequencing data, rather than building operational taxonomic units (OTUs) from sequence similarity. Taxonomy was assigned to each ASV using the SILVA database (Pruesse et al. 2007) (release 128, September 07 2016, https://www.arb-silva.de/documentation/release-128) via QIIME2-2018.2 q2-feature-classifier (Bokulich et al. 2018). We excluded plastid, mitochondrial, or cyanobacterial ASVs based on the SILVA assignment, resulting in 57,827 total bacterial ASVs (Table S2.2). The universal V1-V2 16S rRNA primer pair used did not recover archaea (Wear et al. 2018).

Statistical analyses

All bacterial community ASV (cyanobacteria removed) analyses were conducted using the "vegan" package (v2.4.4; https://cran.r-project.org/web/packages/vegan/) in R (v3.4.1) (Oksanen et al. 2017). For each sample, the Shannon diversity index was calculated to estimate community diversity. Hierarchical clustering based on Bray-Curtis dissimilarity (Bray and Curtis 1957) of bacterial amplicon sequences relative abundance was calculated to compare community compositions between samples. The relative read proportion of bacterial ASVs were calculated by dividing the ASV count by the total reads in each sample. These relative read proportions were log2 transformed for better visualization. All base plots used in the included figures were generated using the R package "ggplot2" (v2.2.1; https://ggplot2.tidyverse.org) (Wickham 2016).

Pelagibacterales and SAR324 phylogenetic reconstructions

For high-resolution Pelagibacterales diversity analyses, a total of 139 near full-length 16S rRNA gene sequences representing Pelagibacterales were retrieved from the SILVA database (release 128) and through the blastn search from GenBank. These 139 sequences (including one *Escherichia coli* and one *Magnetococcus marinus* as an outgroup) were aligned using MAFFT (Katoh and Standley 2013) with default parameters and gaps were masked using trimAl v1.4 (Capella-Gutiérrez et al. 2009). Phylogenetic inferences were made using Maximum Likelihood methods

implemented in RAxML (Stamatakis 2014) under gamma corrected GTR model of evolution with 1,000 bootstrap replicates based on 1,303 homologous positions. Another Maximum Likelihood inference was made using PhyML 3.0.1 (Guindon et al. 2010) with the same substitution model and 100 bootstrap replicates. Additional phylogenetic reconstructions were performed in MrBayes 3.2.6 (Ronquist et al. 2012) with the parameters of lset nst=6 rates=invgamma, ncat=6, ngenval=10000000, samplefreqval=1000 and tempval=0.200. The final tree was visualized with FigTree 1.4.0 (http://tree.bio.ed.ac.uk/software/figtree) with topology from RAxML (Supplemental Fig. 2.1).

For high-resolution SAR324 diversity analyses, a total of 107 near full-length 16S rRNA gene sequences representing SAR324 were retrieved from the SILVA database (release 128) and through the blastn search from GenBank. These 107 sequences (including three *Nitrospinaceae*, two *Desulfobulbaceae*, and three *Desulfovibrionaceae* as an outgroup) were aligned using MAFFT (Katoh and Standley 2013) with LINSI parameters and gaps were masked using trimAl v1.4 (Capella-Gutiérrez et al. 2009). Phylogenetic inferences were made by Maximum Likelihood methods implemented in RAxML (Stamatakis 2014) under gamma corrected GTR model of evolution with 1,000 bootstrap replicates based on 1,227 homologous positions. Additional phylogenetic reconstructions using PhyML and MrBayes were conducted as described above. The final tree was visualized with FigTree 1.4.0 and topology from RAxML (Supplemental Fig. 2.2).

Phylogenetic amplicon assignment

In addition to resolving ASVs, sequenced amplicons were phylogenetically placed using PhyloAssigner v6.166 (Vergin et al. 2013), which performs a profile alignment of amplicon sequences to a multiple sequence alignment using HMMER (Eddy 2011) and assigned phylogenetic positions in an unmasked reference tree based on Maximum Likelihood methods using PPLACER (Matsen, Kodner, and Armbrust 2010). The amplicon sequences were run against a reference alignment and tree of 16S rRNA gene sequences (Vergin et al. 2013) to identify Pelagibacterales and SAR324 sequences. The Pelagibacterales amplicon sequences were retrieved based on their taxonomic assignment to the 16S rRNA gene reference tree (Vergin et al. 2013). The amplicons identified as Pelagibacterales were then run in PhyloAssigner using our fine scale Pelagibacterales reference tree to phylogenetically place amplicon sequences into clades and subclades. SAR324 amplicons were also retrieved based on their taxonomic assignment in the 16S rRNA gene reference tree (Vergin et al. 2013), and placed using PhyloAssigner and our SAR324 reference tree to bin amplicon sequences into SAR324 clades.

To examine only the Pelagibacterales component of the bacterial communities, the relative read proportion was calculated for each subclade identified in the Pelagibacterales phylogenetic tree. Hierarchical clustering based on Bray-Curtis similarity (Bray and Curtis 1957) of Pelagibacterales amplicon sequences relative

abundance per sample was used to compare the Pelagibacterales community composition between samples. The same analyses were performed for the SAR324 component of the communities.

Results

Focusing in or near the Monterey Canyon located in the eastern North Pacific Ocean with sampling in two seasons and years, we examined the distribution of bacterial groups throughout the water column. We specifically examined heterotrophic bacteria (that is, excluding taxa responsible for oxygenic photosynthesis) using both V1-V2 16S rRNA gene amplicons coupled with flow cytometric cell enumerations across 2 to 1,978 m depths. The five stations sampled were located in relatively nutrient-rich, cold coastal waters (Fig. 2.1). The base of the photic zone varied between 25 and 150 m during the sampling periods and across locations, based on the deepest depth with phytoplankton present as measured by flow cytometry. Chlorophyll-*a* was highest in the photic zone (0.032 – 9.952 mg m^{-3}) and no station exhibited a deep chlorophyll maximum. Dissolved inorganic nutrients followed expected depth profiles, with increased phosphate, silicate and nitrate concentrations with depth. Each of the stations exhibited a subsurface nitrite maximum, between 15 m – 70 m depending on the station, and nitrite then decreased with greater depth. The overall range in temperature was 2.0 to 17.3°C, with the

colder bottom depths being at the stations with greatest bottom depth (1820 - 1978 m). The range in salinities was 33.26 – 34.61, with salinity increasing with increasing depth.

Bacterial cell abundances

Within the photic zone, bacterial abundance (based on stained bacteria and removal of counts from photosynthetic bacteria) varied 10x between stations and periods sampled, ranging from 305,500 (CY1978m, May 2016) to 3,499,152 (WF633m, September 2016) cells ml^{-1} (Fig. 2.2). Those sampled in September 2015 exhibited the most variable surface (2 m) abundances, ranging from 485,782 (WF1820m) to 2,482,909 (CY1833m) cells ml^{-1}. While these two stations are about the same distance from shore, measured chlorophyll-*a* corresponded to the bacterial abundances (0.68 mg m^{-3} WF1820m and 1.91 mg m^{-3} CY1833m). At the base of the deepest photic zone, about 150 m, abundances were approximately 500,000 cells ml^{-1} at all of the stations, regardless of distance from shore, seafloor depth, season, or year. In 2016, the lowest surface (2 m) abundances (720,000 – 1,400,000 cells ml^{-1}) occurred in May, while in September they ranged between 2,000,000 to 3,000,000 cells ml^{-1}.

Bacterial cell abundance decreased by 1.5 orders of magnitude between the photic zone and 1,978 m, the deepest station sampled (Fig. 2.2). For the deepest samples at

CY1978m, bacterial cell abundances were 50,000 cells ml^{-1}, and did not appear to vary moving upwards into the mesopelagic zone (200 – 1000 m depth). The samples collected closest to shore (WF633m; 21.67 km offshore) had the highest abundances overlying the seafloor (200,000 cells ml^{-1}) compared to stations with deeper bottom depths, and abundance increased rapidly upwards through the mesopelagic zone at the two stations closest to shore (WF633m and WF1018m – 29.77 km offshore) as these bottom depths are already in the mesopelagic zone.

To examine the abundance variance at a single depth, samples were collected at 600 m water depth from multiple stations at each sampling time. For each sample the technical duplicates were examined, with bacterial cell abundances of 136,277 ± 27,235 cells ml^{-1} (n = 10). This showed that under the conditions and locations studied, bacterial abundance in the middle of the mesopelagic zone varied maximally by 20% across sites. When the shallowest site (WF633m) was excluded, an appropriate step given that its bottom depth corresponds to the mesopelagic mid-measurement, that variability dropped to 16%, demonstrating that cell abundance is quite stable in the mesopelagic. Assessing the technical reproducibility of cell enumeration using duplicate samples from the five collection times showed low variability between duplicates with cell abundances of 173,937 ± 8,758 cells ml^{-1} (5.0%; WF633m, September 2015), 107,753 ± 995 cells ml^{-1} (0.9%; CY1978m, May 2016), 119,766 ± 15,218 cells ml^{-1} (12.7%; WF1018m, May 2016), 157,823 ± 2,553 cells ml^{-1} (1.6%; WF1018m, September 2016), and 122,107 ± 4,556 cells ml^{-1} (3.7%; CY1978m, September 2016).

General bacterial community composition

Bacterial diversity exhibited clear depth-related changes at all sampled stations as reflected by the Shannon diversity index (computed after removal of cyanobacterial sequences). Alpha diversity increased with depth, with the sharpest increase occurring near the base of the photic zone. Alpha diversity remained high throughout mesopelagic and bathypelagic samples (Fig. 2.2). The Shannon diversity index value was not correlated with the number of sequences per sample (Supplemental Fig. 2.3), further rarefaction curves showed a plateau for each depth profile performed, indicating that we did capture the full diversity of the bacterial communities in each sample (Supplemental Fig. 2.4).

Bacterial community vertical distribution variability

Hierarchical clustering (Supplemental Fig. 2.5) of bacterial communities based on amplicon sequence variants (ASVs) Bray-Curtis dissimilarities showed depth associated clusters with distinct photic (2 – 250 m), mesopelagic (300 – 750 m) and bathypelagic (900 – 1 978 m) groups (Fig. 2.3). Further, the photic zone samples cluster into upper (2 – 30 m), mid (30 – 70 m) and lower (70 – 200 m) depths, with a

distinct May 2016 upper photic sample cluster (2 – 25 m). Across the full water column, the bacterial phyla with the highest relative abundances were Actinobacteria, Bacteroidetes, Marinimicrobia, Nitrospinae, Proteobacteria (classes Alphaproteobacteria, Deltaproteobacteria, Gammaproteobacteria), and Verrucomicrobia (Fig. 2.3, Supplemental Fig. 2.6).

We next examined the top 50 most abundant ASVs in each of the three major depth-related ASV community composition based clusters. ASVs belonging to specific bacterial lineages often exhibited variable relative read proportion patterns across depths, that is, high microdiversity, that showed depth related patterns. Within the photic zone, we observed finer scale patterns that appeared connected to seasonality, than seen in the mesopelagic or bathypelagic. For example, the relative abundance in May 2016 of Alphaproteobacteria *Rhodobacteraceae* (24.2% of all sequences; 14.70% ± 9.59 relative read proportion in all photic samples; 26.04% ± 15.25 relative read proportion of May 2016 upper photic samples) appears to be influencing the clustering of the upper photic (2 – 25 m) samples. Bacteroidetes are mostly present in photic zone samples (12.7% of all sequences; average 18.86% ± 6.81 relative read proportion in photic samples; 0.04% ± 0.11 mesopelagic; 0.05% ± 0.13 bathypelagic) with the highest relative abundance of Bacteroidetes ASVs observed in May 2016 (average 24.98% ± 4.79 upper photic samples) coinciding with the increase in relative read proportion of *Rhodobacteraceae*. Overall, while there are finer scale seasonality patterns of bacteria found in photic zone samples, connecting

with the higher variability in environmental parameters, we did not observe site-related or seasonal differences of bacteria in bathypelagic or mesopelagic samples.

Alphaproteobacteria dominated photic zone communities, with ASVs classified as SAR11 surface 1 and ASVs classified as *Rhodobacteraceae* exhibiting the highest relative abundances (average 18.8% ± 6.7 and 13.8% ± 9.0, respectively). The mesopelagic and bathypelagic zone samples were dominated by Deltaproteobacteria SAR324 (8.7% of all sequences; average 14.9% ± 3.3 relative read proportion in mesopelagic and bathypelagic) and Gammaproteobacteria *Oceanospirillales* (14.2% of all sequences; average 14.6% ± 2.7 relative read proportion in mesopelagic and bathypelagic). Marinimicrobia (SAR406) were mostly present in bathypelagic samples (6.3% of all sequences; average 13.6% ± 1.6 relative read proportion in bathypelagic). Actinobacteria were present throughout the water column (5.4 ± 2.2% relative read proportion at all depths). Nitrospinae were more abundant at lower photic and mesopelagic depths (2.5% of all sequences; average 4.0 ± 0.8% relative read proportion in lower photic and mesopelagic). Verrucomicrobia were mostly abundant in September 2015 surface samples (4.6% of all sequences; 4.6% ± 2.4 relative read proportion in September 2015 surface).

While ASVs classified as Gammaproteobacteria *Oceanospirillales* dominated the bacterial community in the mesopelagic and bathypelagic, they exhibited high relative abundances throughout the water column with the patterns of distribution being variable among the ASVs. Four of the *Oceanospirillales* ASVs were more abundant at mesopelagic (3.66% ± 0.79, 1.92% ± 0.43, 1.60% ± 0.58, 1.29% ± 0.49)

and bathypelagic depths (3.11% ± 0.28, 2.78% ± 0.41, 2.3% ± 0.35, 1.42% ± 0.25). Only one ASV made up over one percent of the photic samples (1.56% ± 0.86), though constituted a much lower relative abundance in the mesopelagic (0.58% ± 0.57) and bathypelagic depths (0.02% ± 0.02). The remaining *Oceanospirillales* ASVs were present at all depths at less than 0.5% relative abundances. ASVs classified as Actinobacteria exhibited variable relative abundances throughout the water column, with distinct ASVs consisting of the top 50 ASVS from each zone. Four ASVs were distinctly found at bathypelagic depths (1.74% ± 0.54, 0.91% ± 0.28, 0.67% ± 0.21, 0.48% ± 0.14) while nearly absent at photic and mesopelagic depths. In the mesopelagic, there were two Actinobacteria ASVs that were found (0.61% ± 0.27, 0.55% ± 0.25) while nearly absent at other depths.

As a comparison to the 100% ASV method employed here, sequence analysis was also performed at 99% OTU clustering. As expected, the ASV analysis provided finer detail within each bacterial group than the 99% OTU clusters (Callahan et al. 2015; Eren et al. 2013, 2015; Needham et al. 2017) with the 57,827 ASVs clustering into 26,530 99% OTUs. For example, of the 50 most abundant ASVs identified here for each major depth zone, we found that for Deltaproteobacteria SAR324 there were 20 100% ASVs which collapsed into eight 99% OTU clusters. Further, these OTUs masked the vertical distribution patterns identified with the ASVs. Likewise, for the Gammaproteobacteria *Oceanospirillales* JL-ETNP-Y6, 14 ASVs clustered into six 99% OTUs and depth related patterns were obscured.

Phylogenetic analyses of Alphaproteobacteria Pelagibacterales and Deltaproteobacteria SAR324

To understand the evolutionary relationships within Pelagibacterales using the most recent data available we performed a phylogenetic reconstruction of known Pelagibacterales sequences and previously unrecognized Pelagibacterales sequences in environmental studies (Fig. 2.4). The resulting tree topology corresponds well with previously published phylogenetic trees (Brown et al. 2012; Grote et al. 2012; Jimenez-Infante et al. 2017; Morris et al. 2005; Ngugi and Stingl 2012; Thrash et al. 2014; Tsementzi et al. 2016; Vergin et al. 2013) and expands these known topologies with three additional subclades. Within clade I, there are three previously recognized subclades; Ia and Ib are found in the surface ocean globally while Ic is distributed in bathypelagic depths. In addition, our phylogenetic reconstruction includes the formation of two more subclades within clade I. The near full length 16S rRNA gene sequences forming clade N1 were sampled from the Northeast subarctic Pacific Ocean (Allers et al. 2013) at 500 m (HQ672883) and 2 000 m (HQ674333) depths and from the Guaymas Basin hydrothermal plume at 1 996 m (FJ980771), indicating a potential mesopelagic and bathypelagic distribution. The sequences forming clade N2 were sampled from the Northeast subarctic Pacific Ocean (Allers et al. 2013) at 500 m (HQ672635) and from the Atlantic Ocean (Bergauer et al. 2018) at 367 m (KX427628), indicating a potentially global mesopelagic distribution.

In our 16S rRNA gene phylogenetic reconstruction, clade II has three subclades. Subclade IIb agrees with previous distinctions as consisting of mesopelagic and bathypelagic samples. In our topology, a closer branching subclade is the previously unrecognized N3 subclade, which consists of mesopelagic and bathypelagic samples collected from the Northeast subarctic Pacific Ocean (Allers et al. 2013) at 500 m (HQ672443) and Atlantic Ocean (Bergauer et al. 2018) at 2750 m (KY194455). Branching basal to subclade IIb and N3 is subclade IIa, with a known photic zone distribution. For the remainder of the tree, we recognize clade IV and clade V (subclade Va and Vb) as initially described by Grote and Vergin and colleagues (Grote et al. 2012; Vergin et al. 2013). Statistical analyses were carried out to confirm support of the clade distinctions. Subclade Ia sequences have 100-69.8% identity (98% RAxML robust bootstrap support) while subclade N1 sequences have 100-99.0% identity (92% RAxML robust bootstrap support) with the sequence identity between these two subclades being 97.7–69.6%. Subclade Ib sequences have 100-37.4% identity (95% RAxML robust bootstrap support) and there is 97.3–37.3% identity between subclade N1 and subclade Ib. Basal to subclade Ib is subclade N2 with 100-99.3% sequence identity (98% RAxML robust bootstrap support). Between subclade Ib and subclade N2 there is 95.6–36.7% sequence identity. Subclade Ic is basal to subclade N2 (98% RAxML robust bootstrap support) and has 100-93.6% sequence identity. Between subclade N2 and subclade Ic, there is 95.3-90.8% sequence identity. Basal to subclade Ic is subclade IIb with 100–68.4% identity (86% RAxML robust bootstrap support), and 94.4–67.4% identity to subclade Ic. Subclade

N3 is branches sister to subclade IIb (100% RAxML robust bootstrap support) and has 100-98.6% sequence identity. Between subclade IIb and subclade N3 there is 96.8-68.6% sequence identity. Basal to subclade N3 is subclade IIa with 100-66.2% identity (97% RAxML robust bootstrap support), and 95.2-65.8% identity to subclade N3. Basal to clade I and II is clade III, split into two subclades. Subclade IIIa has sequence identities of 100-90% (98% RAxML robust bootstrap support)and subclade IIIb has sequence identities of 100-94.0% (100% RAxML robust bootstrap support). Between subclade IIa and IIIa sequence identities are 882.-607% and between subclade IIIa and IIIb identities are 90.9-84.5%. Basal to clade II is clade IV, with sequence identities of 100-54.5% (100% RAxML robust bootstrap support), and 83.5-43.2% identities between the two clades. Basal to clade IV is clade V, split into two subclades. Subclade Vb consists of sequences with 100-70.4% identity (100% RAxML robust bootstrap support), and 84.7-46.5% identities to clade IV. Subclade Va has sequence identities of 100-70.4% (100% RAxML robust bootstrap support), and its sequences are 85.4-61.0% similar to subclade Vb.

Next, we implemented this new 16S rRNA gene Pelagibacterales phylogenetic reconstruction to examine the vertical distributions of Pelagibacterales amplicons in our data (Fig. 2.4). In the phylogenetic analysis of this dataset we identified vertical distributions of subclades that correspond to previously recognized distributions while also expanding on the depth ranges of several subclades. Considering the complete dataset, Pelagibacterales consisted of an average of 46.58% ± 9.27 of the amplicon sequences in a sample, indicating this is a highly abundant group of bacteria

at all depths. Subclade Ia are the most abundant overall subclade, dominating photic zone samples with a sample maximum consisting of 92% of the total Pelagibacterales and 60% of reads per proportion of total bacteria. Subclade Ib are one of the most abundant subclades in the mesopelagic and bathypelagic samples (maximum 33% of Pelagibacterales, 16% of bacteria). Subclade Ic exhibits high relative abundances in bathypelagic samples, though is less relatively abundant in mesopelagic depths, and a limited presence in photic zone samples (maximum 16% of Pelagibacterales, 6% of bacteria). Subclade N1 exhibits high relative abundance in mesopelagic and bathypelagic samples (maximum 12% of Pelagibacterales, 6% of bacteria)**,** which was expected given that the sequences consisting of this subclade within the phylogenetic reconstruction were collected from mesopelagic and bathypelagic depths. Also as expected, subclade N2 exhibits low relative abundance in mesopelagic samples (maximum 2% of Pelagibacterales, 1% of bacteria).

Within Pelagibacterales clade II, subclade IIb dominates the mesopelagic and bathypelagic samples (maximum 45% of Pelagibacterales, 17% of bacteria) while subclade N3 exhibits low relative abundance in mesopelagic samples (maximum 2% of Pelagibacterales, 1% of bacteria). Subclade IIa exhibits high relative abundances in the photic zone, decreasing in relative abundance with increasing depth (maximum 15% of Pelagibacterales, 8% of bacteria).

Subclade IIIa exhibits a limited presence in the photic zone and are not detected in the mesopelagic and bathypelagic samples (maximum 0.27% of Pelagibacterales, 0.14% of bacteria). while subclade IIIb (also referred to as LD12) is a distinctly

freshwater subclade of Pelagibacterales. There are no matches of amplicons from my samples to this freshwater subclade.

Subclade IV is found at limited relative abundances throughout the water column, though slightly higher in lower photic and mesopelagic samples (maximum 2% of Pelagibacterales, 1% of bacteria). Subclade Va exhibits limited abundance or is not detected in mesopelagic and bathypelagic samples and a low relative abundance in the upper photic zone (maximum 2% of Pelagibacterales, 1% of bacteria). Subclade Vb exhibits moderate relative abundances in mesopelagic and bathypelagic samples, and low relative abundances in the photic zone (maximum 4% of Pelagibacterales, 2% of bacteria).

To understand the evolutionary relationships within SAR324 using the most recent data available we made a phylogenetic reconstruction of near full length 16S rRNA gene sequences (Fig. 2.5). The resulting tree topology corresponds with previously published phylogenetic trees (Brown and Donachie 2007; Cao et al. 2016; Pham et al. 2008; Sheik et al. 2014; Swan et al. 2011) and expands these known topologies with two additional clades that branch basal to the previously described clades. The original three clades of SAR324 were grouped by temperature and depth distributions (Brown and Donachie 2007). SAR324 clade II consists of samples from cold water including polar surface water and deep samples from temperate and tropical latitudes. SAR324 clade I and clade SAR276 consist of samples from less than 250 m depth at tropical and subtropical latitudes. Brown and Donachie (2007) found these same clades when examining ITS sequence phylogenetic reconstructions. Our 16S rRNA

gene phylogenetic reconstruction of the most up to date near full length sequences available in GenBank continue to support these same clade distinctions. Clade II sequences have 100-96.8% identity (61% RAxML robust bootstrap support) while clade I sequences have 100-98.1% identity (99% RAxML robust bootstrap support) with the sequence identity between these 2 clades being 96.6-94.5%. Clade SAR276 sequences have 100-97.4% identity (100% RAxML robust bootstrap support) and there is 90.7-89.9% identity between clade I and clade SAR276. Basal to clade SAR276 is candidate clade III which consists of photic zone sequences from temperate and subtropical latitudes with 100-98.9% sequence identity (100% RAxML robust bootstrap support). Between clade SAR276 and candidate clade III there is 89.5-87.5% sequence identity. Candidate clade IV is basal to candidate clade III, and consists of subseafloor surface sequences that were included in previous trees(Cao et al. 2016; Sheik et al. 2014), though were not supported as being a distinct clade (91% RAxML robust bootstrap support) and have 100-86.1% sequence identity. Between candidate clades III and IV, there is 86.8-84.9% sequence identity.

Next, we implemented this new 16S rRNA gene SAR324 phylogenetic reconstruction to examine the vertical distributions of SAR324 amplicons in our data (Fig. 2.5). In the phylogenetic analysis of this dataset we identified vertical distributions of clades that correspond to previously recognized distributions while also expanding on the abundances based on the candidate clades. This study focused on the vertical distributions of SAR324 because of highly resolved vertical sampling employed here, providing the opportunity to distinguish fine scale abundance

differences within a phylogenetic context. SAR324 are a highly abundant group of bacteria throughout the water column (8.7% of all sequences in dataset), though are predominantly found below the photic zone (average 14.9% ± 3.3 relative read proportion in mesopelagic and bathypelagic). SAR324 clade II is the most abundant clade overall, reaching a maximum 19.8% of all bacteria and 94.5% of all SAR324 in a sample. The highest relative abundances occur at mesopelagic depths, followed by bathypelagic depths, and surprisingly surface samples. Clade I and clade SAR276 exhibit similar distributions, predominantly at upper mesopelagic and low photic depths. Clade I makes up a maximum 1.1% of all bacteria and 7.6% of all SAR324 in a sample, while clade SAR276 makes up maximum 0.4 % of all bacteria and 42.1% of all SAR324 in a sample. Candidate clades III and IV occur at very low abundances throughout the water column and exhibit distinct depth patterns. Candidate clade III is mostly found at photic depths and not detected at mesopelagic and bathypelagic depths, a maximum of 0.04% of all bacteria and 16.7% of all SAR324 in a sample. Candidate clade IV is mostly found at mesopelagic and bathypelagic depths and not detected from photic depths, exhibiting a maximum 0.07% of all bacteria and 4.7% of all SAR324 in a sample. Even with the strong support of the topology of the SAR324 reconstruction, a number of amplicons were classified as SAR324, but unable to be placed as belonging to a specific clade, mostly at mesopelagic and bathypelagic depths (maximum 1.6% of all bacteria and 11.7% of all SAR324 in a sample).

Discussion

Submarine canyon ecosystems have been understudied for the vertical distribution of bacterial abundance and diversity. Our bacterial cell abundances mirrored trends reported in a previous epifluorescence microscopy-based enumeration of non-photosynthetic bacteria in a study of Mediterranean submarine canyons. The absolute abundances of our study in and near Monterey Canyon were greater (5 m: $2.0 \times 10^6 \pm 8.7 \times 10^5$ cells ml^{-1}; 1200 – 1978 m: $6.71 \times 10^4 \pm 1.23 \times 10^4$ cells ml^{-1}) than the values reported in the Mediterranean canyons (5 m: $4.8 \times 10^3 \pm 1.79 \times 10^3$ cells ml^{-1}; 1500 – 2600 m: $2.95 \times 10^4 \pm 1.14 \times 10^4$ cells ml^{-1}) (Diociaiuti et al. 2019). The latter study further reported that depth-related trends in bacterial cell abundance and biomass both in and out of the canyons, was similar (Diociaiuti et al. 2019). Likewise, DAPI counts at well characterized sites like the Bermuda Atlantic Time-Series (BATS) in the North Atlantic Ocean and Station ALOHA in the North Pacific Subtropical Gyre (Morris et al. 2004; Steinberg et al. 2008) show similar trends though absolute values differ with photic zone abundances highest at BATS > our study > Station ALOHA and similar absolute values at mesopelagic depths across all locations. Additionally, using SYBR green epifluorescence microscopy for cell enumeration at the coastal San Pedro Time-series (SPOT) off of Southern California, similar vertical trends and absolute abundances were observed in bacterial abundances as identified in our study (Cram et al. 2015). A flow cytometric study along a latitudinal transect in the South Atlantic Ocean reported that bacterial abundances also decreased to the same absolute values as our study with increasing depth, and there was a latitudinal trend of higher

abundances at higher latitudes with photic zone absolute values between 40 - 60°S most similar to photic bacterial abundances in our study (De Corte et al. 2016). Collectively, our study of a canyon system in the eastern North Pacific and these other studies from around the world show that while bacterial abundances can vary $10^5 – 10^8$ fold in the photic zone, they decrease with depth such that they are relatively stable in the mesopelagic, and in the bathypelagic, although lower in the latter.

We found that bacterial taxonomic diversity exhibited clear depth-related increases in diversity. Previous studies of bacterial taxonomic diversity with depth have yielded mixed results. Similar to our results, greater diversity was reported below the photic zone, 800 m at BATS (Bryant et al. 2012), in the northern Gulf of Mexico at 450 – 750 m and 1500 m (Easson and Lopez 2019), and in the Mediterranean Sea at 500 and 2000 m (Pommier et al. 2010). In addition to diversity increasing with depth, bacterial community structure was found to be water mass specific in the North Atlantic Ocean (Agogué et al. 2011) and the Southern Ocean (Signori et al. 2014), an aspect that was not part of our study design.

Other SSU rRNA gene amplicon sequencing studies have reported highest bacterial diversity in mesopelagic waters throughout the Pacific Ocean, relative to underlying or overlying water (Jing et al. 2013; Walsh et al. 2016), as well as no diversity trend with vertical distribution at Station ALOHA (Bryant et al. 2012; Kembel et al. 2011). The mixed results of taxonomic diversity with depth from previous studies may be due to differing environmental conditions, selection

mechanisms or decreasing absolute abundances with increasing depths at each of these locations. For instance, Walsh et al. (2016) found the lowest taxonomic diversity at surface depths and the highest diversity within the oxygen minima of the mesopelagic zone, suggesting the role of respiration in shaping bacterial richness in these samples. The surface ocean is subject to more short-term, variable conditions while the bathypelagic communities may be structured by connectivity through ocean circulation. Examination of multiple sites in the Pacific Ocean found bathypelagic bacterial communities to be similar to each other though distinct from photic communities, with the bathypelagic communities appearing to be more stable while the photic communities are affected by fluctuating environmental factors (Jing et al. 2013). With lower absolute abundances in deeper water, it may be easier to capture the rare or less abundant bacteria in each sample, especially if the sequencing depth for the water depths sampled did not reach saturation in the rarefaction curves. While the bacterial cell abundances in our study are highest at depths within the photic zone, the lower diversity in these samples is most likely due to changing environmental conditions throughout the year leading certain bacterial groups to dominate the community as the conditions become more favorable for their survival success.

Previous examinations of bacterial diversity in Monterey Bay from the surface to 200 m depth found greater variability among surface samples (0 m) than at 200 m (Rich et al. 2011). As seen at other Pacific Ocean sites (Jing et al. 2013), the 200 m samples were more similar to each other (Rich et al. 2011). Comparisons between Monterey Bay and Station ALOHA with SSU rRNA gene fosmids indicated that

diversity, as measured as an operational ‘order richness’ index, was higher in gyre samples, though there were patterns of depth partitioning at each site with different bacteria dominating at discrete depths between 0 and 770 m (Pham et al. 2008).

Surface water studies using pairwise association analysis over time have suggested that the abundance of particular bacteria tend to be best predicted by the abundance of other microorganisms rather than variability of measured environmental parameters (Chow et al. 2013, 2014; Fuhrman and Steele 2008; Steele et al. 2011). The bacterial vertical distribution patterns found in this study are similar to previously described communities (Arístegui et al. 2009; Delong et al. 2006; Zinger et al. 2011) with Pelagibacterales present across all depths and an increase of Deltaproteobacteria and Actinobacteria with depth. The vertical distribution of prokaryotic diversity in photic, mesopelagic and bathypelagic zones has been comprehensively studied and compared across the global oceans (Agogué et al. 2011; Brown et al. 2009; De Corte et al. 2016; Delong et al. 2006; Ghiglione et al. 2008; Jing et al. 2013; Medina-Silva et al. 2018; Nunoura et al. 2015; Signori et al. 2014; Tseng et al. 2015; Walsh et al. 2016).

Although relatively few high resolution time-series characterize microbial communities, those that do have revealed strong seasonal patterns in bacterial community structure in the photic zone of both open ocean gyre sites as well as coastal sites. The reported seasonal shifts vary in magnitude between locations (Carlson et al. 2009; Cram et al. 2015; Delong et al. 2006). For example, the upper 200 m of the water column at BATS exhibits seasonal variability of the bacterial community structure, found to be related to seasonal mixing and stratification

(Carlson et al. 2009; Morris et al. 2005). In contrast, the mesopelagic communities at Station ALOHA in the North Pacific Subtropical Gyre are less seasonally variable than BATS in the North Atlantic, but variation has been reported to occur between depths within the mesopelagic zone (Delong et al. 2006). At SPOT, microbial diversity was found to be partially driven by the exchange of bacteria between depths, due to physical mixing, and diversity was highest at mesopelagic depths (150 - 500 m) where communities exhibited the least month to month variation (Cram et al. 2015). Seasonal shifts in ITS Automated Ribosomal Intergenic Spacer Analysis (ARISA) clone library bacterial OTUs were also observed at the bottom depth (890 m) of the SPOT station, shifts that were attributed to variability in particles sinking from the surface ocean and their accumulation on the seafloor (Cram et al. 2015).

Mestre et al. (2018) found the most abundant (> 50%) bacterial 99% OTUs in the bathypelagic (3105 – 4000 m) were surface (3 m) derived OTUs. Whereas we found a few reads (<10%) of the more relatively abundant (>50%) bathypelagic ASVs in photic zone samples. The presence of the same ASVs in both surface and deep sea communities suggests the connection between these communities, potentially via colonized sinking particles (Mestre et al. 2018), and changes in relative abundance on particles as they descend. To test this theory in our own study, it would be necessary to filter seawater into multiple size fractions, instead of only using 0.2 μm filters, with this same high resolution vertical depth sampling. Thus, several of the overall trends seen in our abundance as well as sequence-based diversity and community composition analyses connected well to trends seen in other environments.

Comparisons where results deviated may reflect differences in the environments studied, and also likely reflect differences in the methods and analytical approaches used.

Pelagibacterales vertical distribution

We also sought to understand the evolutionary relationships between the organisms present at our site, especially for the more abundant lineages. Our Pelagibacterales phylogenetic reconstruction incorporated a suite of new full-length 16S rRNA gene sequences and identified three subclades not been recognized in prior studies. Our analysis indicated that clade II has three subclades, whereas prior 16S rRNA based studies have either not identified discrete clade II subclades due to fewer sequences aligned (Brown et al. 2012; Grote et al. 2012; Jimenez-Infante et al. 2017; Morris et al. 2005) or fewer 16S rRNA gene positions considered (Ngugi and Stingl 2012), or have reported two subclades (Tsementzi et al. 2016; Vergin et al. 2013). However, prior ITS based (naming convention phylotypes instead of clades as with 16S) analyses have identified three subphylotypes in clade II (phylotype 2 for ITS) (Brown et al. 2012; Jimenez-Infante et al. 2017; Ngugi and Stingl 2012). Brown et al. (2012) named the subphylotypes P2.1, P2.2, and P2.3 where P2.1 consists of sequences from the surface ocean in tropical and temperate climates, P2.2 consists of Antarctic sequences from a single study (García-Martínez and Rodríguez-Valera

2000), and P2.3 consists of sequences from mesopelagic and bathypelagic depths. While subphylotypes P2.1 and P2.3 include sequences that can be placed into subclades IIa and IIb in our 16S rRNA gene phylogenetic reconstruction, subphylotype P2.2 does not correspond to either of these or subclade N3 in our study. Sequences from subphylotype P2.3 in Brown et al. (2012) ITS phylogenetic reconstruction were placed in subclade IIb as named by Vergin et al. (2013) 16S rRNA gene phylogenetic reconstruction, and agrees with previous classifications as consisting of mesopelagic and bathypelagic samples. In our topology, a third subclade in clade II is the previously unrecognized N3 subclade. This previously unrecognized subclade N3 does not appear to correspond to ITS subphylotype P2.2. The sequences from the Antarctic study that formed subphylotype P2.2 do not contain the first half of the 16S rRNA gene (the primers start at position 818 within 16S V5), so due to their short length they were not included in our phylogenetic reconstruction, though they exhibited 93.45% sequence identity to clade IIa. A BLAST search of these Antarctic sequences (AF151230) found the highest nucleotide percent identity to a Northeast subarctic Pacific Ocean sample from 500 m (95.47%; HQ715235). This subarctic sequence is also not included in our 16S rRNA gene phylogenetic reconstruction, as once again the Forward PCR primer for this sequence began too far into the 16S rRNA gene, at position 1054. Comparisons to our subclade N3 sequences using BLASTn rendered identities <92%. This confirms that the Antarctic sequences classified as subphylotype P2.2 (Brown et al. 2012) are not part of subclade N3. Sequences in subclade IIa are also found with the subclade IIa

classification in the Vergin et al. (2013) 16S rRNA gene phylogenetic reconstruction and with subphylotype P2.1 in Brown et al. (2012) ITS phylogenetic reconstruction. The addition clade N3 in the Pelagibacterales phylogeny identifies clade N3 as being more closely related evolutionarily to clade IIb, while clade IIa is a more basal clade, forming what appears to be a separate clade within our reconstruction. Taken together, it appears that there are at least four clade II subclades.

Expanding on the previously known biogeography of Pelagibacterales clades, assignment of amplicons to this reference tree provided new insights of clade depth distributions. Subclade Ib exhibited higher relative abundance in mesopelagic and bathypelagic samples when compared to the photic zone samples. Previous work on photic depths showed that Pelagibacterales diversified into clades across different water depths and seasonal conditions (Vergin et al. 2013). In our study, subclade IIb was found to exhibit similar relative abundances in mesopelagic and bathypelagic samples, all well oxygenated depths compared to their known peak at anoxic depths within an oxygen minimum zone (Tsementzi et al. 2016) and builds on the upper mesopelagic depth distribution at BATS during spring (Carlson et al. 2009, 2010). Adding to the known distribution of subclade Vb in the surface ocean (Giovannoni 2017), our study found subclade Vb at all depths throughout the water column. Future sampling in different regions of the ocean and at different depths will continue to strengthen our knowledge of Pelagibacterales clade vertical distributions.

SAR324 vertical distribution

We also performed a phylogenetic reconstruction of the SAR324 lineage that incorporated new full-length 16S rRNA gene sequences. Here, the SAR324 sequences formed five statistically supported clades that correspond to three clades reported in prior reconstructions and identified two new candidate clades. Two previous studies (Pham et al. 2008; Sheik et al. 2014) use the same clade name (ctg_NISA008) corresponding to our clade II. Moreover, not all previously published 16S rRNA gene trees describe distinct SAR324 sequence groups (Cao et al. 2016; Chitsaz et al. 2011; Swan et al. 2011). The only clade distinction in Sheik et al. (2014) is for clade ctg_NISA008, corresponding to our clade II. In an earlier study six SAR324 clades were reported (Pham et al. 2008), all with statistical support (parsimony method), specifically, ctg_NISA008 (corresponding to our clade II), SAR324 (corresponding to our clade I), SAR21, SAR276 (corresponding to our clade SAR276), euphotic, and FS142-32B-02. The available sequences for what has been identified as clade SAR21 are unfortunately too short to be included in our phylogenetic reconstruction, but have highest identities of 93.23% and 93.63% to clade SAR276 in our reconstruction. The sequences in the euphotic clade and clade FS142-32B-02, while classified as SAR324 by Pham et al. (2008), were not high enough sequence identity (88.03 – 83.06% and 87.39 – 80.24 %, respectively) to the SAR324 sequences contributing to our phylogenetic reconstruction, so they were not included in our analysis.

Analysis of our 16S rRNA gene amplicons against the SAR324 reference tree both supports and adds to previously known vertical distributions. SAR324 clade II was previously described as occurring in cold waters, > 100m depth in the Arctic Ocean, and coastal and subarctic northeast Pacific Ocean. This same finding is supported by our samples with a predominantly mesopelagic and bathypelagic distribution. Surprisingly, clade II amplicons also exhibited a higher relative abundance in samples collected just below the surface (15-50 m) during both May and September samplings. Due to their location near the surface, the water temperatures are much warmer than those existing at mesopelagic and bathypelagic depths. This highlights that even though there are low counts of SAR324 at these depths, clade II is still the dominate clade. The distributions of clade I and clade SAR276 supported previously known distributions, being found in our lower photic and upper mesopelagic samples. Candidate clade III was expected to have a photic distribution given the information available on the included near full length 16S sequences in the reconstruction. The placement of our amplicons was in agreement with these sequences, being only found in samples from the photic zone and mostly absent at mesopelagic and bathypelagic depths. Candidate clade IV in the SAR324 reconstruction is made of surface sediment sequences. In our dataset, the candidate clade IV amplicons were found at mesopelagic and bathypelagic depths, and mostly absent at photic depths. While most of the 16S amplicons were placed in a clade from the reconstruction, more than expected were classified as SAR324 but not placed into a clade. These amplicons are mostly from mesopelagic and bathypelagic depths suggesting that more full length

16S sequences need to be added to sequencing databases in order to better distinguish the clade placement.

Conclusions

Using highly resolved approaches for sequence analysis facilitated our observations of the vertical distributions of bacterial groups throughout the water column in and near Monterey Bay. With multiple depths sampled from the surface ocean to the seafloor over multiple seasons, we identified that the bacterial community of the photic zone was more variable than communities deeper in the water column, potentially influenced by the changing environmental conditions by season. Bacterial communities of the mesopelagic and bathypelagic were more stable, with limited variations. These findings support those of global studies in both the surface ocean and deep sea (e.g. Salazar et al. 2016; Sunagawa et al. 2015) with deeper sampling and improved sampling of diversity. The new 16S rRNA gene phylogenetic reconstructions presented here highlight the evolutionary diversity of the highly abundant Pelagibacterales and SAR324 bacteria. Placement of our amplicons on these phylogenetic trees provided new insights into vertical distributions of Pelagibacterales and SAR324 clades. Future rRNA gene based studies from more locations globally should utilize these reconstructions to better compare

diversity within the Pelagibacterales and SAR324 clades, respectively, and their vertical distributions.

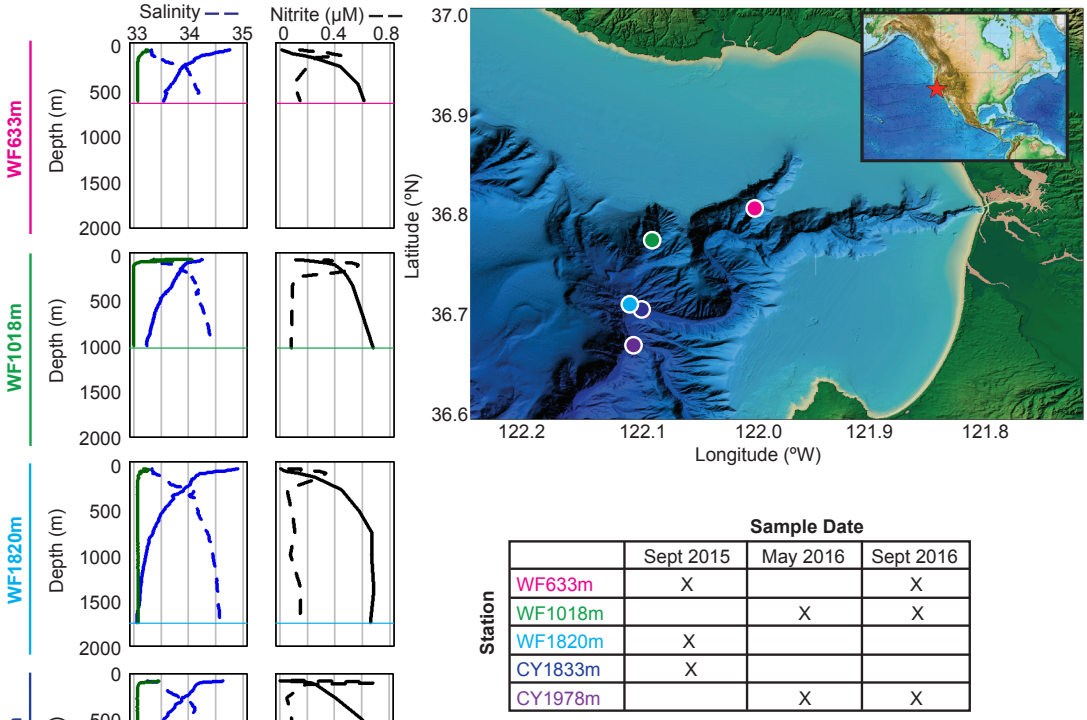

Figure 2.1

Sampling locations for this study are indicated on the map while the representative profiles for each station display the water column characteristics. The enlarged map displays the stations sampled in the eastern North Pacific Ocean and in Monterey Bay overlying seafloor bathymetry displayed via color while the insert map indicates the location of the enlarged region along the eastern North Pacific Ocean. Station names beginning with WF indicate a whale fall on the seafloor while CY indicates a Monterey Canyon location. Two representative profiles for each station include fluorescence, temperature, and salinity as well as nitrate and nitrite. Horizontal colored lines in each profile indicate that station's bottom depth. A table of sample

dates indicates when the water column at each of the stations was sampled.

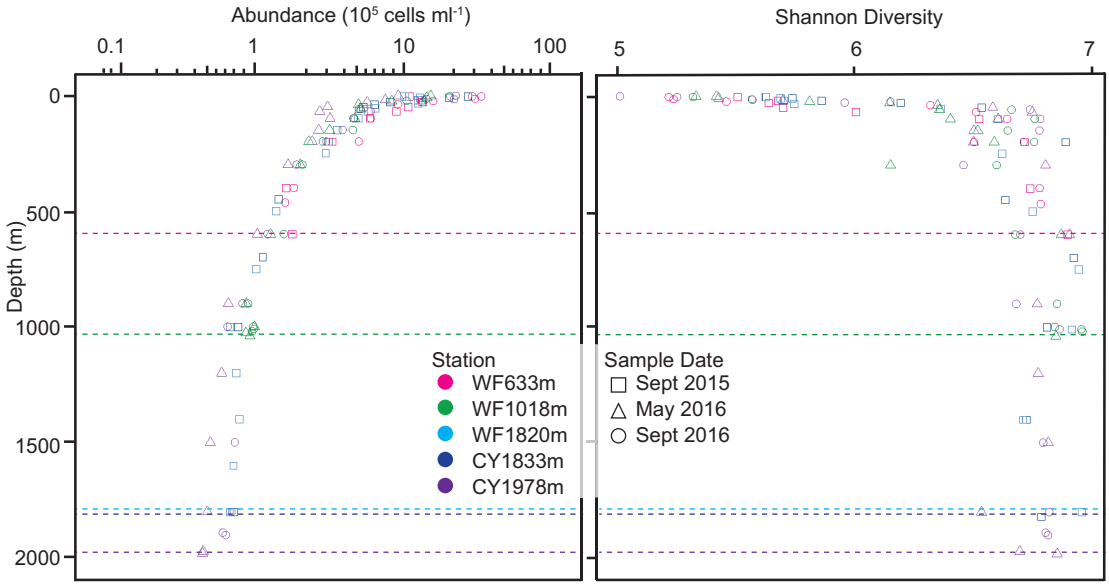

Figure 2.2

Bacterial cell abundance decreases with depth by 1.5 orders of magnitude from the surface ocean to 1,978 m depth while alpha diversity increases with depth. (left panel) Flow cytometry bacterial cell abundances in cells ml^{-1} using SYBR Green I stain and (right panel) calculated Shannon diversity index from amplicon data. Colors represent the station sampled, shapes represent the sampling date, and the horizontal color dotted lines represent the bottom depth for that station. Note that analysis of replicate flow cytometry samples from individual sampling dates revealed a variance of 16% (n = 8) that can be attributed to methodology.

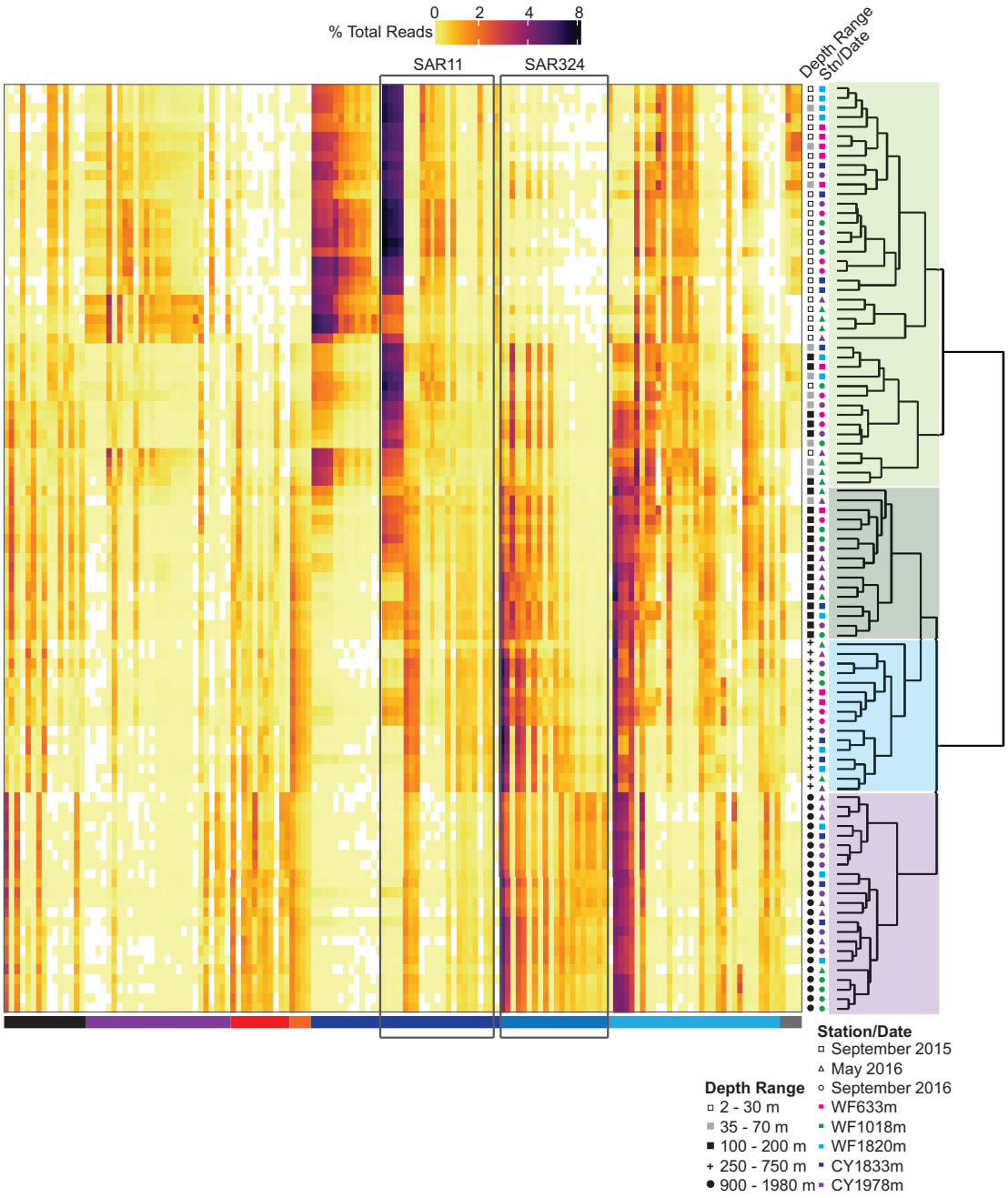

Figure 2.3

Percent relative abundance of the 50 most abundant 100% amplicon sequence variants (ASVs) from each cluster. Heat map columns represent the most abundant ASVs ordered by phylum (as indicated by horizontal color bars). Rows represent individual water samples with hierarchical clustering of samples based on Bray-Curtis dissimilarities of bacterial community ASVs. Sample clusters are apparent in

association with depth gradients: photic (green), mesopelagic (blue), and bathypelagic (purple). Colored shapes indicate the station (color) and sampling date (shape) of each sample. Gray scale shapes indicate the depth range corresponding each sample. Photic zone samples are dominated by Alphaproteobacteria *Rhodobacteraceae* and SAR11, mesopelagic and bathypelagic zone samples are dominated by Deltaproteobacteria SAR324 and Gammaproteobacteria *Oceanospirillales*. Pelagibacterales (SAR11 clade) and SAR324, are highlighted by boxes overlying the heat map. Bacterial Phyla ordered from left to right: Actinobacteria, Bacteroidetes, Marinimicrobia, Nitrospinae, Alphaproteobacteria, Deltaproteobacteria, Gammaproteobacteria, Verrucomicrobia.

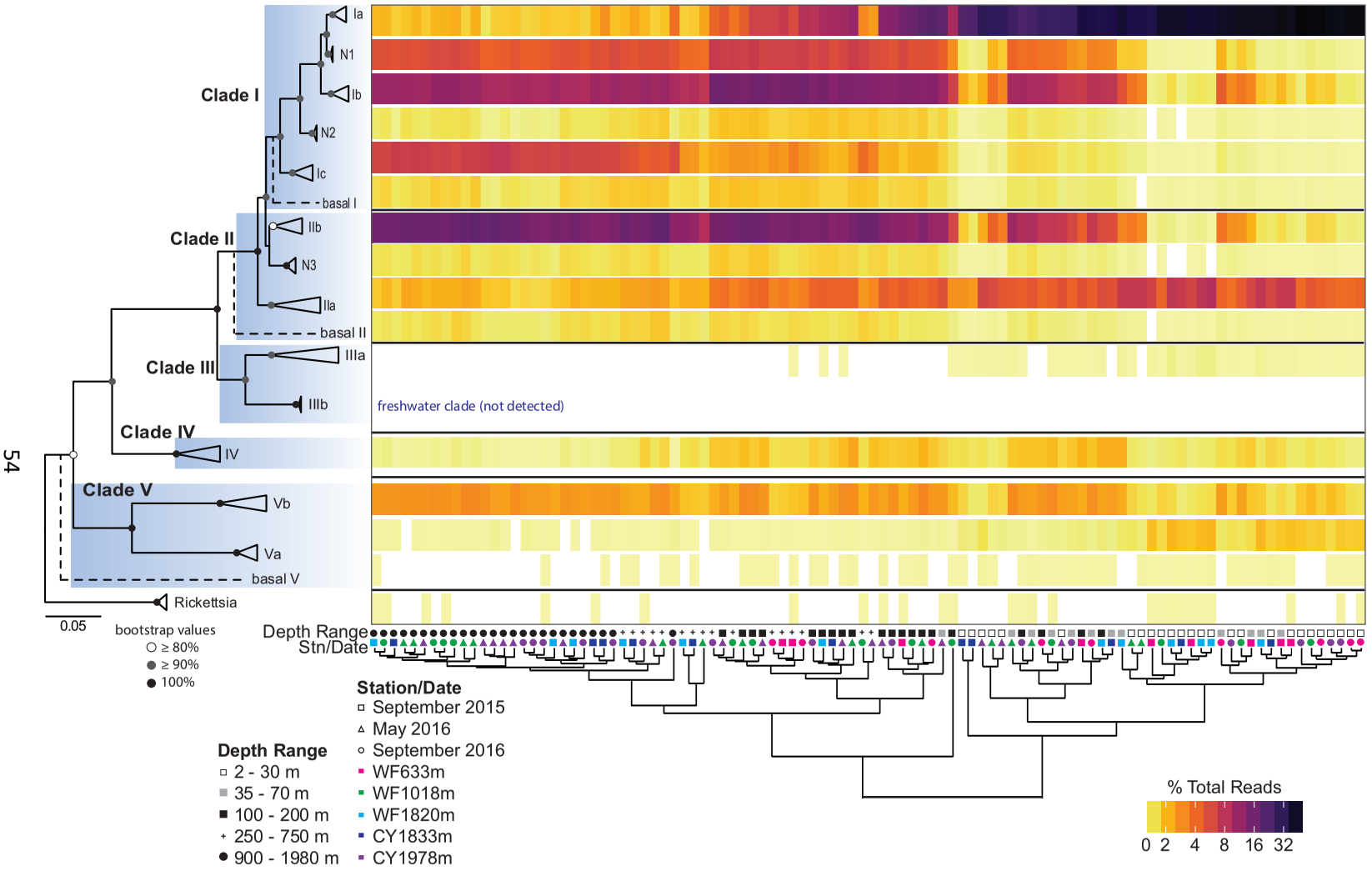
Clade I
Ia
N1
Ib
N2
Ic
basal I
Clade II
IIb
N3
IIa
basal II
Clade III
IIIa
IIIb
freshwater clade (not detected)
Clade IV
IV
Clade V
Vb
Va
basal V
Rickettsia
0.05
bootstrap values
≥ 80%
≥ 90%
100%
Depth Range
Stn/Date
Station/Date
September 2015
May 2016
September 2016
WF633m
WF1018m
WF1820m
CY1833m
CY1978m
Depth Range
2 - 30 m
35 - 70 m
100 - 200 m
250 - 750 m
900 - 1980 m
% Total Reads
0 2 4 8 16 32

Figure 2.4

Pelagibacterales 16S rRNA gene Maximum Likelihood tree reconstruction and percent relative abundance of Pelagibacterales clades. Heat map columns represent individual water samples ordered by hierarchical clustering based on the Bray-Curtis similarities of the Pelagibacterales composition, with samples generally clustering by depth. Colored shapes indicate the station (color) and sampling date (shape) of each sample. Gray scale shapes indicate the depth range corresponding to sample depth. The phylogenetic tree identifies three statistically supported previously unrecognized Pelagibacterales clades. Phylogenetic classifications of the V1-V2 16S rRNA gene amplicons in this study suggest novel subclade N1 to be highly relatively abundant in mesopelagic and bathypelagic depths while subclades N2 and N3 are found with low relative abundance at mesopelagic depths. This reconstruction was performed in collaboration with Chang Jae Choi.

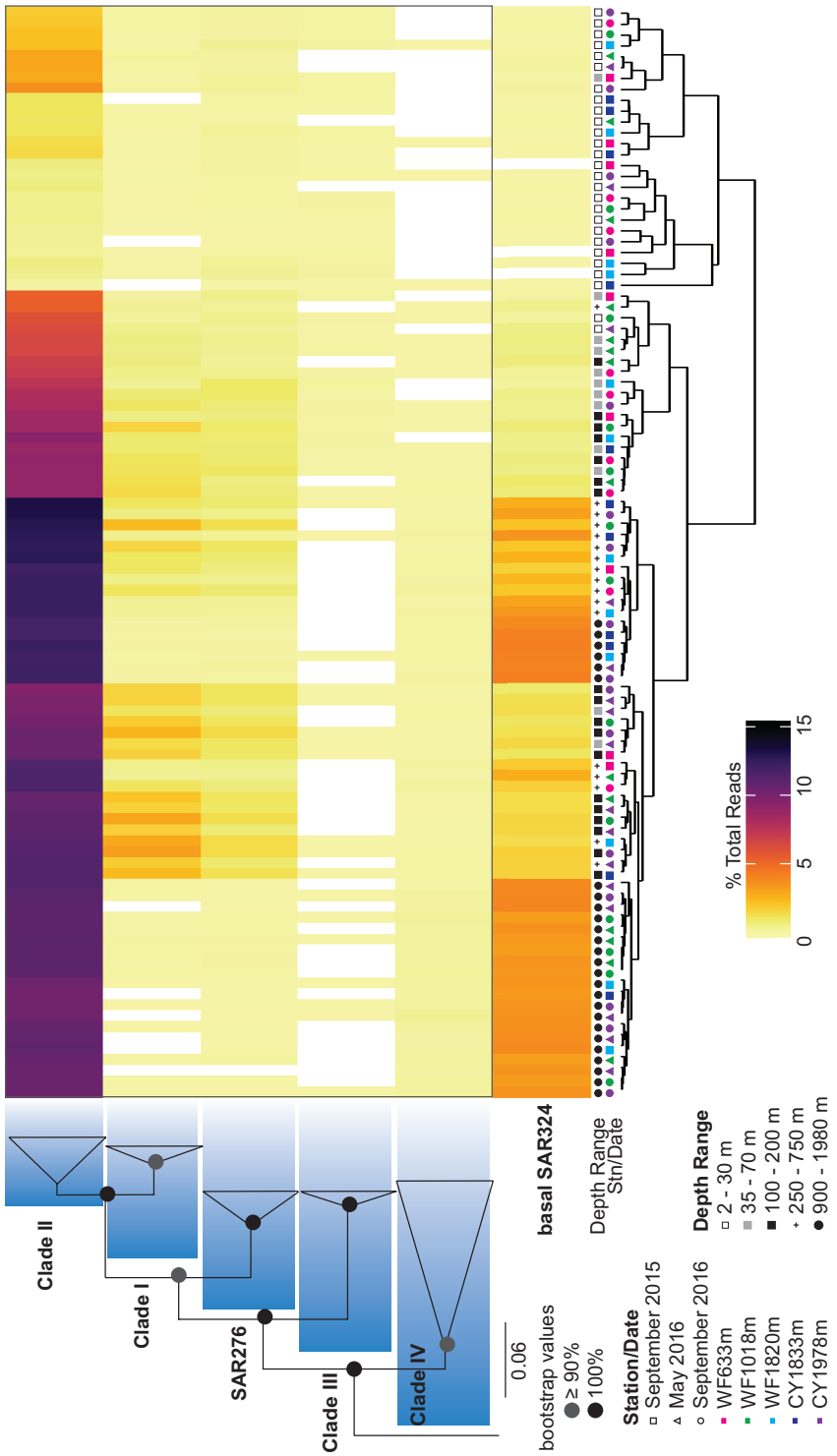
Clade II
Clade I
SAR276
Clade III
Clade IV
basal SAR324
0.06
bootstrap values
≥ 90%
100%
Depth Range
Stn/Date
Station/Date
September 2015
May 2016
September 2016
WF633m
WF1018m
WF1820m
CY1833m
CY1978m
Depth Range
2 - 30 m
35 - 70 m
100 - 200 m
250 - 750 m
900 - 1980 m
% Total Reads
0
5
10
15

Figure 2.5

SAR324 16S rRNA Maximum Likelihood tree reconstruction and percent relative abundance of SAR324 clades. Heat map columns represent individual water samples ordered by hierarchical clustering based on the Bray-Curtis similarities of the SAR324 composition, with samples generally clustering by depth. Colored shapes indicate the station (color) and sampling date (shape) of each sample. Gray scale shapes indicate the depth range corresponding to the sample depth. The phylogenetic tree includes two previously unrecognized SAR324 clades. Phylogenetic classifications of the V1-V2 16S rRNA gene amplicons in this study suggest candidate SAR324 clade III to be found at low relatively abundance at photic depths while clade IV is found with low relative abundance at mesopelagic and bathypelagic depths.

Chapter 3: Bacterial community variability in Monterey Canyon and associated submarine fan sediments

Abstract

Organic matter depositional histories influence bacterial communities in deep sea surface sediments. We conducted replicated sampling of deep sea surface sediments in a submarine canyon ecosystem and associated submarine fan ecosystem in and near Monterey Bay, CA, USA, with seafloor depths ranging from 633 m to 3,562 m. Bacterial community composition was assessed using V1-V2 16S rRNA gene amplicons analyzed at 100% nucleotide identity as amplicon sequence variants (ASV). Biological replicates (n = 3 sediment push cores) were sampled at each of the five stations, with biological replicates within each sediment push core (n = 3 per core) sequenced for a total of nine samples analyzed from <1 m apart within each station. Replicated sampling on a submeter scale allowed assessment of the amount of replication needed to describe the bacterial community composition within a specific location. Permutational multivariate analysis of variance (PERMANOVA) found no significant difference between replicates at the submeter scale, at any station. However comparisons between stations >10 km away showed bacterial communities to be significantly different ($p < 0.05$). The surface sediment bacterial community compositions at the four stations from Monterey Canyon were more similar to each

other than to the submarine fan sediments. A fine scale vertical analysis of 1- or 3-cm intervals of the upper 20 cm of the sediments found the Shannon diversity index to be higher than that of the water column, with Monterey Canyon sediments maintaining a similar level of diversity down core while the submarine fan sediments decreased in Shannan diversity with increasing sediment depth. Canonical correspondence analysis (CCA) of geochemical measurements and their potential influence on vertical bacterial community composition of Monterey Canyon sediments identified nitrate (NO_3^-) and dissolved inorganic carbon (DIC) as having a significant ($p < 0.05$) influence. The most abundant bacteria in terms of relative amplicon abundance across all stations were the Deltaproteobacteria *Desulfobacteraceae* (8.75% of all amplicons) and *Desulfobulbaceae* (6.5% of all amplicons). The well-known deep sea bacteria Gammaproteobacteria JTB255-marine benthic group (MBG) made up 3.3% of bacterial amplicons, and exhibited higher relative abundances at the more offshore submarine fan surface sediments (0 – 3 cm below seafloor: average 6.8% ± 0.8 relative abundance). The analyses also showed that while the surface sediments are at the interface between seawater and the subseafloor, the bacterial communities within the sediments were distinct from the overlying seawater. These analyses indicate that in the sediment types studied herein, submeter homogeneity (< 1 m apart) is considerable when sampling is performed at the same depth horizon, however down core sampling renders differing changes in diversity index profiles depending on the type of sediments sampled.

Introduction

Seafloor bacterial abundances are impacted by organic matter availability in sediments. Further, organic matter content has been shown to be associated with significant differences in bacterial community structure in deep sea sediments (Bienhold et al. 2016; Danovaro et al. 2016). The distribution patterns of deep sea (> 200 m seafloor depth) surface sediment bacteria showed higher dissimilarities with increasing distance from compared sites than pelagic communities, indicating that physical mixing plays a fundamental role in "homogenizing" distributions in pelagic environments (Zinger et al. 2011) and that transport through sediments is more difficult than through water. Horizontally isolated assemblages suggest that specific surface sediment bacterial groups may be widely dispersed over scales of a few kilometers but the local environmental conditions select for particular assemblages (Hewson et al., 2007). This highlights the need for higher taxonomic resolution studies in sediments to identify the parameters most influencing specific particular bacterial assemblages.

Many benthic microbial diversity studies have focused on either hot spot ecosystems, such as hydrothermal vents and cold seeps, or open ocean abyssal plain habitats. Submarine canyons can also be considered hot spots and typically differ from surrounding open environments in terms of both quantity and quality of organic matter deposited and may support higher prokaryotic (Polymenakou et al. 2008) and

faunal abundances (Cunha et al. 2011; Duineveld et al. 2001; Escobar Briones et al. 2008; De Leo et al. 2010; Vetter and Dayton 1998) than surrounding abyssal sediments.

Here, we sampled sediments throughout Monterey Canyon and a station 170 km offshore onto the associated submarine fan in the eastern North Pacific Ocean. The goals of our study were first to examine variability within sediment communities by performing biologically replicated sampling, and second to characterize variations in community structure at sites with different depositional histories. To this end we analyzed V1-V2 16S rRNA gene amplicon sequences from samples collected at 1- or 3- cm intervals over the upper 20 cm of deep sea sediments. The analyses were used to compare sediment bacterial community structure to that of the overlying seawater community and to assess variations over the vertical sediment profile.

Materials and Methods

Oceanographic sampling

Three research cruises were conducted onboard the R/V *Western Flyer* in September 2015, September 2016, and May 2017 in or near Monterey Bay, in the eastern North Pacific Ocean. Five stations were sampled for sediments and the

overlying seawater: SF3562m, CY1833m, CY1040m, WF1018m, and WF633m. Station name letters indicate being at a location where a whale carcass existed on the sea floor (WF, whale fall), while "CY" corresponds to a submarine canyon site and "SF" corresponds to the more offshore submarine fan, neither of which has a such known unusual attribute. Number values in names indicate the bottom depth at the station.

Seawater was collected 1 m above the seafloor using a Niskin bottle mounted on a conductivity/temperature/depth (CTD) rosette or on the remotely operated vehicle (ROV) *Doc Ricketts*. Samples for DNA extraction were collected by filtering 1 L of seawater onto a 0.2 μm 47 mm Supor filter (Pall Gelman, East Hills, NY, USA) in duplicate and immediately frozen at -80°C.

Seafloor sediment samples were obtained using a ROV to collect push cores of 21 cm length and 7 cm inner diameter. After collection, the sediments were extruded from the push cores on board the ship and sampled for nucleic acid analysis. At each site one core was also sampled for porewater geochemistry as described below. Cored sediments were sectioned into 1-cm or 3-cm intervals by extruding the sediment upward through the polycarbonate plastic core tube. Triplicate 1-cc plugs of sediment were collected into cryovials, flash frozen in liquid nitrogen and stored at -80°C.

Geochemical analysis

Porewater was extracted from 1- or 3-cm sediment intervals under argon using a pressurized gas sediment squeezer (KC Denmark A/S, Silkeborg, Denmark) (Reeburgh 1967) into argon flushed syringes prior to distribution through a 0.2 μm polyethersulfone (PES) syringe filter for various measurements. Sulfide dissolved in sediment pore waters was preserved by the immediate precipitation as ZnS through the addition of 0.5M Zn-acetate in a 1:1 ratio with water samples. Concentrations were then determined spectrophotometrically by the Cline assay (Cline 1969). Water samples for anion and cation analysis (Na^+, K^+, Mg^{2+}, Ca^{2+}, formate, acetate, Cl^-, Br^-, NO_3^-, SO_4^{2-}) were stored at -20°C after filtration. After thawing, aliquots were diluted 1:20 with 18.2 MW Milli-Q water and were subsequently analyzed on a dual channel Dionex ICS-2000 ion chromatography system in the Caltech Environmental Analysis Center. Water samples were split and simultaneously separated with cation and anion exchange columns at 0.25 ml min^{-1} and 30°C. Cations were separated isocratically with 20 mM methanesulfonic acid using an IonPac CS12A column and guard column, and anions were separated isocratically with 20 mM KOH using an IonPac AG19 column and guard column. Water samples for DIC measurements were filtered directly into helium flushed, 12 ml exetainer vials (Labco Ltd, Lampeter, UK) that had been pre-weighed after the addition of 100 μl ~40% phosphoric acid. Samples were stored upright at room temperature. Vials were sampled using a GC-PAL autosampler (CTC Analytics, Zwingen, Switzerland) equipped with a double-holed needle that transferred headspace using a 0.5 ml min^{-1} continuous flow of helium to a 50 μm sample loop before separation by a PoraPlotQ fused silica column (25m; i.d.

0.32 mm) at 72°C. CO_2 was then introduced to a Delta V Plus IRMS using a ConFlo IV interface (Thermo Scientific, Bremen, Germany) in the Caltech Stable Isotope Facility. A sample run consisted of three reference CO_2 gas peaks, 10 replicate sample injections, and two final reference CO_2 peaks. A concentrated solution of $NaHCO_3$ was used to establish a standard curve for μmol CO_2 determination by adding a range of volumes to additional exetainer vials, which were interspersed with samples. The concentration of DIC (μM) in samples was calculated after determining sample volume by re-weighing exetainers and by comparing the average of the combined mass 44, 45, and 46 CO_2 peak areas to the standard curve (n = 20, R2 = 0.99). Due to low porewater levels at SF3562m, there was not enough volume to measure all parameters, so we do not have measurements of DIC, total Fe, Fe^{2+} or HS. (Table S3.1).

DNA extraction, PCR and sequencing

Seawater DNA was extracted from filters using a modification of the QIAGEN DNeasy Plant kit (Qiagen, Valencia, CA, USA), including the addition of a bead beating step (Demir-Hilton et al. 2011). Sediment DNA extracts were attained using the Qiagen RNA Powersoil DNA elution accessory kit (Qiagen, Valencia, CA, USA). At each station sampled, three push cores were selected for DNA analysis. For one of these push cores, one replicate of sediment DNA was extracted from each depth

interval. For technical replicates, one depth interval was selected, and DNA was extracted for two additional push cores (3 push cores total) at the identical depth interval. For biological replicates, DNA was extracted from triplicate 1-cc plugs of sediment samples within the selected depth interval of the three push cores (n = 9 replicates per station).

DNA was quantified with the QuBit dsDNA high-sensitivity assay (Invitrogen, Carlsbad, CA, USA) and diluted to 5 ng μl^{-1} with TE pH 8. Polymerase chain reactions (50 µl) were set up as previously described (Hamady et al. 2008) with 5 µl of 10x buffer, 1 U of HiFi-Taq, 1.6 mM $MgSO_4$ (Invitrogen, Carlsbad, CA, USA), 5 ng of template DNA, 200 nM of the forward primer (27FB, 5′-AGRGTTYGATYMTGGCTCAG-3′) and the reverse primer (338RPL, 5′-GCWGCCWCCCGTAGGWGT-3′) (Fortunato et al. 2012). The PCR cycling parameters were 94°C for 2 min; 30 × 94°C for 15 s, 55°C for 30 s, 68°C for 1 min and a final elongation at 68°C for 7 min. Following the PCR, an aliquot was run on a 1% Agarose gel to verify the desired V1-V2 16S rRNA gene product (~ 300 nt in length) had been amplified. Samples were sequenced using Illumina MiSeq 2x300 bp paired-end reads.

V1-V2 16S rRNA gene amplicon quality control

Amplicon sequence reads were processed with USEARCH v9 (Edgar 2010) to trim low quality bases using a 10% read length window with a Q25 running-quality threshold and to merge paired-end sequences (≥ 50-nucleotide overlap, minimum sequence length of 200 nucleotides, and maximum 5% mismatches). A filtering step was performed to discard low-quality merged sequences with a maximum expected error >1. Primers were removed from the sequences with cutadapt (Martin 2011). The resulting total amplicon read count was 15,172,576. Libraries contained between 80,826 and 771,343 sequences (average = 199,639 ± 92,047, median = 176,733, n = 76; Table S3.2).

Amplicon sequence variant resolution

Merged amplicon sequences were resolved into amplicon sequence variants (ASVs) of 100% pairwise nucleotide identity with USEARCH v10.0.240 (Edgar 2010). Implementation of the unoise3 algorithm (Edgar 2016) infers exact ASVs from the sequencing data, instead of building operational taxonomic units (OTUs) from sequence similarity. Taxonomies were assigned to each ASV using the SILVA database (Pruesse et al., 2007; release 128, September 07 2016, https://www.arb-silva.de/documentation/release-128) via QIIME2-2018.2 q2-feature-classifier (Bokulich et al. 2018) with a default confidence level threshold of 0.7. We filtered the ASVs into the non-photoautotrophic bacterial component by excluding the amplicons

with taxonomies matching plastid, mitochondrial, or cyanobacterial sequences based on the SILVA assignment, resulting in 99,406 total bacterial ASVs (Table S3.2). The V1-V2 16S rRNA primer pair used was bacterial and plastid specific and did not allow for comparison of archaea (Wear et al. 2018).

Statistical analyses

All bacterial community ASV analyses were conducted using the "vegan" package (v2.4.4; https://cran.r-project.org/web/packages/vegan/) in R (v3.4.1) (Oksanen et al. 2017). Prior to performing a canonical correspondence analysis (CCA), the "step" function in vegan was used to automatically select constraints in the model using forward stepwise selection and Akaike's information criterion with 999 permutation tests at each step. Five geochemical parameters were found to be uncorrelated with the others (formate, acetate, nitrate, sulfate and dissolved inorganic carbon) and were applied using the "cca" function. To evaluate the significance of the canonical axes, a Monte Carlo test with 999 permutations was used. Statistical significance of the individual geochemical parameters was assessed using the marginal effects of the terms. For each sample, the Shannon diversity index was calculated to estimate community alpha diversity. Hierarchical clustering based on Bray-Curtis dissimilarity (Bray and Curtis 1957) of bacterial ASV relative abundances was calculated to compare beta diversity of community compositions between samples. Permutational

multivariate analysis of variance (PERMANOVA) was run using the "adonis" function on the Bray-Curtis distance matrices to quantitatively evaluate the effects on bacterial community compositions of interval depth within a push core, between replicates within a station and between stations. First, a PERMANOVA was run between all replicates within a station and between all replicates between different stations. A PERMANOVA was also run to compare the bacterial community composition of sediments between all of the depth intervals within a full length push core and compared to each station. The relative read proportion of bacterial ASVs were calculated by dividing the ASV count by the total reads in each sample. These relative read proportions were log10 transformed for better visualization. Differential abundances of ASVs between biological replicates within each station were identified based on a negative binomial distribution model using "DESeq2" package (v1.22.2; https://bioconductor.org/packages/release/bioc/html/DESeq2.html) (Love et al. 2014) and estimated effect size shrinkage to rank ASVs was performed using 'apeglm' package, an approximate posterior estimation for a generalized linear model (v1.4.2; https://bioconductor.org/packages/release/bioc/html/apeglm.html) (Zhu et al. 2018). All base plots used in the included figures were generated using the R package "ggplot2" (v2.2.1; https://ggplot2.tidyverse.org) (Wickham 2016).

Results

The different sampling stations provided the opportunity to compare coastal sediments from within a submarine canyon ecosystem and sediments offshore from a submarine fan, as well as to assess the influence of a previous organic matter perturbation more than a decade after the input. The four stations sampled in the Monterey Canyon are influenced by the hydrography and sedimentology of the canyon while the one station sampled from the submarine fan in the eastern North Pacific Ocean is influenced by more transitional surface ocean conditions typical between the coast and oligotrophic open ocean.

Geochemical parameters were measured at every depth interval in one push core at each station (Fig. 3.1) across two sedimentary ecosystems, a submarine canyon and the associated submarine fan. The submarine fan ecosystem represented by SF3562m exhibited conservative vertical profiles, the same concentration of Na^+, K^+, Mg^{2+}, Ca^{2+}, formate, acetate, Cl^-, Br^-, NO_3^-, and SO_4^{2-} from the top to the bottom of the core. The canyon stations exhibited more variability in their geochemical vertical profiles. SO_4^{2-} exhibited conservative vertical profiles at WF633m, WF1018m, and CY1833m (29.60 mM ± 0.67), while at CY1040m, SO_4^{2-} reached a minimum of 26.65 mM at 12-15 cm below seafloor (cmbsf) indicating the potential occurrence of sulfate reduction (Jørgensen 1982) with increasing sediment depth. NO_3^- decreased with increasing sediment depth at WF633m, CY1040m, and CY1833m, which has previously been shown to indicate potential nitrate reduction or denitrification occurring with increasing sediment depth (Sørensen 1978). The surface concentration at CY1833m (4.10 mM) was much lower than the other canyon stations (WF633m,

WF1018m, CY1040m: 11.83 mM ± 0.49). At WF1018m, NO_3^- exhibited a sharp decline to a minimum of 1.00 mM at 3-4 cmbsf, drastically increased to a maximum of 19.40 mM at 5-6 cmbsf and was similar to the surface concentration (11.50 mM) at the bottom interval of 12-15 cmbsf (10.10 mM). In contrast to NO_3^-, acetate concentration gradually increased with depth at all of the canyon stations, with a peak maximum at WF1018m at 4-5 cmbsf, directly below the NO_3^- minimum. At WF1018m, the surface concentration of acetate was more than double (35.20 mM) the concentration of other canyon locations (14.40 mM ± 2.36). Formate exhibited variable vertical profiles at all the canyon stations. At WF633m and CY1833m, formate alternated between increasing and decreasing in concentration with depth. At CY1040m, formate was drawn down to nearly 0 mM by 4-5 cmbsf and remained at this concentration down through the core. At WF1018m, formate concentration at the surface was the highest (36.00 mM) and was drawn down to a minimum of 1.80 mM at 3-4 cmbsf, increasing again to 15.20 mM ± 4.26 for the remainder of the core. DIC exhibited a conservative profile at WF1018m and gradually increased at CY1040m with a surface concentration of 2.66 mM reaching a similar concentration as WF1018m by 12-15 cmbsf (3.13 mM ± 0.09). Both WF633m and CY1833m exhibited slightly increased DIC with depth to 6-9 cmbsf and then decreasing to the bottom of the core. In summary, while each station exhibited unique geochemical profiles, WF1018m and CY1040m showed similar trends in geochemistry across the core profile, while SF3562m differed from all of the submarine canyon stations (Fig. 3.1).

Sedimentary bacterial communities are horizontally homogenous on a submeter scale

The technical and biological replicate sampling of deep sea sediments at five stations allows us to fill the knowledge gap about the homogeneity of bacterial communities within one location. The technical replicates consisted of the individual push cores at a single station, with triplicate push cores collected. Of these three push cores, a single depth interval near the surface was selected. Within each of the push cores at this depth interval, triplicate biological replicates were sampled. In total, nine samples were sequenced at each station to assess within core and between core variability. Overall, the bacterial communities are horizontally homogenous within a station, with PERMANOVA analyses identifying no statistical difference, indicating that the biological and technical replicates are not different from each other. PERMANOVA analyses between stations did find a statistical difference ($p<0.05$). While there are similar bacterial community compositions across the stations, there are also unique amplicon sequence variants (ASVs) at each station.

To more closely analyze the most abundant ASVs of the replicates at each station, the top 50 most abundant ASVs from each station's determined via hierarchical clustering were identified (Fig. 3.2). This resulted in 93 total ASVs examined for their replication variability, indicating strong overlap of the most abundant ASVs across

the five stations. When examining the top 50 most abundant ASVs at each station, SF3562m, the submarine fan station, was the most homogenous between replicates. The canyon ecosystem stations, while not statistically different, did exhibit some variability between replicates (Fig. 3.2). Differential abundance analyses between the three technical replicate push cores within a station identified the percent of ASVs that were significantly (adjusted $p < 0.1$) different in their relative abundances between each push core. At CY1833m, there was the most variability between push cores with 0.225%, 13.2% and 13.9% of ASVs exhibiting differential relative abundances out of the 2,206 shared ASVs considered. Station WF1018m was the next most variable between push cores with 0.75%, 4.8% and 13.2% of ASVs exhibiting differential relative abundances out of the 2,675 shared ASVs considered. The variability within sediments at WF633m and CY1040m were similar with 0.49%, 2.24% and 4.8% of ASVs exhibiting differential relative abundances out of the 3,134 shared ASVs considered at WF633m, and 0.356%, 2.33% and 3.63% of ASVs exhibiting differential relative abundances out of the 3,233 shared ASVs considered at CY1040m. In agreement with the analysis of the 50 most abundant ASVs, SF3562m exhibited the least variability in relative abundances with differences of 0.566%, 0.908% and 3.39% out of the 2,643 shared ASVs considered.

Sediment bacterial community fine scale vertical variability

Examination of the upper 20 cm of deep sea sediments, divided into 1- or 3-cm intervals from surface to the bottom of the core, provides a fine scale vertical profile. An analysis of the Shannon diversity index found high diversity throughout the sediments (Fig. 3.3A). The four Monterey Canyon stations exhibit similar levels of diversity from the surface down to 20 cmbsf in the sediments. Station SF3562m exhibits a decrease in Shannon diversity index with increasing depth into the sediments. PERMANOVA analysis showed no significant difference between the bacterial communities within the vertical profile of an individual push core, however a comparison of one push core from each station did reveal a significant difference (p<0.05) over all depth intervals between stations. This difference between stations agrees with our analyses of the replicate samples between stations. Within the sediments, many of the bacterial taxa classifications consist of multiple ASVs, indicating there are many unique V1-V2 16S rRNA gene amplicon sequences for the same bacteria. While each station consists of a statistically significant different bacterial community, there are more similarities in the most abundant ASVs found in the canyon ecosystem stations compared to the submarine fan sediments.

To more closely analyze the most abundant ASVs throughout the upper 20 cm of deep sea sediments and the overlying sweater, the top 50 most abundant ASVs from the clusters determined via hierarchical clustering were identified in the seawater, SF3562m sediment, and canyon station's sediment (Fig. 3.4). This resulted in 143 total ASVs examined for their fine scale vertical distribution within the sediments and the overlying seawater. As expected, the same bacterial taxa are found in the full

length push cores as the replicate dataset from the same stations. The most abundant sedimentary bacteria were the Deltaproteobacteria *Desulfobacteraceae* (8.75% of all sedimentary reads; average 8.9% ± 3.4 relative abundance) and *Desulfobulbaceae* (6.5% of all sedimentary reads; average 6.8% ± 3.0 relative abundance). There are four highly abundant *Desulfobacteraceae* ASVs found in the sediments at all stations, exhibiting an increase in relative abundance with increasing depth into the sediments (0 – 3 cmbsf: 5.7% ± 2.1; 3 – 12 cmbsf: 8.8% ± 2.9; 12 – 18 cmbsf: 12.1% ± 3.3 relative abundance). Of the 143 most abundant ASVs, 18 ASVs are Deltaproteobacteria Desulfobulbaceae genus *Desulfobulbus*, found in sediments at all stations exhibiting a decreasing trend in relative abundance with increasing depth into the sediments (0 – 3 cmbsf: 7.4% ± 2.9; 3 – 12 cmbsf: 7.3% ± 2.6; 12 – 18 cmbsf: 4.8% ± 3.7 relative abundance). Of these 18 Desulfobulbus ASVs, six ASVs are almost exclusively found at SF3562m, eight ASVs are almost entirely found at all of the Monterey Canyon stations, and four ASVs are found at all five stations. Interestingly, 5.0% of all sedimentary reads are unclassified bacteria indicating there remains many unknown bacteria in sediments, with an increase in relative abundance with increasing depth (0 – 3 cmbsf: 3.7% ± 0.5; 3 – 12 cmbsf: 4.8% ± 1.1; 12 – 18 cmbsf: 6.5% ± 1.8 relative abundance). Chloroflexi *Anaerolineaceae* also makes up 5.0% of all sedimentary reads, with four highly abundant ASVs found at all stations, increasing in relative abundance with increasing depth (0 – 3 cmbsf: 3.0% ± 1.1; 3 – 12 cmbsf: 4.6% ± 1.6; 12 – 18 cmbsf: 9.0% ± 2.2 relative abundance). Deltaproteobacteria NB1-j makes up 3.5% of all sedimentary reads (4.1% ± 1.1

relative abundance) with eight abundant ASVs. While all eight NB1-j ASVs are found at all stations, the relative abundances vary between the four canyon stations and SF3562m. In the canyon, NB1-j increase in relative abundance with increasing depth (0 – 3 cmbsf: 2.6% ± 1.0; 3 – 12 cmbsf: 3.5% ± 0.9; 12 – 18 cmbsf: 4.5% ± 1.7 relative abundance) while NB1-j decreases in relative abundance at SF3562m (0 – 3 cmbsf: 4.1% ± 0.6; 3 – 12 cmbsf: 2.0% ± 0.5; 12 – 18 cmbsf: 0.8% ± 0.6 relative abundance). Gammaproteobacteria JTB255-marine benthic group (MBG) makes up 3.3% of the sedimentary sequences (average 3.0% ± 1.8 relative abundance), with the five most abundant JTB255-MBG ASVs found at SF3652m. The relative abundance of JTB255-MBG decreases with increasing depth at SF3652m (0 – 3 cmbsf: 6.8% ± 0.8; 3 – 12 cmbsf: 2.3% ± 0.2; 12 – 18 cmbsf: 0.2% ± 0.2 relative abundance), as well as at the canyon stations though at much lower relative abundances (0 – 3 cmbsf: 3.2% ± 0.8; 3 – 12 cmbsf: 2.9% ± 0.9; 12 – 18 cmbsf: 1.4% ± 0.7 relative abundance). Bacteroidetes *Flavobacteriaceae* consist of 3.1% of sedimentary sequences (average 3.2% ± 2.2 relative abundance), with two mostly abundant ASVs at the canyon stations, one of which is also found at SF3562m. The relative abundance of *Flavobacteriaceae* decreases with increasing depth at the canyon stations (0 – 3 cmbsf: 7.0% ± 1.9; 3 – 12 cmbsf: 3.3% ± 0.9; 12 – 18 cmbsf: 1.3% ± 0.9 relative abundance), as well as at SF3562m at much lower relative abundances (0 – 3 cmbsf: 3.4% ± 0.2; 3 – 12 cmbsf: 0.7% ± 0.3; 12 – 18 cmbsf: 0.04% ± 0.05 relative abundance). Actinobacteria OM1 clade make up 2.6% of sedimentary reads (average 2.5% ± 1.2 relative abundance). There are two abundant OM1 clade ASVs

predominantly found at SF3562m. OM1 clade decreases in relative abundance with increasing depth at SF3562m (0 – 3 cmbsf: 4.1% ± 0.8; 3 – 12 cmbsf: 4.3% ± 1.6; 12 – 18 cmbsf: 0.7% ± 0.4 relative abundance), while maintaining similar relative abundances with depth at the canyon stations (0 – 3 cmbsf: 2.6% ± 1.7; 3 – 12 cmbsf: 2.1% ± 0.5; 12 – 18 cmbsf: 2.4% ± 1.0 relative abundance).

Next, we used canonical correspondence analysis (CCA) to identify the sediment geochemical conditions associated with community composition changes (ter Braak and Verdonschot 1995). For statistical analyses only, parameters for which there was data from every station were used. In addition, at SF3562m, SO_4^{2-} which is known to be at equilibrium with seawater in the surface sediments (Jørgensen et al. 2019) was below expected values, indicating there was a methodological issue between sampling and analysis that left us cautious about the actual values measured, therefore we excluded SF3562m sediments in the CCA so this station would not unnaturally skew the analysis. The CCA was therefore based on Monterey Canyon sediments only, and used formate, acetate, SO_4^{2-}, NO_3^-, and DIC, which were found to be independent of the other compounds, while Cl^-, Na^+, K^+, Mg^{2+}, Ca^{2+} were correlated (Fig. 3.3B). Of the uncorrelated parameters, DIC and NO_3^- were found to be statistically significant ($p<0.05$), influencing the bacterial community compositions throughout the upper 20 cm of deep sea sediments. The CCA ordination diagram (Fig. 3.3B) of the first two axes indicates that there are bacterial community composition distinctions by station (horizontal CCA1 axis, 21% of variation

explained) and distinctions by vertical profile within each push core (vertical CCA2 axis, 16% of variation explained).

Overall, sediment bacterial communities are more diverse than the communities of overlying seawater, and unlike in seawater, there are no dominate sediment ASVs (Fig. 3.4). The surface sediments at each station contain very few seawater ASVs.

Building on previous work in the water column (Chapter 2) at these stations in the Monterey Canyon, the bacterial community of the upper 20 cm of deep sea sediments was compared to the community of the overlying bottom seawater. Rarefaction curves generated from the sequencing datasets did reach a plateau, indicating that the full diversity of the samples was revealed by the amount of sequencing carried out (not shown). The seawater and sediment communities were found to be distinctly different, with hierarchical clustering of samples based on Bray-Curtis dissimilarities of bacterial community ASVs (Fig. 3.4). The seawater sample communities consist of marked dominants, such as Deltaproteobacteria SAR324 and Gammaproteobacteria *Oceanospirillales*, highly influencing the shaping of these communities. Within the submarine canyon ecosystem, the seawater samples also contain sediment ASVs at very low abundances, whereas very few sediment ASVs are found in the overlying seawater at the submarine fan station (Fig. 3.4).

Discussion

The submarine canyon's quick descent of seafloor depth relatively close to shore positions deep sea depths within a coastal environment. Submarine canyons are considered highly heterogeneous ecosystems displaying strong gradients in the frequency of physical disturbance events (e.g. sediment slumps, dense water cascading events, tidal forcing and storm-induced gravity flows) and resource availability (De Leo et al. 2014; Pasqual et al. 2011; Tesi et al. 2008). These factors are thought to have a strong influence on prokaryotic activities in sediments of these systems (Šimek et al. 2005). Our study additionally compared sites known to have had massive episodic input of organic matter, in the form of a deposited dead whale, with a single large whale carcass potentially providing the equivalent of 2000 years of accumulated background particulate organic carbon flux to the deep seafloor (Smith and Baco 2003). In 2004, a dead whale carcass was deposited in the Monterey Canyon at 1018 m seafloor depth (Lundsten et al. 2010), which we sampled 131 months later. Hence, in addition to looking at sub-meter heterogeneity we could compare sites within the same canyon that presumably had very different communities within the last 11 years, as well as comparing to the submarine fan ecosystem site.

Previous studies on diversity of bacteria in sediment environments have typically either focused on the surface sediments (i.e. 0 to 2 or 5 cmbsf) (e.g. Bienhold et al., 2016; Dyksma et al., 2016; Goffredi & Orphan, 2010; Gong et al., 2015; Hewson et al., 2007; Probandt et al., 2017) and/or deeper subsurface sediments (>1 m below seafloor) (e.g. Bienhold et al. 2016; Durbin and Teske 2011; Walsh et al. 2016; Zinke

et al. 2017). Few have assessed a fine scale vertical profile in the upper 20 cmbsf at 1- to 3- cm intervals (e.g. Peoples et al. 2019).

The replicated sampling of the sediments at each station allowed for the assessment of the horizontal homogeneity at each location. Station SF3562m was found to be the most homogenous between replicates, due to its location towards the open ocean instead of the canyon ecosystem. These sediments are more compact than sediments in Monterey Canyon, and visually the seafloor is more uniform. At the Monterey Canyon stations, the surface sediments constantly interact with the overlying seawater, with sediments being resuspended and mixed. This mixing potentially allows for more variability as bacterial communities from different depth intervals within the sediment may be introduced to other areas at the same station. Overall, the bacterial communities within a station are not different between technical replicates. Knowing that the sediments are less heterogenous than we had expected supports the potential to conduct robust *in situ* incubation experiments with ecologically thoughtful experimental design within a station. Replicates from an *in situ* incubation experiment can be considered true replicates. This replication is supported at different seafloor depths at all four stations within Monterey Canyon as well as at the one submarine fan station (Fig. 3.2).

One of the unique opportunities of this study was to assess the influence of a previous organic matter perturbation, deposition of a whale carcass, and compare this to sediments ~100 m away. Previous studies have identified that the influence of this sudden deposition of organic matter spreads away from the source as a dispersing

front of whale-associated nutrients (Goffredi and Orphan 2010). We sampled sediments at this previous whale fall site 11 years (131 months) after it was initially deposited. Comparison of the bacterial community at this station (WF1018m) to a reference canyon station ~100 m away (CY1040m) found that these bacterial communities are more similar to each other than to any of the other stations included in this study (Fig. 3.2, 3.3B, 3.4). In a previous study that assessed the bacterial diversity in sediments underlying whale falls at 1820 and 2893 m in Monterey Canyon, they found less diversity compared to reference sediments 10 - 20 m away sampled 7 months post deposition, yet by 70 months post deposition the diversity of the reference sediments had also decreased (Goffredi and Orphan 2010). The similarity in diversity between WF1018m and CY1040m in this study suggests that the organic matter perturbation to the sediments that was initiated by the deposition of the whale carcass has spread to at least 100 m away and is now influencing these sediments. Alternatively, enough time has passed since the initial organic matter perturbation and this influence has dissipated from the underlying sediments, with the community at this previous whale fall now resembling a previously unperturbed site. To verify which scenario is more likely to be influencing today's bacterial communities, it is necessary to sample multiple distances from the whale fall at the same seafloor depth ~1000 m, such as 10 m, 500 m and 1000 m, to best capture the edge of the dispersing front.

While oxygen was not directly measured in the sediments sampled here, the changing concentrations of measured SO_4^{2-}, NO_3^-, and acetate and the high relative

abundance of anaerobic bacterial groups suggest the anaerobic redox reactions that are occurring throughout the canyon ecosystem. The most abundant sedimentary bacteria were the Deltaproteobacteria Desulfobacteraceae and Desulfobulbaceae genus *Desulfobulbus*, both of which are known to be sulfate reducing bacteria that respire anaerobically and incompletely oxidize organic compounds to acetate (Kuever 2014; Kuever et al. 2015). While there is a decrease in SO_4^{2-} at CY1040m, geochemically supporting the presence of sulfate reducers, SO_4^{2-} remains unchanged with increasing sediment depth at the other canyon stations. The unchanging SO_4^{2-} concentrations may occur even while sulfate reduction reactions are happening as a consequence of the bioturbation at these stations (Chen et al. 2017). Macrofauna moving vertically through the sediments may be introducing overlying seawater that is higher in SO_4^{2-} concentrations, replenishing SO_4^{2-} at the same rate it is being microbially reduced. While SO_4^{2-} is not decreasing, nitrate is decreasing with depth, indicating the occurrence of nitrate reduction or denitrification though this is not supported by the identified abundant bacterial communities. We are unable to confirm if the NO_3^- decrease is due to nitrate reduction or denitrification because we did not measure the respective end products of either reaction, NH_3 or N_2. One possibility is that nitrate reduction or denitrification is being carried out by very low abundance bacterial groups that are endemic to specific locations. It is also possible that the sulfate reducing bacteria we identified are using NO_3^- as an electron acceptor. This has been documented in other sulfate reducing bacteria such as a few *Desulfovibrio* species (Keith and Herbert 1983; McCready, Gould, and Cook 1983; Mitchell, Jones,

and Cole 1986; Seitz and Cypionka 1986), *Desulfobulbus propionicus* (Widdel and Pfennig 1982), and *Desulfobacterium catecholicum* (Moura et al. 1997; Szewzyk and Pfennig 1987), and noted that nitrate may be a preferred electron acceptor over sulfate (Seitz and Cypionka 1986). A likely scenario is that nitrate is being utilized as a nutrient source by methanotrophic archaea (ANME) partnered with the sulfate reducing bacteria (Green-Saxena et al. 2014) or nitrate reduction is being carried out by other archaea present (Martínez-Espinosa et al. 2001). As the V1-V2 16S rRNA gene primer set used for this study does not include archaea, we are unable to currently determine which archaea were present alongside the identified bacteria.

While bacterial groups known to be ubiquitous throughout deep sea (>1000 m) surface sediments are present at SF3562m, their relative abundances are much lower than previous global studies found (Bienhold et al. 2016; Mußmann et al. 2017). Gammaproteobacteria JTB255-MBG was found to be a cosmopolitan surface sediment bacterial group, identified in all 27 global deep sea surface sediments assessed (Bienhold et al. 2016) and occurring in high relative sequence abundances in multiple benthic habitats such as coastal, deep sea, organic-rich and organic-poor sediments (Mußmann et al. 2017). A study of submarine canyons in the Mediterranean Sea also found JTB255-MBG as one of the most abundant bacterial groups (Corinaldesi et al. 2019). In our study, the very low relative abundances to complete absence in canyon station sediments of JTB255-MBG indicates that while these globally cosmopolitan bacterial groups can still be found, this ecosystem

preferentially selects for bacterial groups that thrive under anaerobic conditions instead.

The bacterial diversity between pelagic communities and surface benthic communities has been found to differ greatly globally, with surface sediments more rich than overlying water (Probandt et al. 2017; Walsh et al. 2016; Zinger et al. 2011), in which our findings agree. The similar bacterial diversity identified within the canyon ecosystem stations is due to the similar influences on these communities. The Monterey Canyon stations are coastal and impacted by the submarine canyon. In order, the stations are located 21.67 km (WF633m), 29.77 km (WF1018m and CY1040m), 32.36 km (CY1833m) and 170 km (SF3562m) from shore. These factors combined lead the deep sea sediments within this ecosystem to receive more nutrients and organic matter than deep sea sediments underlying oligotrophic water (D'hondt et al. 2015). The sediments within Monterey Canyon are very fluffy, easily interacting with the bottom currents of the overlying seawater and resuspending, leading to greater mixing of these sediments with seawater. The constant resuspension of sediment particles in the seawater causes sediment bacterial ASVs to be found in the seawater bacterial communities (Fig. 3.4). In another study at several sites in the Pacific Ocean, the most abundant sediment bacterial sequences were also present at very low relative abundances in the overlying seawater, suggesting that marine sedimentary bacteria are dispersed via seawater with advective transport through the water column providing the simplest explanation of microbial input to the sediments (Walsh et al. 2016).

At all stations sampled herein, the surface sediments also contain seawater bacterial ASVs, as this is the interface between the distinct habitats of the seawater and subseafloor. There is greater bioturbation at the canyon stations, with macrofauna visually identified while sampling these sediments. This bioturbation appears to result in at least some transport of sediments vertically, potentially mixing sediment and water column bacterial communities. A similar disturbance was previously identified in the near-surface sediments of Aarhus Bay, Denmark, where it was hypothesized that macrofauna inhabiting the sediments have a 'homogenizing' effect causing similar vertical profiles of bacterial abundances (Chen et al. 2017). The sediments at SF3562m were less "fluffy" such that there was minimal resuspension of surface sediments in the overlying seawater. There was also no noticeable bioturbation when sampling these sediments, suggesting that vertical stratification is more defined in these sediments, potentially leading to the observed lower bacterial diversity with increasing sediment depth.

Different bacterial communities exist in the seawater and sediments because these different substrates require varying lifestyles to survive, leading each of these habitats to be poised to contribute to biogeochemical cycles differently. Within the sediments, some of the bacterial taxa classifications consist of many ASVs, meaning many unique sequences are identified as the same bacteria. This suggests that in sediments there are potentially multiple ecological niches for these bacteria to occupy. The sediment grains create barriers for the porewater so more variable conditions exist

across small spatial scales, leading the sediments to have greater bacterial diversity to inhabit these spatially close but distinct ecological niches.

Conclusions

Replicated sampling of sediments <1 m and >10 km apart provided a characterization of the heterogeneity of the bacterial community composition at different spatial scales. While the bacterial communities of sediments >10 km apart are significantly different, bacterial communities of sediments <1 m apart are fairly homogenous and not significantly different, at least in the environments we studied. The homogenous nature of bacterial community composition at small scales supports the potential to conduct robust *in situ* incubation experiments with ecologically thoughtful experimental design within a station. Between stations sampled within Monterey Canyon, DIC and NO_3^- significantly influence the bacterial community composition. While the surface sediments are at the interface between seawater and the subseafloor, the bacterial communities within the sediments are distinct from the overlying seawater. Future sediment studies can benefit from the replicated sampling of our study to inform their sampling strategies.

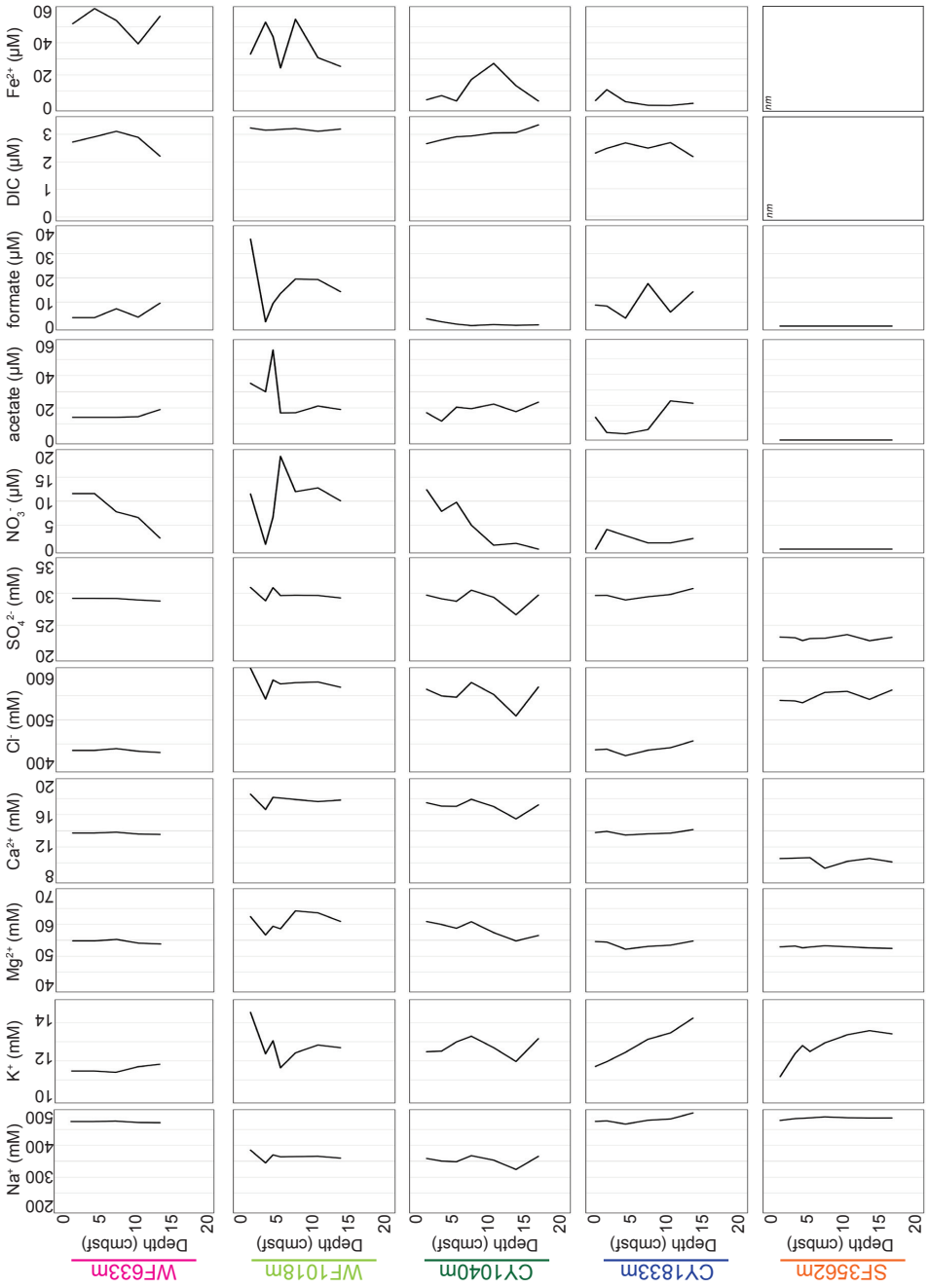

Figure 3.1

Distributions of Na^+, K^+, Mg^{2+}, Ca^{2+}, SO_4^{2-}, NO_3^-, acetate, formate, DIC and Fe^{2+} concentrations with depth below the seafloor at WF633m, WF1018m, CY1040m, CY1833m, and SF3562m. Based on the below expected values of SO_4^{2-} at SF3562m, the actual values of all geochemical components measured at SF3562m were not considered for analysis, only the vertical profile trends.

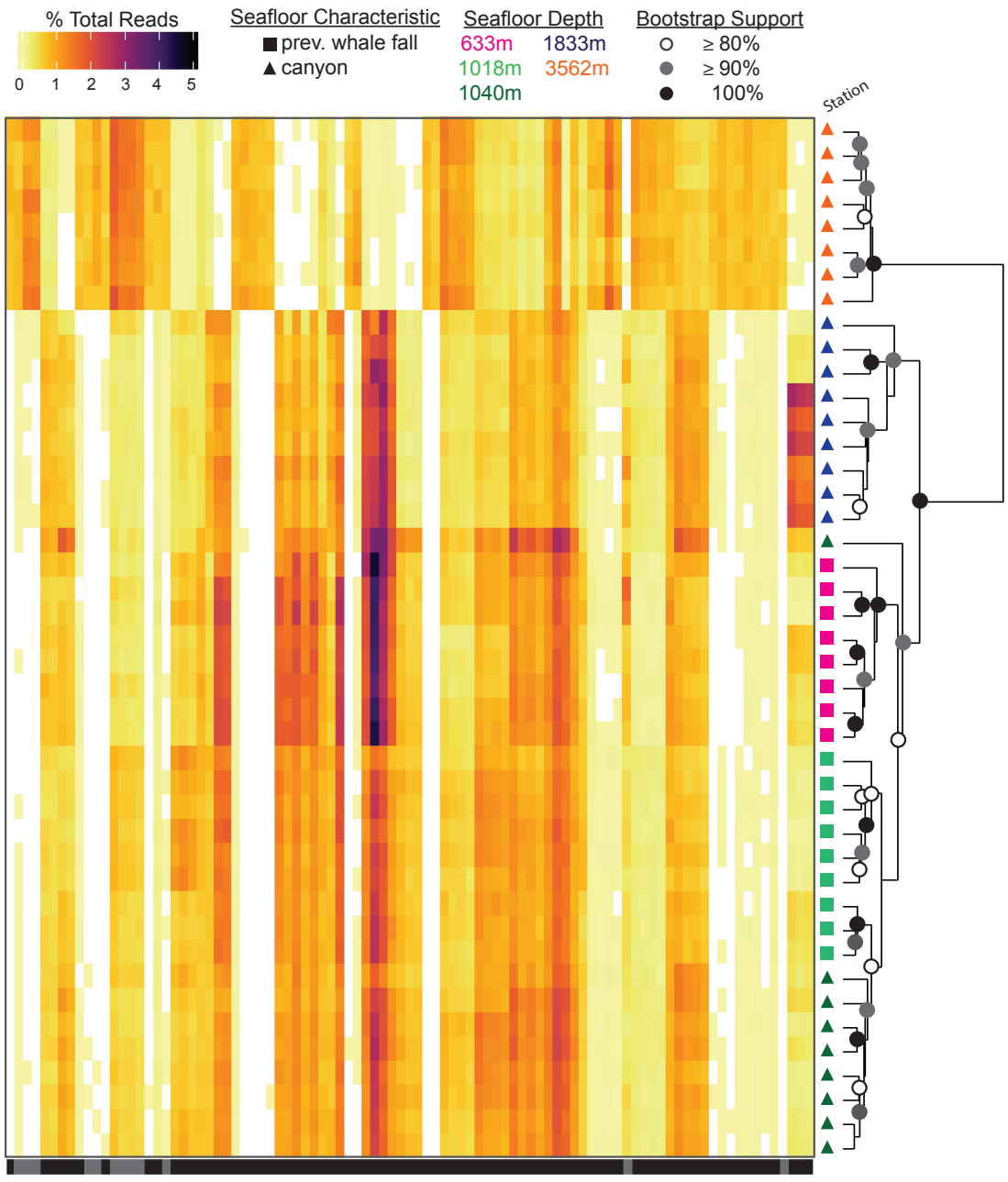

Figure 3.2

Percent relative abundance of the most abundant 100% amplicon sequence variants (ASVs) from replicate sediment push cores. Heat map columns represent the most abundant ASVs ordered by phylum (as indicated by horizontal black and gray bars at bottom). Row represents individual samples with hierarchical clustering of samples based on Bray-Curtis dissimilarities of bacterial community ASVs. There are clear

sample clusters by station (color): 3,562 m (orange), 1,833 m (blue), 1,040 m (dark green), 1,018 m (light green), and 633 m (pink). Shapes indicate the seafloor characteristic of each sample. At each station, triplicate push cores were sampled (technical replicates). From each push core, one depth interval was selected. Triplicate biological replicates were sequenced from this depth. Within a station the bacterial community composition was fairly homogenous across triplicate push cores (<1 m apart). The bacterial communities were more heterogeneous between different stations (>10 km apart). The ASV composition was most similar among stations located within the canyon ecosystem, while the submarine fan community consisted of other bacteria. Bacterial Phyla ordered from left to right: Acidobacteria, Actinobacteria, Bacteroidetes, Chloroflexi, Gemmatimonadetes, Ignavibacteriae, Nitrospinae, Betaproteobacteria, Deltaproteobacteria, Epsilonproteobacteria, Gammaproteobacteria, SBR1093, and Verrucomicrobia.

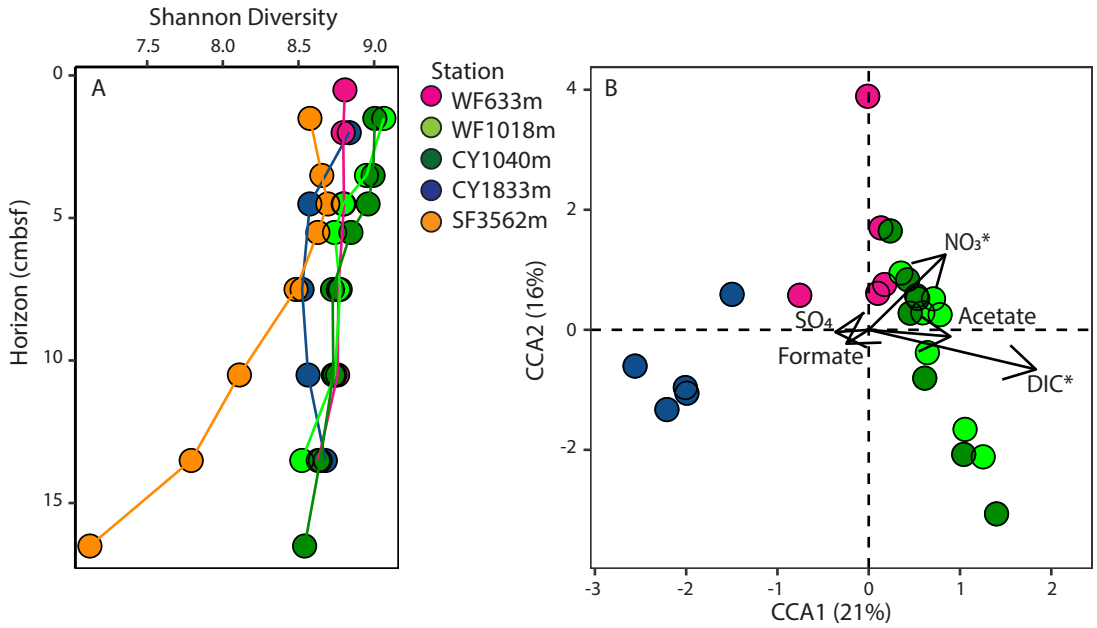

Figure 3.3

Shannon diversity index through full length sediment push cores and canonical correspondence analysis (CCA) of the geochemical data corresponding to the bacterial ASV communities of the full length push cores. A. Down core depth profile of bacterial community Shannon diversity index at all five stations. Shannon diversity index was similar at the surface depth interval across all stations. Bacterial community composition diversity is represented as a circle for each depth interval sampled, with color indicating the sample. For the stations within the canyon ecosystem, the diversity was relative constant through push core (upper 20 cm of the sediments). At the submarine fan station, Shannon diversity index decreased down through the core. B. CCA ordination diagram of the first two axes, with percentage of variation in the bacterial community composition explained by each axis indicated in the parentheses after the axis label. The constrained sets of environmental variables analyzed are indicated as vectors: formate, acetate, SO_4^{2-}, NO_3^- and dissolved inorganic carbon (DIC). The bacterial community composition for each sediment depth interval is represented as circles; the colors indicate the station the sediment was sampled from. The samples along the vertical axis correspond to the interval within the push core, with surface sediments near the top of the plot and deeper sediments near the bottom. The statistical significance of nitrate and DIC ($p < 0.05$) are indicated with an asterisk next to the corresponding vectors.

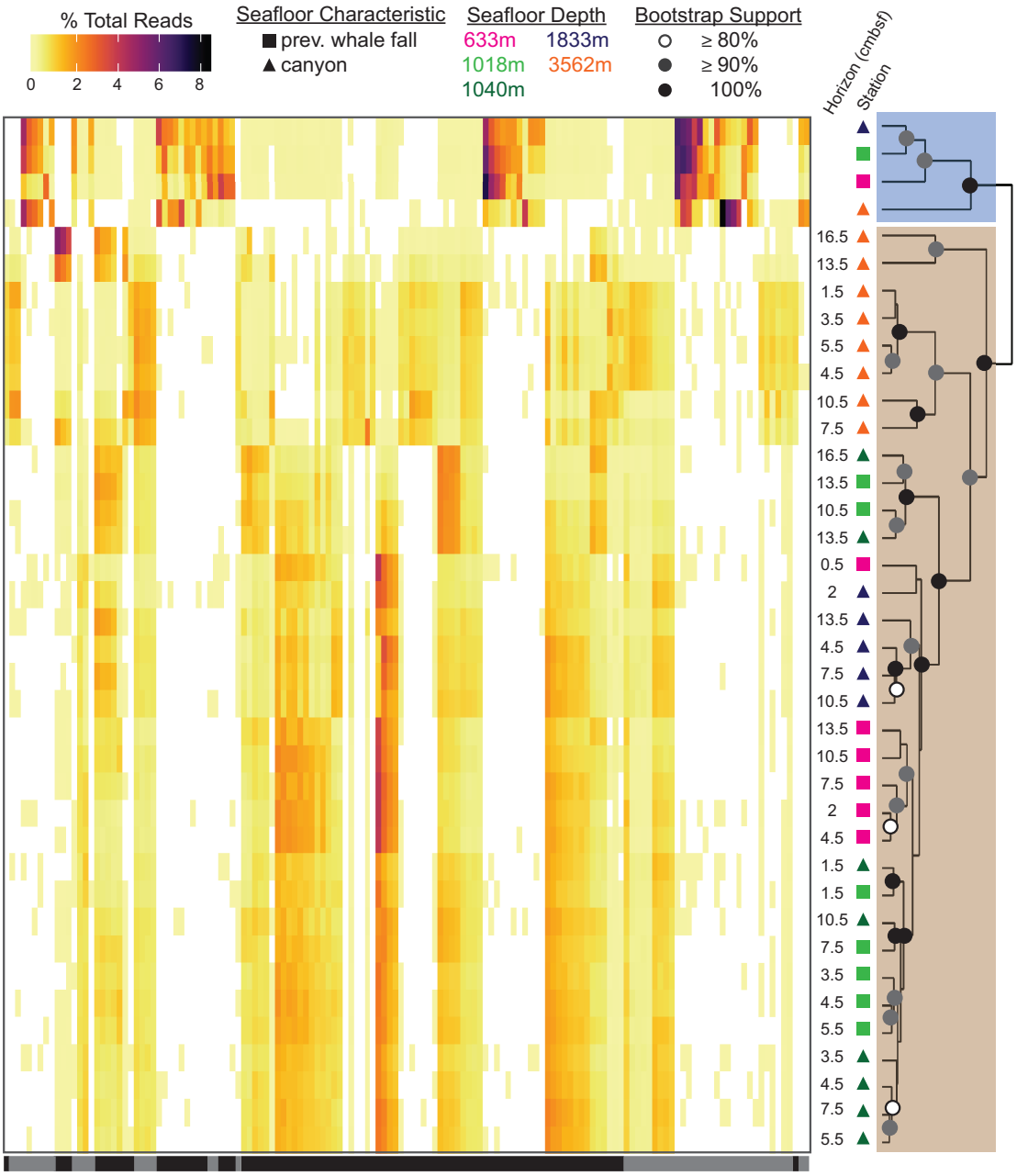

Figure 3.4

Percent relative abundance of the most abundant 100% amplicon sequence variants (ASVs) from full length sediment push cores and overlying seawater. Heat map columns represent the most abundant ASVs ordered by phylum (as indicated by horizontal black and gray bars at bottom). Row represents individual samples with hierarchical clustering of samples based on Bray-Curtis dissimilarities of bacterial community ASVs. There are clear sample clusters by substrate: seawater (blue) and sediment (brown). Colored shapes indicate the station (color) and seafloor

characteristic (shape) of each sample. The midpoint of each sampled push core depth interval is included next to the corresponding sample. Distinct dominant ASVs were found in the overlying seawater bacterial communities compared to the sediment communities. Fine scale vertical variability of bacterial communities within push cores from surface to ~20 cm below. Bacterial phyla ordered from left to right: Acidobacteria, Actinobacteria, Atribacteria, Bacteroidetes, Chloroflexi, Ignavibacteriae, Marinimicrobia, Nitrospinae, Alphaproteobacteria, Betaproteobacteria, Deltaproteobacteria, Gammaproteobacteria, SBR1093, and Verrucomicrobia.

Chapter 4: *In situ* exploration of bacterial responses to phytodetritus amendments

Abstract

Deep sea bacteria degrade surface ocean derived particulate organic matter (POM). We developed and deployed an *in situ* incubator to examine changes in microbial community composition in response to phytodetritus additions. Initial *in situ* incubation experiments were carried out at seafloor depths of 1,040 m and 3,562 m in the eastern North Pacific Ocean. Bathypelagic water and the resident bacterial community at these depths was incubated in unamended control bags or treatment bags amended with phytodetritus derived from cultures of diatom *Chaetoceros* or prasinophyte *Micromonas*. Bacterial cell abundances significantly increased ($p < 0.05$) over the length of both control experiments after 60 days (1,040 m) and 240 days (3,562 m) compared to initial time points (1 day: 1,040 m; 0 day: 3,562 m). V1-V2 16S rRNA gene amplicon sequence analysis of 100% nucleotide identity amplicon sequence variants (ASVs) of 1,040 m control incubations revealed an increase in bacterial ASVs that appeared to be connected to the 60 day confinement period or other related community changes. ASV analyses of the phytodetritus amended treatments at both 1,040 m and 3,562 m led to two time point-associated ASV-based clusters for each experiment, one cluster with Niskin controls and <1 week incubations and the second cluster consisting of multi-month incubations. The relative abundance of Gammaproteobacteria Oceanospirillales increased in the 4 day

incubations, and continued to increase in the multi-month incubations. Bacterial groups known to degrade algal polysaccharides in the surface ocean, such as Bacteroidetes Flavobacteria and Planctomycetes, increased in relative abundance in the multi-month incubations. These deep sea *in situ* incubation experiments further our understanding of the bacteria actively responding to phytodetritus at the seafloor and first insights into the timescales on which they respond to fresh inputs of phytodetritus.

Introduction

Carbon remineralization and sequestration in the deep sea remain major unknown components in most carbon cycle models. Dissolved organic carbon flux supports ~ 10% of the respiration in the mesopelagic zone (Arístegui et al., 2002), with the bulk (~ 90%) of the respiration being supported by sinking particulate organic carbon (POC). Only a portion of the surface produced organic carbon is exported to the deep sea via mineral ballasting, aggregates, fecal pellets, eddy-driven subduction, and large zooplankton sinking or vertical migration (Alldredge et al., 1993; Armstrong et al., 2002; Katija et al., 2017; Lebrato et al., 2013; Omand et al., 2015; Robison et al., 2005; Wilson et al., 2013). Once on the seafloor, phytodetritus and fecal pellets become a food source for the organisms living in the surface sediments and the overlying seawater. Sinking POC can exhibit seasonal, interannual and episodic flux

variations, with strong connectivity to surface ocean conditions (Smith et al., 2013). The abyssal community appears to be sustained by episodic pulses of food from surface production, based on research at Station M, a long term study site in the Northeast Pacific Ocean (4000 m seafloor depth). The recalcitrant organic matter that is not readily consumed by the benthic community is sequestered into the sediments and is thought to be increasingly utilized by the benthic fauna during periods of low food supply (Smith et al., 2013).

Small particles (11- 64 μm) contribute significantly to particle flux in oligotrophic regions (Durkin et al., 2015). At the Bermuda Atlantic Time Series (BATS), the flux of small particles increases with depth which may contribute significantly to carbon flux (39 ± 20% of modeled total carbon flux) through aggregation and disaggregation, physical mixing and direct gravitational settling (Durkin et al., 2015). Denaturing gradient gel electrophoresis (DGGE) fingerprint analysis showed that when surface production at BATS is dominated by small size cells, small eukaryotes and cyanobacteria contribute to sinking particle flux via packaging as aggregates and fecal pellets (Amacher et al., 2013). During periods of high POC influxes, the magnitude of carbon flows within the deep sea microbial loop appear to decline (Dunlop et al. 2016). This same study found that the benthic community primarily relies on the more stable food source of semi-labile detritus during periods of low POC flux.

Multiple incubation experiments of deep sea samples have been carried out shipboard, providing a rich literature resource. An early shipboard study (Boetius and Lochte 1996) of deep sea (1000 m seafloor depth) Arctic sediments tested the hydrolytic potentials and growth of bacteria when enriched for over 63 days with a variety of organic compounds. The enrichment with starch, lipid and cellulose did not cause detectable bacterial growth. The chitin and glucose enrichments resulted in significant biomass production after a lag phase of up to 10 days.

Here, we performed a series of dep sea in situ incubations to identify the deep sea bacterial taxa that are poised to degrade organic matter. We designed a deep sea *in situ* incubation sampler, deployable via remotely operated vehicle (ROV), to perform experiments at the sediment-water interface at 1040 m and 3562 m seafloor depths in the eastern North Pacific Ocean. These samplers experimentally simulate arrival of phytodetritus in the deep sea in a confined setting to further our understanding of which deep sea bacteria actively consume carbon and the timescale of responses to fresh inputs of organic material.

Materials and Methods

Phytodetritus preparation

Algal cultures were grown to be used as the phytodetritus substrate for each experiment. For the coastal experiment, cultures of the diatom *Chaetoceros mulleri* Lemmermann (CCMP1316) were grown at 125 μE m^{-2} s^{-1} PAR in L1 medium in a defined artificial sea water (ASW) base. Culture growth was measured via fluorometery and by counting the cells using a Sedgewick Rafter under an epifluorescence microscope. For the more offshore experiment, the prasinophyte *Micromonas commoda* (RCC299) was grown at 125 μE m^{-2} s^{-1} PAR in L1 medium in ASW. Culture growth was measured using an Accuri (BD, San Jose, CA, USA) flow cytometer. For both cultures, cells were harvested in their exponential phase (6 x 10^5 and 7 x 10^6 cells ml^{-1} for CCMP1316 and RCC299, respectively) by centrifugation at 10,000 x g for 30 minutes at 4°C and the supernatant removed and discarded. The remaining cell pellets were frozen at -80°C until use. To prepare the phytodetritus solution for a 0.35 μM carbon addition to each sample, cells were resuspended in sterile ASW, vortexed and sonicated.

Incubator and experimental design

Deep water *in situ* incubation samplers were designed to perform experiments on the seafloor near the sediment-water interface. Each sampler consists of a stand with a base that rests on the seafloor and a post that holds up to six sample bags. The sample bags were made of fluoroethyl polymer (FEP) film and were gas permeable under

atmospheric pressure (OriGen Biomedical, Austin, TX, USA). Either 1- or 2- L bags were used. A manifold is attached at the top of the stand with Tygon tubing that connects to each sample bag (Fig. 4.1A). The sample bags were either empty or prefilled with the appropriate carbon substrate solution (more details below). To fill them with *in situ* seawater, the manifold was connected to a submersible pump (Sea-Bird Scientific, Bellevue, WA, USA) attached to remotely operated vehicle (ROV) *Doc Ricketts* and the local water was pumped into the bags (fill volumes were targeted at 1 L at 1,040 m and 2 L at 3,562 m). After filling, the pump was turned off and the interface removed from the stand. The stand was then placed onto the seafloor and remained there for the designated time period. One stand was used for each of the experimental time points.

Based on a study by Peltzer & Hayward (1996) conducted in the North Pacific subtropical gyre, the expected natural contribution of labile carbon at our study sites was 0.1% (0.035 μM) of the total organic carbon (35 μM). For the experiments, we targeted a 1% labile carbon (0.35 μM) addition, an order of magnitude above the expected natural contribution, which in order to ensure that a detectable response signal was acquired for downstream analysis. At the 1040 m location, the 1-liter sample bags (OriGen Biomedical, Austin, TX, USA) were preloaded with 0.35 μg phytodetritus and at the 3,562 m location, the 2-liter sample bags were preloaded with 0.7 μg phytodetritus in a sterile laminar flow hood before boarding the ship to target this 0.35 μM addition.

Paired with each organic matter (OM) incubation experiment, incubation controls were conducted to identify bag effects that were independent of OM addition. This consisted of an incubation sampler with three bags attached, no OM addition, filled with deep water at the seafloor and remaining for the designated time point. Niskin bottles mounted on the ROV were also used to sample the same local water as had been pumped into the experimental bags. This Niskin water was used as a control for seawater that had not been introduced to the experimental sample bags.

Oceanographic sampling

Four deep sea *in situ* incubation experiments were carried out in the eastern North Pacific Ocean onboard the R/V *Western Flyer*. Two experiments occurred at 1,040 m seafloor depth 29.77 km from shore in Monterey Bay while the other two occurred at 3,562 m seafloor depth located 170 km from shore. At 1,040 m, the time course of OM incubations was 0, 2, 4, and 120 days and the time course of control incubations was 1 and 60 days (Fig. 4.1B). At 3,562 m, the time course of OM incubations was 0, 4, 240, and 365 days and the time course of control incubations was 0, 5, and 240 days (Fig. 4.1B). Every incubation time point and Niskin control was carried out in triplicate.

The total volume of collected seawater in each incubation bag was measured shipboard after retrieval and ranged from 50 – 860 ml (1 L bags) and 1558 - 2868 ml

(2 L bags). While a targeted fill volume was made for each incubation, the bags did not fill evenly, leading to variability in volumes within and between timepoints. Bags with less than 440 ml were not included in further analyses after a preliminary assessment. From the 1 L bags, of the total volume collected, 100 ml was filtered onto a 0.2 μm Supor filter (Pall Gelman, East Hills, NY, USA) for total DNA. Filters were frozen and stored at -80°C. Flow cytometry samples (3 ml) were preserved in glutaraldehyde (EM grade, 0.25% final concentration, Electron Microscopy Services, Hatfield, PA, USA) at room temperature in the dark for 20 min, flash frozen in liquid nitrogen and stored at -80°C (Marie et al. 2001). The remaining volume of water was filtered onto a 0.2 μm Supor filter (Pall Gelman, East Hills, NY, USA) for RNA. Filters were frozen and stored at -80°C.

From the 2 L bags, of the total volume collected, 500 ml was filtered onto a 0.2 μm Supor filter (Pall Gelman, East Hills, NY, USA) for total DNA. Filters were frozen and stored at -80°C. Flow cytometry samples were preserved in 3 mL volumes with glutaraldehyde (EM grade, 0.25% final concentration, Electron Microscopy Services, Hatfield, PA, USA) at room temperature in the dark for 20 minutes (during which they were aliquoted into one ml volumes) and flash frozen in liquid nitrogen. Corresponding nutrient samples (~25 ml) were taken as previously described (Pennington and Chavez 2000) from each bag. The remaining volume of seawater was filtered onto a 0.2 μm Supor filter (Pall Gelman, East Hills, NY, USA) for additional DNA or RNA that has yet to be analyzed. Filters were flash frozen in

liquid nitrogen and stored at -80°C. All volumes sampled were recorded and added at the end to calculate the total volume of water for each sample.

Flow cytometry

Bacterial cell counts were measured by flow cytometry using a BD Influx flow cytometer (BD Biosciences, San Jose, CA, USA). After thawing, preserved seawater samples were stained with SYBR Green I (0.5X final concentration; Molecular Probes, Inc., Eugene, OR, USA) for 15 min at room temperature in the dark (Marie et al. 2001). Two types of fluorescent polystyrene beads, 0.75 μm yellow-green and 0.5 μm green (Polysciences, Inc., Warrington, PA, USA), were added to the stained sample for reference. Samples were run at 25 μl min^{-1}, as measured with an inline flow meter (SENSIRION SLG-1430), using a 200 mW 488 nm laser to interrogate cells. Each sample was pre-run 2 min, then bacterial populations were resolved by green fluorescence (520/35nm band pass, trigger) and Forward Angle Light Scatter (FALS). Events were collected for 2 min, and the volume analyzed was confirmed by weight measurements. Flow cytometry data were analyzed in WinList 3D 8.0 (Verity Software House, Topsham, ME, USA).

DNA extraction, PCR and amplicon sequencing

DNA was extracted from filters using a modification of the QIAGEN DNeasy Plant kit (Qiagen, Valencia, CA, USA), including addition of a bead beating step (Demir-Hilton et al. 2011), and quantified with the QuBit dsDNA high-sensitivity assay (Invitrogen, Carlsbad, CA, USA). Prior to PCR, templates were diluted to 1 ng μl^{-1} with TE pH 8 (Thermo Fisher Scientific, Waltham, MA, USA). Polymerase chain reactions (50 µl) were set up as previously described (Hamady et al. 2008) with 5 µl of 10x buffer, 1 U of HiFi-Taq, 1.6 mM $MgSO_4$ (Invitrogen, Carlsbad, CA, USA), 5 ng of template DNA, 200 nM each of the forward primer (27FB, 5′-AGRGTTYGATYMTGGCTCAG-3′) and the reverse primer (338RPL, 5′-GCWGCCWCCCGTAGGWGT-3′) (Fortunato et al. 2012). The PCR cycling parameters were 94°C for 2 min; 30 × 94°C for 15 s, 55°C for 30 s, 68°C for 1 min and a final elongation at 68°C for 7 min. Following the PCR, an aliquot was run on a 1% Agarose gel to verify the desired V1-V2 16S rRNA gene product (~ 300 nt in length) had been amplified. Samples were amplicon sequenced using Illumina MiSeq 2x300 bp paired-end reads.

V1-V2 16S rRNA gene amplicon quality control

Amplicon sequence reads were processed with USEARCH v9 (Edgar 2010) for quality control and to merge paired-end reads. Low quality bases were trimmed from

the sequences using a 10% read length window with a Q25 running-quality threshold. Paired-end sequences were merged with a ≥ 50-nucleotide overlap, minimum sequence length of 200 nucleotides, and maximum 5% mismatches. A filtering step was performed to discard low-quality merged sequences with a maximum expected error >1. Primers were removed from the sequences with cutadapt (Martin 2011). For each sample, between 132,127 and 317,549 amplicons were generated (average = 208,520 ± 56,916, median = 206,169, n = 30).

Amplicon sequence variant resolution

Merged amplicon sequences were resolved into amplicon sequence variants (ASVs) of 100% pairwise nucleotide identity with USEARCH v10.0.240 (Edgar 2010). The unoise3 algorithm (Edgar 2016) infers exact ASVs from the sequencing data, instead of building operational taxonomic units from sequence similarity. Taxonomies were assigned to each ASV using the SILVA database (Pruesse et al. 2007) (release 128, September 07 2016, https://www.arb-silva.de/documentation/release-128) via QIIME2-2018.2 q2-feature-classifier (Bokulich et al. 2018). We filtered the ASVs into the non-phototrophic bacterial component by excluding the amplicons with taxonomies matching plastid, mitochondrial, or cyanobacterial sequences based on the SILVA assignment, resulting in 53,134 total bacterial ASVs. The V1-V2 16S rRNA primer pair used was

bacteria and plastid specific and did not allow for comparison of archaea (Wear et al. 2018).

Statistical analyses

Differences in bacterial cell abundances over the length of each incubation were calculated using a one-way ANOVA. All non-phototrophic bacterial community ASV analyses were conducted using the "vegan" package (v2.4.4; https://cran.r-project.org/web/packages/vegan/) in R (v3.4.1) (Oksanen et al. 2017). Hierarchical clustering based on Bray-Curtis dissimilarity (Bray and Curtis 1957) of bacterial amplicon sequences relative abundance was calculated to compare community compositions between samples. The relative read proportion of bacterial ASVs were calculated by dividing the ASV count by the total reads in each sample. These relative read proportions were log2 transformed for better visualization. Differential abundances of ASVs between biological replicates within each station were identified based on a negative binomial distribution model using "DESeq2" package (v1.22.2; https://bioconductor.org/packages/release/bioc/html/DESeq2.html) (Love et al. 2014) and estimated effect size shrinkage to rank ASVs was performed using 'apeglm' package, an approximate posterior estimation for a generalized linear model (v1.4.2; https://bioconductor.org/packages/release/bioc/html/apeglm.html) (Zhu et al. 2018).

All base plots used in the included figures were generated using the R package "ggplot2" (v2.2.1; https://ggplot2.tidyverse.org) (Wickham 2016).

Metagenomic sequencing

DNA was extracted from triplicate control Niskin samples and triplicate 1,040 m 120 day OM incubation filters using a modification of the QIAGEN DNeasy Plant kit (Qiagen, Valencia, CA, USA), including addition of a bead beating step (Demir-Hilton et al. 2011) and exclusion of RNase. DNA was quantified with the QuBit dsDNA high-sensitivity assay (Invitrogen, Carlsbad, CA, USA) and sequenced using Illumina HiSeq 4000 2x150 bp paired-end reads. These sequences were not further analyzed herein but future directions will focus on identifying potential pathways responding to the phytodetritus addition.

Results

The experiments in this study were among the first deep water *in situ* incubation experiments to be conducted that address bacterial diversity. The primary other existing deep water *in situ* incubation experiment that analyzed members of the microbial community (Pachiadaki et al. 2016) addressed protistan grazing on

prokaryotes at multiple depths throughout the water column. Our hope is that by conducting *in situ* experiments and applying multiple sequencing approaches, of which amplicon analyses were completed herein and future directions include metagenomic analyses, we can generate insights into the deep sea bacterial taxa that actively respond to fresh pulses of organic matter, at least those that degrade phytodetritus.

Bacterial cell abundances increase over long incubations

The bacterial cell abundances were assessed to identify how abundances were impacted by the bacterial communities existing in isolated incubation bags over time compared to their initial abundances from the 0 or 1 day timepoint. Measured from triplicate samples at 1,040 m, the control Niskin communities exhibited the lowest bacterial abundances (31,024 ± 1,079 cells ml^{-1}) compared to the communities incubated over time (not shown). While there was a slight increase in bacterial cell abundances after a 1 day incubation (39,787 ± 7,344 cells ml^{-1}), there was a significant increase ($p < 0.05$, one-way ANOVA) between the 1 day and 60 day incubations (140,363 ± 8,571 cells ml^{-1}) (Fig. 4.2A). Measured from triplicate samples at 3,562 m, the Niskin control communities exhibited more variability (31,851 ± 11,364 cells ml^{-1}) though similar cell abundances as the community at 1,040 m (not shown). The short incubations at 3,562 m exhibited a decrease in

bacterial cell abundances: 0 days (26,688 ± 5,336 cells ml^{-1}) and 5 days (20,407 ± 5,336 cells ml^{-1}; duplicates). By the 240 day incubation, cell abundances had increased dramatically (116,154 ± 39,335 cells ml^{-1}) again similar to the long incubation at 1,040 m, and was a significant increase compared to the 0 day incubation ($p < 0.05$, one-way ANOVA) (Fig. 4.2C). Overall, by isolating deep water into incubation bags, bacterial abundance increased over time. The reasons behind this are unclear, but may include damage to the grazer community during the set up of our experiment.

The organic matter (OM) amendments at 1,040 m exhibited similar trends in bacterial abundances as the control incubations (Fig. 4.2B). The Niskin control (125,267 ± 1,811 cells ml^{-1}; duplicates), 0 day OM amended incubation (136,436 ± 6,365 cells ml^{-1}), 2 day OM amended incubation (133,558 ± 2,717 cells ml^{-1}) and 4 day OM amended incubation (135,546 ± 4,873 cells ml^{-1}) exhibited similar bacterial cell abundances. The 120 day incubation (180,012 ± 49,549 cells ml^{-1}) exhibited a significant increase ($p < 0.05$, one-way ANOVA) in bacterial cell abundances compared to the 2 day incubation, and there was greater variability between replicates. At 3,562 m, the OM incubations exhibited a different pattern in bacterial cell abundances over time as compared to the control incubations (Fig. 4.2D). The Niskin control exhibited the lowest overall bacterial cell abundances (34,944 ± 6,521 cells ml^{-1}; duplicates). There was the same increase in the short incubations of 0 days (52,632 ± 4,177 cells ml^{-1}) and 4 days (52,908 ± 2,852 cells ml^{-1}) relative to the

Niskin community. There was a significant decrease ($p < 0.05$, one-way ANOVA) in abundance between both the 0 day and 4 day incubations to the 240 day incubations (37,819 ± 12,422 cells ml^{-1}). However, it should be noted that there was also more variability between replicates at 240 days such that communities in some bags appeared to have died while in others abundance has increased slightly from the earlier time points. The bacterial cell abundances from the 365 day incubation were more similar to the short incubations and the most variable (56,064 ± 25,280 cells ml^{-1}). Perhaps not surprisingly, the influence of OM addition to the isolated bacterial communities in each incubation bag was less than that of being isolated from the surrounding seawater.

Control incubation influence on bacterial community

Niskin control (n = 1), 1 day (n = 1) and 60 day (n = 1) samples from the 1,040 m control incubation experiment were chosen for V1-V2 16S rRNA gene amplicon sequencing. For the 1,040 m control incubations we performed hierarchical clustering of bacterial communities based on amplicon sequence variants (ASVs) Bray-Curtis dissimilarities. We found the 1 day incubation (n = 1) to be similar to the Niskin control (n = 1), but different from the 60 day incubation (n =1) (Fig. 4.3). To more closely analyze the most abundant ASVs from each sample, the ASVs consisting of the top 50% of the bacterial community from all three samples combined were identified. This resulted in 146 ASVs examined for their change in relative abundance

over the course of the incubation. The bacterial relative abundances were highly similar between the Niskin and 1 day incubation with the most abundant ASVs identified as Actinobacteria Sva0996 marine group, Marinimicrobia, Nitrospinae, Alphaproteobacteria SAR11, Deltaproteobacteria SAR324, Gammaproteobacteria Oceanospirillales JL-ETNP-Y6 and Salinisphaerales ZD0417 marine group, and Verrucomicrobia Arctic97B-4 marine group (Fig. 4.3). These groups with high relative abundances were partially expected as they were the same bacterial groups identified at this depth and location from a previous study (Chapter 2). The most noticeable difference within these groups was the increase of four ASVs classified as SAR11 surface I after the 1 day incubation (Niskin: 0.031%, 0.028%, 0.012%, 0.005%. 1 day: 0.484%, 0.438%, 0.376%, 0.311%, respectively). All of these short incubation ASVs were also found in the 60 day incubation, though at much lower abundances. The most highly abundant ASVs of the 60 day incubation were Alphaproteobacteria Rhodobacterales genus *Sulfitobacter* and *Sneathiellales*, Epsilonproteobacteria Campylobactertales genus *Arcobacter*, and the Gammaproteobacteria Alteromonadales genus *Colwellia*, Cellvibrionales Cellvibionaceae and Spongiibacteraceae BD1-7, Thiotrichales Piscirickettsiaceae and Oceanospirillales Oceanospirillaceae. Almost all of the ASVs making up these 60 day incubation bacterial groups were not detected in the Niskin and 1 day incubations, even though rarefaction curves of samples from this experiment showed a plateau, indicating we did capture the full diversity of the bacterial communities in each sample (not shown).

Deep sea bacterial responses to *in situ* phytodetritus-amended incubations

At 1,040 m, an OM *in situ* incubation experiment was carried out, with incubations of deep water amended with *Chaetoceros mulleri* Lemmermann (CCMP1316). Niskin control (n = 3), 0 day (n = 2), and 120 day (n = 6) samples were selected for V1-V2 16S rRNA gene amplicon analyses for the initial assessment of the bacterial community changes due to the amended incubations. Hierarchical clustering of 1,040 m OM incubation bacterial communities based on ASV Bray-Curtis dissimilarities found two major clusters. The first cluster consisted of the Niskin controls (n = 3) and 0 day incubation (n = 2) while the second cluster was all of the replicates from the 120 day incubation (n = 6) (Fig. 4.4). To more closely analyze the most abundant bacterial ASVs from the Niskin, 0 day incubation and 120 day incubation samples, the top 50% of ASVs from each time point were identified (Niskin: 134 ASVs. 0 day: 157 ASVs. 120 day: 74 ASVs). This resulted in 241 total ASVs examined for their change in abundance due to the incubation of the bacterial communities with the added OM. The ASVs with the highest relative abundances from the Niskin and 0 day samples matched the bacterial groups found in the Niskin and 1 day samples from the control incubation. In addition, the Niskin and 0 day OM incubation samples included Chloroflexi SAR202, and Gammaproteobacteria Oceanospirillales OM182, SAR86 and SUP05. The 0 day incubation samples also

consisted of an increase in the relative abundances of ASVs classified as unclassified Bacteria and Alphaproteobacteria Rhodobacteraceae. The four unclassified Bacteria ASVs increased from an average of 0.014% ± 0.018 to 0.67% ± 0.11 relative abundance, while four of the Alphaproteobacteria Rhodobacteraceae ASVs increased from an average of 0.050% ± 0.067 to 0.972% ± 0.219 relative abundance. Several bacterial groups increased in relative abundance in the 120 day OM incubation as seen in the 60 day control incubation including Alphaproteobacteria Rhodobacteraceae (though not the same ASVs that increased in the 0 day OM incubation), Epsilonproteobacteria Campylobactertales genus *Arcobacter*, and the Gammaproteobacteria Alteromonadales genus *Colwellia* and Thiotrichales Piscirickettsiaceae. In addition to these bacterial groups that seem to be impacted by being incubated in the bags, the 120 day OM incubation exhibited an increased in relative abundance of the Bacteroidetes Flavobacteria genus NS3a marine group, genus *Polaribacter* and genus *Ulvibacter*, Betaproteobacteria Burkholderiales BAL58 marine group and Gammaproteobacteria Oceanospirillales Psuedohongiella. Of the bacteria that increase with the 120 day OM incubation, Bacteroidetes Flavobacteria NS3a marine group was not detected in the Niskin and 0 day incubations.

At 3,562 m, an OM *in situ* incubation experiment was carried out, with incubations of deep water amended with *Micromonas commoda* (RCC299). Niskin control (n = 2), 0 day (n = 3), 4 day (n = 3), 240 day (n = 4) and 365 day (n = 4) samples were chosen for V1-V2 16S rRNA gene amplicon analyses for the initial assessment of the bacterial community changes due to the amended incubations.

Hierarchical clustering of 3,562 m OM incubation bacterial communities based on ASV Bray-Curtis dissimilarities found two major clusters. The first cluster consisted of the Niskin controls (n = 2), 0 day incubation (n = 3), and 4 day incubation (n = 3) while the second cluster consisted of the long incubations, 240 days (n = 4) and 365 days (n = 4) (Fig. 4.5). The short OM incubations grouped by time point within the first cluster while the 240 day and 365 day OM incubations were interspersed throughout the second cluster. To more closely analyze the bacterial ASVs with the highest relative abundances from the control Niskins, as well as 0, 4, 240 and 365 day incubation samples, the top 50% of ASVs from each time point were identified (Niskin: 56 ASVs. 0 day: 73 ASVs. 4 day: 68 ASVs. 240 day: 59 ASVs. 365 day: 55 ASVs). This resulted in 135 total ASVs examined for their change in abundance due to the incubation of the bacterial communities with the added OM. There were no differences in which bacterial group ASVs were most abundant in the Niskin and 0 day incubations. The 4 day incubations included the appearance of Gammaproteobacteria Oceanospirillaceae, which then increased in relative abundance in both long OM incubations (Niskin + 0 day: 0% ± 0; 4 day: 0.02% ± 0.02; 240 + 365 day: 0.77% ± 0.5). Several bacterial groups increased in relative abundance in the 240 and 365 day OM incubations as seen in the 60 day control incubation from 1,040 m including Alphaproteobacteria genus *Sneathiella*, Epsilonproteobacteria Campylobactertales genus *Arcobacter*, and Gammaproteobacteria Cellvibrionales. In addition to these bacterial groups that seem to be impacted by being incubated in the bags, the 240 and 365 day OM incubations exhibited an increased in relative

abundance of the Bacteroidetes Flavobacteria genus *Aquibacter* and genus *Fluviicola*, and Planctomycetes genus *Planctomyces*. These bacteria that seem to increase in response to the 240 and 365 day OM incubations were also present in the short incubations and Niskin samples but at low relative abundances. Of the bacterial groups in high relative abundance in the Niskin, 0 and 4 day OM incubations, Deltaproteobacteria SAR324 was not detected in the 240 and 365 day OM incubations.

Discussion

The four *in situ* incubation experiments presented here aim to identify how our incubator set up influenced the community, as well as to identify which bacteria were actively responding to the provided phytodetritus that simulated sinking OM arriving into the deep sea. Flow cytometric cell enumerations from our control *in situ* incubations indicated an increase in bacterial abundances over incubation times greater than 5 days (Fig. 4.2A, C). This suggests that there is an influence on the bacterial communities just from being isolated in the incubation bags. Potentially the bags themselves were providing a surface for some bacteria to adhere to, as there was a high surface area to volume relative to natural bathypelagic conditions with bag volumes ranging from 50 – 860 ml (1 L bags) and 1558 - 2868 ml (2 L bags), encouraging bacterial growth. Whether or not these taxa would have contributed to

our counts is unclear, as we did not attempt to sample the bag walls. There is also the possibility that the bacteria that survive on dissolved organic carbon (DOC) were thriving due to a potential increase in DOC leaching from the bags themselves which were made of fluoroethyl polymer (FEP) film. While the incubation bags were sterile, we did not prefill the bags with MilliQ water to determine if there were carbon compounds that would leach into the experiments. A previous year long incubation experiment of bathypelagic water (2100 m) collected from the Northwestern Mediterranean Sea with no external input of carbon examined the prokaryotic community dynamics in a 600 L HDPE container (Sebastián et al. 2018). Flow cytometric abundances of 14 timepoints over the course of the year demonstrated alternating increases and decreases in prokaryotic abundances, similar to the trends we observed in our control incubations.

Flow cytometric cell enumeration from both of the *in situ* OM incubations also indicated an increase in bacterial abundance over incubation times greater than 4 days, though the increase was less pronounced and more variable compared to the control incubations (Fig. 4.2B, D). The long incubation times of 120, 240 and 365 days led each of the replicates to turn into unique mesocosms rather than existing as true replicates to each other, as the individual communities captured within each bag were isolated for lengths of time that potentially allowed for multiple cycles of microbial success and turnover. This could be seen, for example, in the 365 day OM incubation at SF3652m where one replicate drastically decreased in bacterial cell abundances (23,264 cells ml^{-1}) and one replicate greatly increased (94,076 cells ml^{-1})

compared to the 0 day incubation (52,632 cells ml^{-1} ± 4,177). A previous high molecular weight dissolved organic matter 27 hour incubation experiment of 75 m water from the North Pacific subtropical gyre measured cell densities via flow cytometry, and found that bacteria doubled in the DOM-amended microcosms (McCarren et al. 2010). This quick doubling of cell abundances were not seen in our OM incubations, as our bacterial communities were from bathypelagic depths (1,040 m and 3,562 m) where colder temperatures lead to slower growth than in the photic zone.

The control incubations exhibited a change in the bacterial community composition over time, indicating that not only were bacterial cell abundances increasing, but the bacteria that make up the community were changing as well. The most abundant ASVs in the 60 day incubation, that were initially very rare or not detected in the Niskin and 1 day incubation ASV data, were potentially the most responsive to the conditions inherent in the control incubation, and were considered 'seed' ASVs. The notion of microbial seedbanks has been previously proposed to play a fundamental role in microbial dynamics (Caporaso et al. 2012; Gibbons et al. 2013; Lennon and Jones 2011; Shade et al. 2014), and has been demonstrated in both short-term (Aanderud et al. 2015; Baltar et al. 2016) and long-term (Sebastián et al. 2018) incubation experiments. For the previous long-term incubation of seawater from 2100 m in the Mediterranean Sea, the shift in responsive 97% operational taxonomical units (OTUs) was suggested to have been triggered by the introduction of fresh organic carbon by chemolithoautotrophic Thaumarchaeota for four months of

the incubation. As the V1-V2 hypervariable region of the 16S rRNA gene does not amplify archaea, we could not assess whether chemolithoautrotrophic archaea introduced 'fresh' organic carbon between the 1 day and 60 day timepoints in our incubation. The bacterial groups that responded in our incubations at 60 days appeared to differ from those reported in a prior Mediterranean Sea incubation (Sebastián et al. 2018). This may be due to the primers used for producing amplicons (our use of V1-V2 vs. V4-V5) that potentially have different biases. Alternatively observed differences could be because the volume of water utilized in the incubations was very different or other factors. For example, we performed incubations of 1-2 L while the year long incubation from the Mediterranean Sea involved one 600 L parcel of bathypelagic water. This large volume was used to reduce the confinement effects that are known to influence community composition (McCarren et al. 2010; Schäfer, Servais, and Muyzer 2000). The most responsive ASVs of our 60 day incubation were Alphaproteobacteria Rhodobacterales genus *Sulfitobacter* and Sneathiellales, Epsilonproteobacteria Campylobactertales genus *Arcobacter*, and the Gammaproteobacteria Alteromonadales genus *Colwellia*, Cellvibrionales Cellvibionaceae and Spongiibacteraceae BD1-7, Thiotrichales Piscirickettsiaceae and Oceanospirillales Oceanospirillaceae. Strong enzymatic and genetic evidence suggests that deep sea Epsilonproteobacteria are chemolithoautotrophic (Takai et al. 2005), supporting the increase in relative abundance of genus *Arcobacter* in our 60 day incubation as a metabolic advantage in this control experiment.

The long term OM incubations at both 1,040 m and 3,562 m exhibited an increase in relative abundances of the same bacterial groups that seem to be influenced by incubating in the bag over time, there were also bacteria that increased in relative abundances presumably due to the phytodetritus addition at the start of the incubation. In general, Bacteroidetes are recognized for harboring a variety of genes encoding hydrolytic enzymes to degrade phytoplankton-derived polysaccharides and peptides (Fernández-Gómez et al. 2013; Li et al. 2015). At 1,040 m with the addition of the diatom *Chaetoceros*, Bacteroidetes Flavobacteria genus *Polaribacter* increased in relative abundance. *Polaribacter* has previously been shown to thrive in response to a spring phytoplankton bloom in the North Sea, with genome analyses suggesting the decomposition of sulfated polysaccharides (Xing et al. 2015). In particular, *Polaribacter* has been found to thrive during diatom dominated phytoplankton blooms in the North Sea (Teeling et al. 2012) and Southern Ocean (Williams et al. 2012). Additionally, Betaproteobacteria Burkholderiales BAL58 marine group has been found to be positively influenced by an increase in terrestrially derived DOM, leading to an increased biogeochemical role in the cycling of carbon in the Baltic Sea (Lindh et al. 2015). At 3,562 m with the addition of *Micromonas*, Planctomycetes increased in relative abundance. Note that the *Micromonas* culture used in these experiments was axenic and the ASVs that increased were generally found at much lower relative abundances in control samples as well. A genomic study of a Planctomycetes strain isolated from the Kiel Fjord in the Baltic Sea found the presence of a large number of open reading frames (ORFs) encoding enzymes

required for the degradation of algal polysaccharides (Glöckner et al. 2003), and a proteomic approach suggests the Planctomycetes play a role in the degradation of carbohydrates (Rabus et al. 2002). The validity of these findings for the taxa stimulated in our study must be determined, as the prior studies used surface isolates. In addition, to the increase in relative abundance of polysaccharide degrading bacteria at the multi-month incubations, an increase was already apparent in the 4 day incubation. The Gammaproteobacteria Oceanospirillales increased in relative abundance after 4 days, although not detected in the Niskin and 0 day samples. These groups continued to increase in relative abundance at 240 and 365 days. This increase in relative abundance at 4 days indicates the quick response of members of the bacterial community to an incoming pulse of phytodetritus, suggesting that certain bacterial groups are poised to respond more rapidly than others – even on timescales of days.

Conclusions

This study assesses bacterial abundance and community composition changes in response to *in situ* control incubations and *in situ* phytodetritus amended incubations at bathypelagic depths. Measures of bacterial abundance as well as changes in the flow cytometric signatures of these populations indicated changes were occurring. However the largest insights to changes came through evaluating community

composition shifts that occurred in response to the addition of fresh phytodetritus. In this sense the 16S rRNA gene amplicon analyses were invaluable in revealing major responses as well as characterizing the overall makeup of the communities and indications of which bacterial groups responded. The unamended control incubations led to an increase in prokaryotic abundances over 240 days, while OM amended incubations exhibited little change, though more variable between replicates, in average prokaryotic abundances. Changes in bacterial community composition occurred over the length of both the control and OM incubation experiments, with bacteria known to degrade polymers and polysaccharides increasing in relative abundances due to the addition of either *Chaetoceros* or *Micromonas* as phytodetritus. A future goal is for the metagenomic sequences generated herein to expand insights gained from the V1-V2 16S rRNA gene amplicon sequencing analysis. The use of new technologies, such as the deep sea *in situ* incubator developed and implemented in the present study, provide the opportunity to assess *in situ* microbial activities with fewer sampling artifacts introduced. An important next step for scientists that seek to replicate *in situ* conditions will be to produce incubation vessels that provide less disruption to natural water dynamics. Given the volumes and sample bag sizes used here, it appears the natural community dynamics in our incubations was influenced by being confined, as seen elsewhere (McCarren et al. 2010; Schäfer et al. 2000). Overall, these methods should improve our understanding of enzyme diversity in deep sea microbes and the responsiveness of different taxa to phytodetrital inputs.

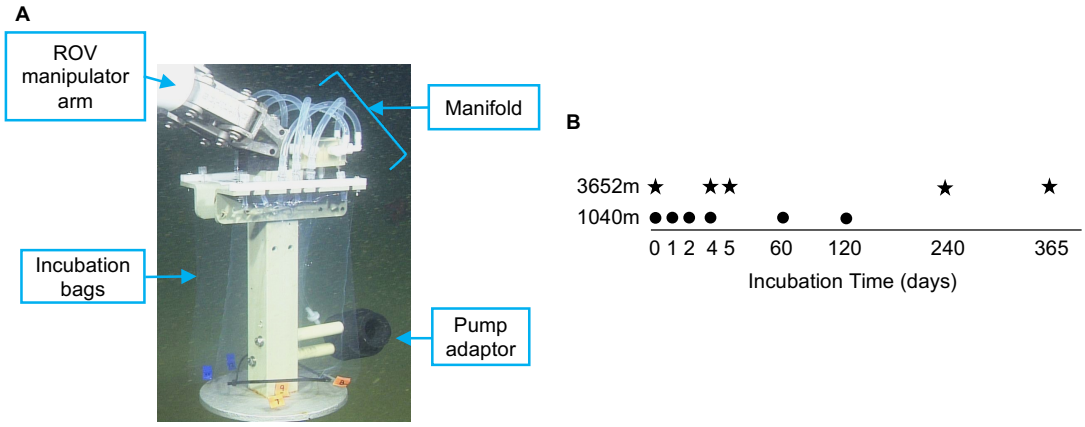

Figure 4.1

(A) Photo of the deep water *in situ* incubation sampler built for this study with the major components labeled. (B) Experimental timelines at the two study sites located at 1,040 m and 3,562 m seafloor depths. Includes incubation times in days for both control and organic matter amended incubations.

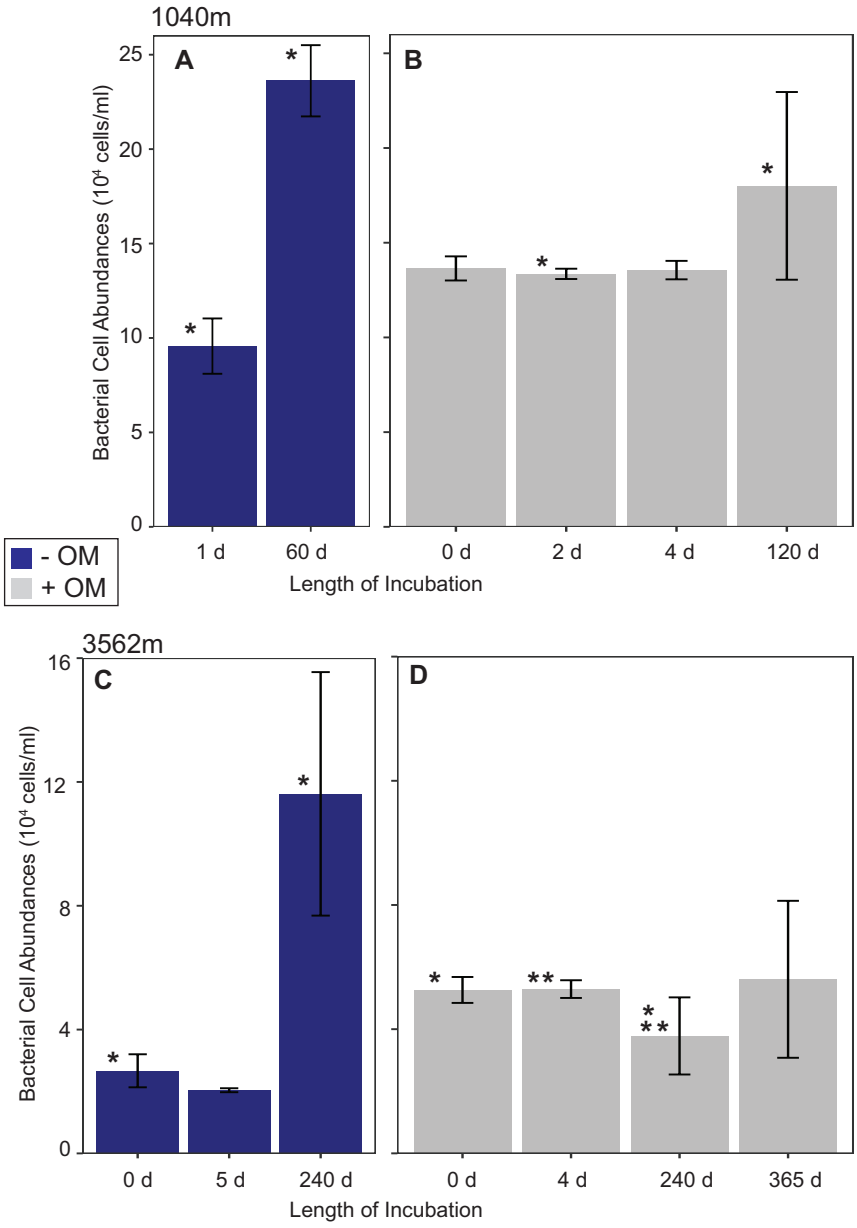

Figure 4.2

Mean bacterial cell abundances per incubation time point with error bars showing the standard deviation of biological triplicates. Control (A) and organic matter (OM) amended (B) incubations conducted at 1,040 m. Bacterial cell abundances increased from the incubation in the bag over the 60 days. The OM added in this experiment was *Chaetoceros mulleri* Lemmermann, and bacterial cell abundances did not change over the first four days of OM incubation but did increase by 120 days. Control (C) and OM amended (D) incubations conducted at 3,562 m. Note, bacterial cell

abundance values are lower than the top panels. Bacterial cell abundances initially decreased over the first five days from the incubation in the bag, but then drastically increased by 240 days. The OM added in this experiment was *Micromonas commoda*, and bacterial cell abundance did not change over the full 365 days incubations. From all four incubations, the longer incubations (120, 240 and 365 days) exhibited more variable bacterial cell abundances per timepoint.

* or ** = significant difference between the two time points within each panel, $p < 0.05$ (one-way ANOVA)

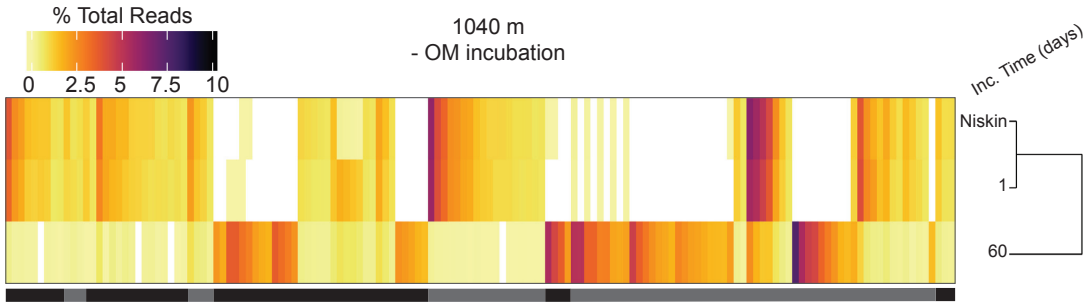

Figure 4.3

Percent relative abundance of the most abundant 100% amplicon sequence variants (ASVs) from a single sample each of the Niskin control and the control incubation conducted at 1,040 m for 1 and 60 days. Heat map columns represent the 50% most abundant ASVs per timepoint ordered by phylum (as indicated by horizontal black-gray bars). Rows represent individual water samples with hierarchical clustering of samples based on Bray-Curtis dissimilarities of bacterial community ASVs. Phyla groups represented from left to right: Actinobacteria, Bacteroidetes, Marinimicrobia, Nitrospinae, Proteobacteria (Alphaproteobacteria, Deltaproteobacteria, Epsilonproteobacteria, Gammaproteobacteria), Verrucomicrobia.

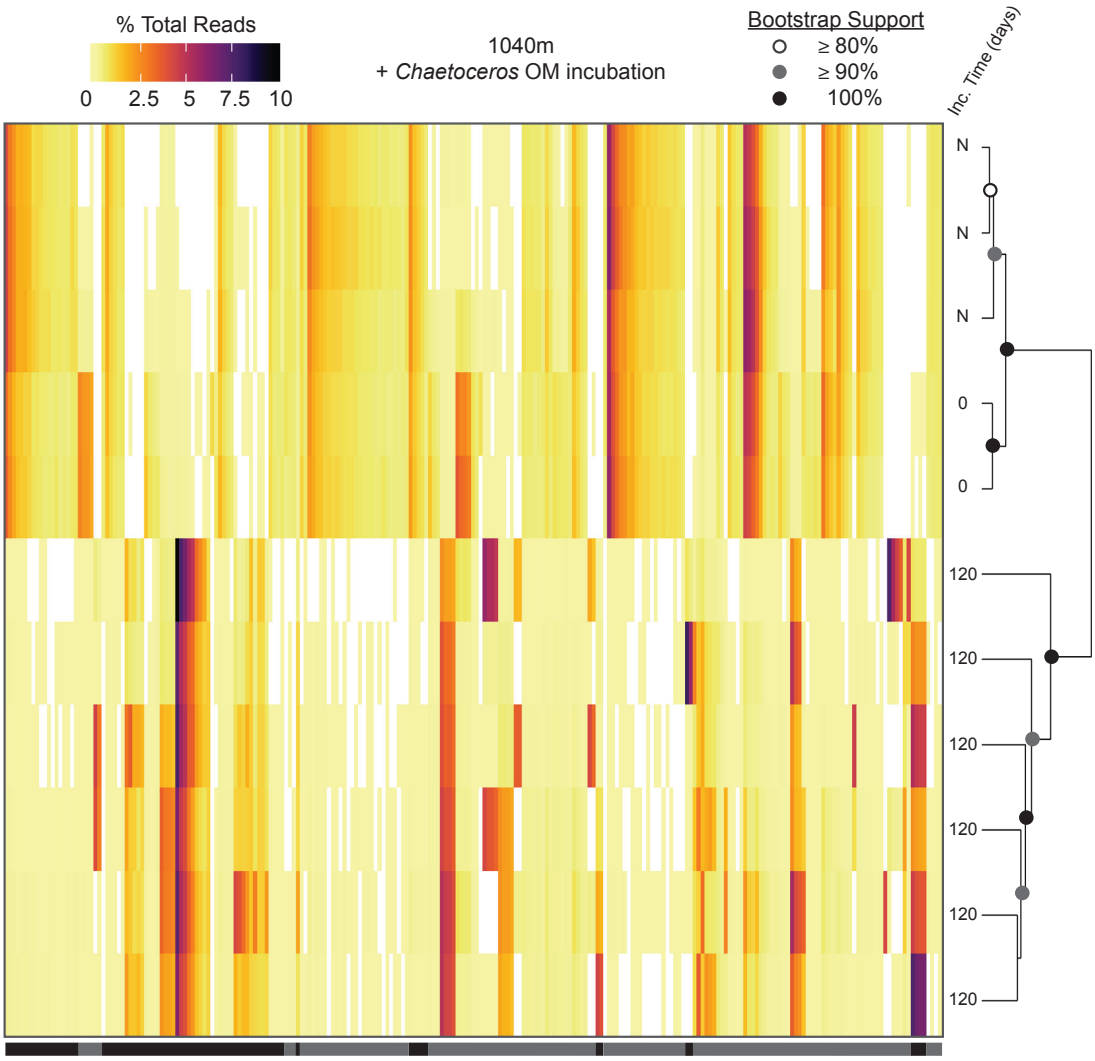

Figure 4.4

Percent relative abundance of the most abundant 100% amplicon sequence variants (ASVs) from the OM amended (*Chaetoceros mulleri* Lemmermann (CCMP1316)) incubation conducted at 1,040 m. Heat map columns represent the 50% most abundant ASVs per timepoint ordered by phylum (as indicated by horizontal black-gray bars). Rows represent individual water samples with hierarchical clustering of samples based on Bray-Curtis dissimilarities of bacterial community ASVs. There are clear sample clusters by incubation times: short (Niskin controls and 0 days) and long (120 days). Bootstrap supports of the hierarchical clustering are indicating for values ≥80. Phyla groups represented from left to right: Actinobacteria, unclassified Bacteria, Bacteroidetes, Chloroflexi, Latescibacteria, Marinimicrobia, Nitrospinae, Proteobacteria (Alphaproteobacteria, Betaproteobacteria, Deltaproteobacteria,

Epsilonproteobacteria, Gammaproteobacteria, unclassified Proteobacteria), Verrucomicrobia.

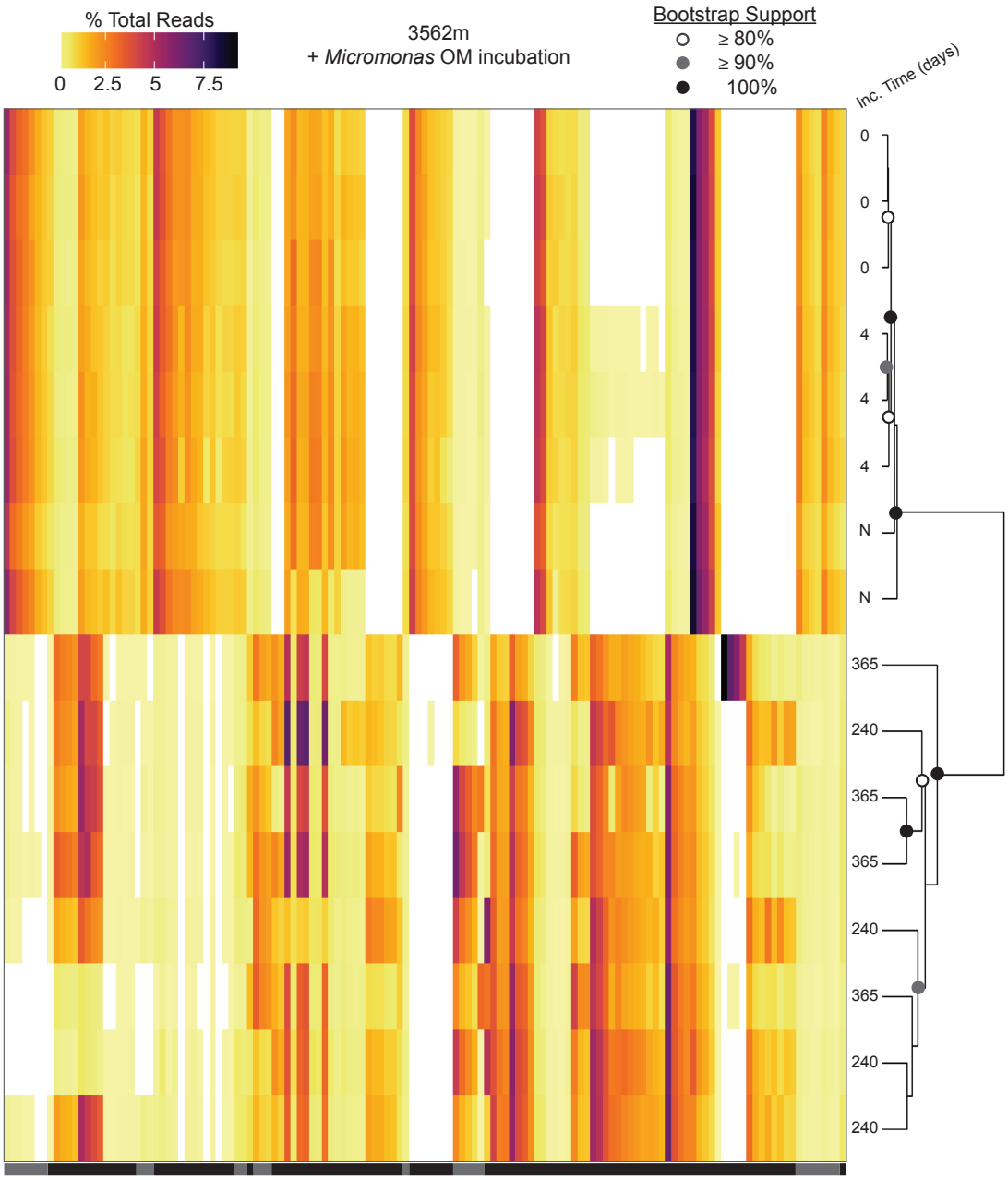

Figure 4.5

Percent relative abundance of the most abundant 100% amplicon sequence variants (ASVs) from the OM amended (*Micromonas commoda* (RCC299)) incubation conducted at 3,562 m. Heat map columns represent the 50% most abundant ASVs per timepoint ordered by phylum (as indicated by horizontal black-gray bars). Rows represent individual water samples with hierarchical clustering of samples based on Bray-Curtis dissimilarities of bacterial community ASVs. There are clear sample

clusters by incubation times: short (Niskin controls, 0 and 4 days) and long (240 and 365 days). Bootstrap supports of the hierarchical clustering are indicating for values ≥80. Phyla groups represented from left to right: Actinobacteria, Bacteroidetes, Chloroflexi, Marinimicrobia, Nitrospinae, Planctomycetes, Proteobacteria (Alphaproteobacteria, Betaproteobacteria, Deltaproteobacteria, Epsilonproteobacteria, Gammaproteobacteria), Verrucomicrobia, unclassified Bacteria.

Chapter 5: Conclusions and Perspectives

Marine microorganisms survive and thrive throughout the water column and underlying sediments, contributing to global biogeochemical cycles. Microbes fulfill a variety of roles to interact with elements such as carbon, nitrogen, phosphorous and sulfur, transforming these elements and influencing the flow of energy through the ecosystems. In order to understand the specific activities of different microbes, it is first necessary to identify the composition of microbial communities and how they vary under different environmental conditions.

In this dissertation, marine bacterial community diversity was characterized from the surface ocean to the seafloor and into deep sea surface sediments with repeated samplings and consistent methods. The research presented leverages remotely operated vehicles and next generation sequencing to deepen understanding of communities in the deep sea. In addition, first steps were made to develop and test an *in situ* incubator that rests on the seafloor.

Characterization of variations in bacterial community structure throughout the water column gives a baseline of current biodiversity at multiple depths. It is necessary to establish a baseline of community compositions in order to compare future deviations resulting from climate change or other perturbations. With repeated sampling of depths in and near Monterey Bay, we found distinct depth related trends in community compositions of the photic zone (0 – 200 m), mesopelagic zone (200 – 1000 m) and bathypelagic zone (>1000 m). There was no detectable variability in

community composition associated with time of year at mesopelagic and bathypelagic depths, though the photic samples exhibited seasonal changes in the bacterial groups present. As bacterial communities below the photic zone are influenced by the flux of surface derived organic matter, identification of the diversity at different depths helps to identify connectivity of communities in the vertical dimension.

The influence of descending organic matter extends to the seafloor, where different depositional histories influence bacterial community structure of deep sea surface sediments. While most deep sea sediments receive surface derived organic matter as phytodetritus, sediments located within a submarine canyon are also influenced by unique hydrology and sedimentology, increasing the quantity and quality of organic matter deposited. An additional organic matter perturbation is the deposition of dead multicellular animals, and in the case of one of our studies sites, a whale carcass. Our sampling in the region of a previously deposited dead whale carcass (our sampling being 11 years later), plus sediments ~100 m away did not detect bacterial community differences that appeared to be associated with this previous perturbation. This suggests that there is no longer an influence from the whale carcass or the influence has spread beyond 100 m from the deposition site. To test these possibilities requires future additional sediments to be sampled at varying distances from the previous whale carcass, preferably at the same seafloor depth of ~1000 m. To date, few if any studies have performed replicated sampling within sediment push cores and between push cores <1 m apart. We found no significant differences in bacterial community composition between either type of replicate.

Depending on the similarities of our sites to other ocean sediment regions, this indicates that in future *in situ* deep sea sediment incubation experiments replicate sediment push cores could be considered technical replicates.

While diversity measurements are the first step in characterizing marine ecosystems, the next direction is to determine microbial functions and assess their activity. One of the important roles of marine bacteria is their function in transforming organic carbon compounds. To connect deep sea bacteria with their role in degrading organic carbon, we developed an *in situ* incubator to characterize which bacteria respond to a simulated flux of organic carbon in the form of phytodetritus. Bacterial groups known to degrade polymers and polysaccharides were found to increase over time in response to the phytodetritus. Further exploration of the metagenome data analyzed here can be carried out to determine the carbohydrate active enzymes present in controls versus the 120 day incubation (with phytodetritus derived from the diatom *Chaetoceros*).

Looking forward, additional DNA analyses can be performed involving stable isotope probing as in these experiments the phytodetritus was labeled with carbon-13. Thus, a future step would be to use stable isotope probing to isolate the specific bacterial groups that consumed and incorporated the ^{13}C labeled phytodetritus into their DNA. This would allow us to identify their activities as being distinct from other bacterial groups that increase for indirect, rather than direct reasons. Understanding the changing conditions within each incubation, such as specific carbon compounds of particulate and dissolved organic carbon may provide clarity on the organic matter

transformations being carried out by individual bacterial groups. Based on the results from these initial *in situ* incubations, future experiments should include time points between 4 days and 60 days as we saw a large response already by 4 days, but are missing any time points immediately after. Ultimately, RNA from these experiments is also available to analyzed. RNA sequencing would identify the specific enzymes stimulated in response to the phytodetritus

The work presented in this dissertation leverages oceanographic sampling capabilities with novel instrumentation to detect bacterial diversity throughout the water column and into surface sediments and links specific deep sea bacteria to organic matter degradation. Together, this research provides statistically sound sampling that provides baseline knowledge of bacterial communities against which future studies can assess change over time and differences from other deep sea environments.

References

Aanderud, Zachary T., Stuart E. Jones, Noah Fierer, and Jay T. Lennon. 2015. "Resuscitation of the Rare Biosphere Contributes to Pulses of Ecosystem Activity." *Frontiers in Microbiology* 6:24.

Acinas, Silvia G., Luisa A. Marcelino, Vanja Klepac-Ceraj, and Martin F. Polz. 2004. "Divergence and Redundancy of 16S RRNA Sequences in Genomes with Multiple Rrn Operons." *Journal of Bacteriology* 186(9):2629–35.

Agogué, Hélène, Dominique Lamy, Phillip R. Neal, Mitchell L. Sogin, and Gerhard J. Herndl. 2011. "Water Mass-Specificity of Bacterial Communities in the North Atlantic Revealed by Massively Parallel Sequencing." *Molecular Ecology* 20(2):258–74.

Alldredge, A. L., U. Passow, and B. E. Logan. 1993. "The Abundance and Significance of a Class of Large, Transparent Organic Particles in the Ocean." *Deep-Sea Research I* 40(6):1131–40.

Allers, Elke, Jody J. Wright, Kishori M. Konwar, Charles G. Howes, Erica Beneze, Steven J. Hallam, and Matthew B. Sullivan. 2013. "Diversity and Population Structure of Marine Group A Bacteria in the Northeast Subarctic Pacific Ocean." *The ISME Journal* 7(2):256–68.

Amacher, Jessica, Susanne Neuer, and Michael Lomas. 2013. "DNA-Based Molecular Fingerprinting of Eukaryotic Protists and Cyanobacteria Contributing to Sinking Particle Flux at the Bermuda Atlantic Time-Series Study." *Deep-Sea Research Part II: Topical Studies in Oceanography* 93:71–83.

Arístegui, Javier, Carlos M. Duarte, Susana Agustí, Marylo Doval, Xosé A. Álvarez-Salgado, and Dennis A. Hansell. 2002. "Dissolved Organic Carbon Support of Respiration in the Dark Ocean." *Science* 298(5600):1967.

Arístegui, Javier, Josep M. Gasol, Carlos M. Duarte, and Gerhard J. Herndl. 2009. "Microbial Oceanography of the Dark Ocean's Pelagic Realm." *Limnology and Oceanography* 54(5):1501–29.

Armstrong, R. A., C. Lee, J. I. Hedges, S. Honjo, and S. G. Wakeham. 2002. "A New, Mechanistic Model for Organic Carbon Flxes in the Ocean Based on the Quantitative Association of POC with Ballast Minerals." *Deep-Sea Res Part II* 49:219–36.

Azam, F., T. Fenchel, J. G. Field, J. S. Gray, L. A. Meyer-Reil, and F. Thingstad. 1983. "The Ecological Role of Water-Column Microbes in the Sea*." *Marine Ecology Progress Series* 10:257–63.

Baltar, Federico, Daniel Lundin, Joakim Palovaara, Itziar Lekunberri, Thomas Reinthaler, Gerhard J. Herndl, and Jarone Pinhassi. 2016. "Prokaryotic

Responses to Ammonium and Organic Carbon Reveal Alternative CO 2 Fixation Pathways and Importance of Alkaline Phosphatase in the Mesopelagic North Atlantic." *Frontiers in Microbiology* 7:1670.

Benner, Ronald, J. Dean Pakulski, Matthew Mccarthy, John I. Hedges, Patrick G. Hatcher, J. Dean Pakulski, Matrhew Mccarthy, John I. Hedges, and Patrick G. Hatcher. 1992. "Bulk Chemical Characteristics of Dissolved Organic Matter in the Ocean." *Science* 255(5051):1561–64.

Bergauer, Kristin, Antonio Fernandez-Guerra, Juan A. L. Garcia, Richard R. Sprenger, Ramunas Stepanauskas, Maria G. Pachiadaki, Ole N. Jensen, and Gerhard J. Herndl. 2018. "Organic Matter Processing by Microbial Communities throughout the Atlantic Water Column as Revealed by Metaproteomics." *Proceedings of the National Academy of Sciences* 115(3):E400–408.

Bienhold, Christina, Lucie Zinger, Antje Boetius, and Alban Ramette. 2016. "Diversity and Biogeography of Bathyal and Abyssal Seafloor Bacteria." *PLoS ONE* 11(1):e0148016.

Boetius, A. and K. Lochte. 1996. "Effect of Organic Enrichments on Hydrolytic Potentials and Growth of Bacteria in Deep-Sea Sediments." *Marine Ecology Progress Series* 140(1–3):239–50.

Bokulich, Nicholas A., Benjamin D. Kaehler, Jai Ram Rideout, Matthew Dillon, Evan Bolyen, Rob Knight, Gavin A. Huttley, and J. Gregory Caporaso. 2018. "Optimizing Taxonomic Classification of Marker-Gene Amplicon Sequences with QIIME 2's Q2-Feature-Classifier Plugin." *Microbiome* 6(1):90.

ter Braak, Cajo J. F. and Piet F. M. Verdonschot. 1995. "Canonical Correspondence Analysis and Related Multivariate Methods in Aquatic Ecology." *Aquatic Sciences* 57(3):255–89.

Bray, J. Roger and J. T. Curtis. 1957. "An Ordination of the Upland Forest Communitites in Southern Wisconsin." *Ecological Monographs* 27(4):325–49.

Brown, M. V, G. K. Philip, J. A. Bunge, M. C. Smith, A. Bissett, F. M. Lauro, J. A. Fuhrman, and S. P. Donachie. 2009. "Microbial Community Structure in the North Pacific Ocean." *The ISME Journal* 3(12):1374–86.

Brown, Mark V., Federico M. Lauro, Matthew Z. Demaere, Les Muir, David Wilkins, Torsten Thomas, Martin J. Riddle, Jed A. Fuhrman, Cynthia Andrews-Pfannkoch, Jeffrey M. Hoffman, Jeffrey B. McQuaid, Andrew Allen, Stephen R. Rintoul, and Ricardo Cavicchioli. 2012. "Global Biogeography of SAR11 Marine Bacteria." *Molecular Systems Biology* 8(595):1–13.

Brown, MV and SP Donachie. 2007. "Evidence for Tropical Endemicity in the Deltaproteobacteria Marine Group B/SAR324 Bacterioplankton Clade." *Aquatic Microbial Ecology* 46:107–15.

Bryant, Jessica A., Frank J. Stewart, John M. Eppley, and Edward F. Delong. 2012. "Microbial Community Phylogenetic and Trait Diversity Declines with Depth in a Marine Oxygen Minimum Zone." *Ecology* 93(7):1659–73.

Buesseler, K. O., T. W. Trull, D. K. Steinberg, M. W. Silver, D. A. Siegel, S. I. Saitoh, C. H. Lamborg, P. J. Lam, D. M. Karl, N. Z. Jiao, M. C. Honda, M. Elskens, F. Dehairs, S. L. Brown, P. W. Boyd, J. K. B. Bishop, and R. R. Bidigare. 2008. "VERTIGO (VERtical Transport In the Global Ocean): A Study of Particle Sources and Flux Attenuation in the North Pacific." *Deep-Sea Research Part II: Topical Studies in Oceanography* 55(14–15):1522–39.

Callahan, Benjamin J., Paul J. McMurdie, and Susan P. Holmes. 2017. "Exact Sequence Variants Should Replace Operational Taxonomic Units in Marker Gene Data Analysis." *The ISME Journal*.

Callahan, Benjamin J., Paul J. Mcmurdie, Michael J. Rosen, Andrew W. Han, Amy Jo Johnson, and Susan P. Holmes. 2015. "DADA2 : High Resolution Sample Inference from Amplicon Data." *Nature Methods* 13(7):581–95.

Cao, Huiluo, Chunming Dong, Salim Bougouffa, Jiangtao Li, Weipeng Zhang, Zongze Shao, Vladimir B. Bajic, and Pei Yuan Qian. 2016. "Delta-Proteobacterial SAR324 Group in Hydrothermal Plumes on the South Mid-Atlantic Ridge." *Scientific Reports* 6(March 2015):1–9.

Capella-Gutiérrez, Salvador, José M. Silla-Martínez, and Toni Gabaldón. 2009. "TrimAl: A Tool for Automated Alignment Trimming in Large-Scale Phylogenetic Analyses." *Bioinformatics* 25(15):1972–73.

Caporaso, J. Gregory, Konrad Paszkiewicz, Dawn Field, Rob Knight, and Jack A. Gilbert. 2012. "The Western English Channel Contains a Persistent Microbial Seed Bank." *The ISME Journal* 6:1089–93.

Carlson, Craig A., Dennis A. Hansell, Norman B. Nelson, David A. Siegel, William M. Smethie, Samar Khatiwala, Meredith M. Meyers, and Elisa Halewood. 2010. "Dissolved Organic Carbon Export and Subsequent Remineralization in the Mesopelagic and Bathypelagic Realms of the North Atlantic Basin." *Deep-Sea Research Part II: Topical Studies in Oceanography* 57(16):1433–45.

Carlson, Craig A., Robert Morris, Rachel Parsons, Alexander H. Treusch, Stephen J. Giovannoni, and Kevin Vergin. 2009. "Seasonal Dynamics of SAR11 Populations in the Euphotic and Mesopelagic Zones of the Northwestern Sargasso Sea." *The ISME Journal* 3:283–95.

Charette, Matthew A., S. Bradley Moran, and James K. B. Bishop. 1999. "234Th as a Tracer of Particulate Organic Carbon Export in the Subarctic Northeast Pacific Ocean." *Deep Sea Research Part II: Topical Studies in Oceanography* 46(11):2833–61.

Chen, Xihan, Thorbjørn Joest Andersen, Yuki Morono, Fumio Inagaki, Bo Barker Jørgensen, and Mark Alexander Lever. 2017. "Bioturbation as a Key Driver behind the Dominance of Bacteria over Archaea in Near-Surface Sediment." *Scientific Reports* 7(1):1–14.

Chitsaz, Hamidreza, Joyclyn L. Yee-Greenbaum, Glenn Tesler, Mary Jane Lombardo, Christopher L. Dupont, Jonathan H. Badger, Mark Novotny, Douglas B. Rusch, Louise J. Fraser, Niall A. Gormley, Ole Schulz-Trieglaff, Geoffrey P. Smith, Dirk J. Evers, Pavel A. Pevzner, and Roger S. Lasken. 2011. "Efficient de Novo Assembly of Single-Cell Bacterial Genomes from Short-Read Data Sets." *Nature Biotechnology* 29(10):915–22.

Cho, Byung C. and Farooq Azam. 1988. "Major Role of Bacteria in Biogeochemical Fluxes in the Ocean's Interior." *Nature* 332(6163):441–43.

Chow, Cheryl Emiliane T., Diane Y. Kim, Rohan Sachdeva, David A. Caron, and Jed A. Fuhrman. 2014. "Top-down Controls on Bacterial Community Structure: Microbial Network Analysis of Bacteria, T4-like Viruses and Protists." *ISME Journal* 8(4):816–29.

Chow, Cheryl Emiliane T., Rohan Sachdeva, Jacob A. Cram, Joshua A. Steele, David M. Needham, Anand Patel, Alma E. Parada, and Jed A. Fuhrman. 2013. "Temporal Variability and Coherence of Euphotic Zone Bacterial Communities over a Decade in the Southern California Bight." *ISME Journal* 7(12):2259–73.

Cline, Joel D. 1969. "Spectrophotometric Determination of Hydrogen Sulfide in Natural Waters." *Limnology and Oceanography* 14:454–58.

Corinaldesi, Cinzia, Michael Tangherlini, Eugenio Rastelli, Emanuela Buschi, Marco Lo Martire, Roberto Danovaro, and Antonio Dell'Anno. 2019. "High Diversity of Benthic Bacterial and Archaeal Assemblages in Deep-Mediterranean Canyons and Adjacent Slopes." *Progress in Oceanography* 171:154–61.

De Corte, Daniele, Eva Sintes, Taichi Yokokawa, Itziar Lekunberri, and Gerhard J. Herndl. 2016. "Large-Scale Distribution of Microbial and Viral Populations in the South Atlantic Ocean." *Environmental Microbiology Reports* 8(2):305–15.

Cram, Jacob A., Cheryl-Emiliane T. Chow, Rohan Sachdeva, David M. Needham, Alma E. Parada, Joshua A. Steele, and Jed A. Fuhrman. 2015. "Seasonal and Interannual Variability of the Marine Bacterioplankton Community throughout the Water Column over Ten Years." *The ISME Journal* 9(3):563–80.

Cunha, Marina R., Gordon L. J. Paterson, Teresa Amaro, Sabena Blackbird, Henko C. de Stigter, Clarisse Ferreira, Adrian Glover, Ana Hilário, Konstadinos Kiriakoulakis, Lenka Neal, Ascensão Ravara, Clara F. Rodrigues, Áurea Tiago, and David S. M. Billett. 2011. "Biodiversity of Macrofaunal Assemblages from Three Portuguese Submarine Canyons (NE Atlantic)." *Deep-Sea Research Part II: Topical Studies in Oceanography* 58(23–24):2433–47.

D'hondt, Steven, Fumio Inagaki, Carlos Alvarez Zarikian, Lewis J. Abrams, Nathalie Dubois, Tim Engelhardt, Helen Evans, Timothy Ferdelman, Britta Gribsholt, Robert N. Harris, Bryce W. Hoppie, Jung Ho Hyun, Jens Kallmeyer, Jinwook Kim, Jill E. Lynch, Claire C. Mckinley, Satoshi Mitsunobu, Yuki Morono, Richard W. Murray, Robert Pockalny, Justine Sauvage, Takaya Shimono, Fumito Shiraishi, David C. Smith, Christopher E. Smith-Duque, Arthur J. Spivack, Bjorn Olav Steinsbu, Yohey Suzuki, Michal Szpak, Laurent Toffin, Goichiro Uramoto, Yasuhiko T. Yamaguchi, Guo Liang Zhang, Xiao Hua Zhang, and Wiebke Ziebis. 2015. "Presence of Oxygen and Aerobic Communities from Sea Floor to Basement in Deep-Sea Sediments." *Nature Geoscience* 8(4):299–304.

Danovaro, Roberto, Massimiliano Molari, Cinzia Corinaldesi, and Antonio Dell'Anno. 2016. "Macroecological Drivers of Archaea and Bacteria in Benthic Deep-Sea Ecosystems." *Science Advances* 2(4):1–12.

Delong, Edward F., Christina M. Preston, Tracy Mincer, Virginia Rich, Steven J. Hallam, Niels-ulrik Frigaard, Asuncion Martinez, Matthew B. Sullivan, Robert Edwards, Beltran Rodriguez Brito, Sallie W. Chisholm, and David M. Karl. 2006. "Community Genomics Among Stratified Microbial Assemblages in the Ocean's Interior." *Science* 311(5760):496–503.

Demir-Hilton, Elif, Sebastian Sudek, Marie L. Cuvelier, Chelle L. Gentemann, Jonathan P. Zehr, and Alexandra Z. Worden. 2011. "Global Distribution Patterns of Distinct Clades of the Photosynthetic Picoeukaryote Ostreococcus." *The ISME Journal* 5(7):1095–1107.

Diociaiuti, Tommaso, Fabrizio Bernardi Aubry, and Serena Fonda Umani. 2019. "Vertical Distribution of Microbial Communities Abundance and Biomass in Two NW Mediterranean Sea Submarine Canyons." *Progress in Oceanography* 175(March):14–23.

Duineveld, Gérard, Marc Lavaleye, Eilke Berghuis, and Peter De Wilde. 2001. "Activity and Composition of the Benthic Fauna in the Whittard Canyon and the Adjacent Continental Slope (NE Atlantic)." *Oceanologica Acta* 24(1):69–83.

Dunlop, Katherine M., Dick van Oevelen, Henry A. Ruhl, Christine L. Huffard, Linda A. Kuhnz, and Kenneth L. Smith. 2016. "Carbon Cycling in the Deep Eastern North Pacific Benthic Food Web: Investigating the Effect of Organic Carbon Input." *Limnology and Oceanography* 61(6):1956–68.

Durbin, Alan M. and Andreas Teske. 2011. "Microbial Diversity and Stratification of South Pacific Abyssal Marine Sediments." *Environmental Microbiology* 13(12):3219–34.

Durkin, Colleen A., Margaret L. Estapa, and Ken O. Buesseler. 2015. "Observations of Carbon Export by Small Sinking Particles in the Upper Mesopelagic." *Marine*

Chemistry 175:72–81.

Dyksma, Stefan, Kerstin Bischof, Bernhard M. Fuchs, Katy Hoffmann, Dimitri Meier, Anke Meyerdierks, Petra Pjevac, David Probandt, Michael Richter, Ramunas Stepanauskas, and Marc Mußmann. 2016. "Ubiquitous Gammaproteobacteria Dominate Dark Carbon Fixation in Coastal Sediments." *ISME Journal* 10(8):1939–53.

Easson, Cole G. and Jose V. Lopez. 2019. "Depth-Dependent Environmental Drivers of Microbial Plankton Community Structure in the Northern Gulf of Mexico." *Frontiers in Microbiology* 9(January):1–13.

Eddy, Sean R. 2011. "Accelerated Profile HMM Searches." *PLoS Computational Biology* 7(10).

Edgar, Robert C. 2010. "Search and Clustering Orders of Magnitude Faster than BLAST." *Bioinformatics* 26(19):2460–61.

Edgar, Robert C. 2016. "UNOISE2: Improved Error-Correction for Illumina 16S and ITS Amplicon Sequencing." *BioRxiv* 081257.

Eren, A. Murat, Loïs Maignien, Woo Jun Sul, Leslie G. Murphy, Sharon L. Grim, Hilary G. Morrison, and Mitchell L. Sogin. 2013. "Oligotyping: Differentiating between Closely Related Microbial Taxa Using 16S RRNA Gene Data." *Methods in Ecology and Evolution* 4(12):1111–19.

Eren, A. Murat, Hilary G. Morrison, Pamela J. Lescault, Julie Reveillaud, Joseph H. Vineis, and Mitchell L. Sogin. 2015. "Minimum Entropy Decomposition: Unsupervised Oligotyping for Sensitive Partitioning of High-Throughput Marker Gene Sequences." *The ISME Journal* 9(4):968–79.

Escobar Briones, Elva, Erika Laura Estrada Santillán, and Pierre Legendre. 2008. "Macrofaunal Density and Biomass in the Campeche Canyon, Southwestern Gulf of Mexico." *Deep-Sea Research Part II: Topical Studies in Oceanography* 55(24–26):2679–85.

Falkowski, Paul G., Tom Fenchel, and Edward F. Delong. 2008. "The Microbial Engine That Drives the Earth's Biogeochemical Cycles." *Science* 320:1034–40.

Fernández-Gómez, Beatriz, Michael Richter, Margarete Schüler, Jarone Pinhassi, Silvia G. Acinas, José M. González, and Carlos Pedrós-Alió. 2013. "Ecology of Marine Bacteroidetes: A Comparative Genomics Approach." *ISME Journal* 7(5):1026–37.

Field, K. G., D. Gordon, T. Wright, E. Urback, K. Vergin, and S. J. Giovannoni. 1997. "Diversity and Depth-Specific Distribution of SAR11 Cluster RRNA Genes from Marine Planktonic Bacteria." *Applied And Environmental Microbiology* 63(1):63–70.

Fortunato, Caroline S., Lydie Herfort, Peter Zuber, Antonio M. Baptista, and Byron C. Crump. 2012. “Spatial Variability Overwhelms Seasonal Patterns in Bacterioplankton Communities across a River to Ocean Gradient.” *ISME Journal* 6(3):554–63.

Fuhrman, Jed A. and Joshua A. Steele. 2008. “Community Structure of Marine Bacterioplankton: Patterns, Networks, and Relationships to Function.” *Aquatic Microbial Ecology* 53(1):69–81.

García-Martínez, J. and F. Rodríguez-Valera. 2000. “Microdiversity of Uncultured Marine Prokaryotes: The SAR11 Cluster and the Marine Archaea of Group I.” *Molecular Ecology* 9(7):935–48.

Georges, Anna A., Heba El-Swais, Susanne E. Craig, William K. W. Li, and David A. Walsh. 2014. “Metaproteomic Analysis of a Winter to Spring Succession in Coastal Northwest Atlantic Ocean Microbial Plankton.” *The ISME Journal* 8(6):1301–13.

Ghiglione, J. F., C. Palacios, J. C. Marty, G. Mével, C. Labrune, P. Conan, M. Pujo-Pay, N. Garcia, and M. Goutx. 2008. “Role of Environmental Factors for the Vertical Distribution (0-1000 m) of Marine Bacterial Communities in the NW Mediterranean Sea.” *Biogeosciences* 5(6):1751–64.

Gibbons, Sean M., J. Gregory Caporaso, Meg Pirrung, Dawn Field, Rob Knight, and Jack A. Gilbert. 2013. “Evidence for a Persistent Microbial Seed Bank throughout the Global Ocean.” *PNAS* 110(12):4651–55.

Giering, Sarah L. C., Richard Sanders, Richard S. Lampitt, Thomas R. Anderson, Christian Tamburini, Mehdi Boutrif, Mikhail V Zubkov, Chris M. Marsay, Stephanie A. Henson, Kevin Saw, Kathryn Cook, and Daniel J. Mayor. 2014. “Reconciliation of the Carbon Budget in the Ocean’s Twilight Zone.” *Nature* 507:480–83.

Giovannoni, S. J. 2005. “Genome Streamlining in a Cosmopolitan Oceanic Bacterium.” *Science* 309(5738):1242–45.

Giovannoni, Stephen J. 2017. “SAR11 Bacteria: The Most Abundant Plankton in the Oceans.” *Annual Review of Marine Science* 9:231–55.

Glöckner, F. O., M. Kube, M. Bauer, H. Teeling, T. Lombardot, W. Ludwig, D. Gade, A. Beck, K. Borzym, K. Heitmann, R. Rabus, H. Schlesner, R. Amann, and R. Reinhardt. 2003. “ Complete Genome Sequence of the Marine Planctomycete Pirellula Sp. Strain 1 .” *Proceedings of the National Academy of Sciences* 100(14):8298–8303.

Goffredi, Shana K. and Victoria J. Orphan. 2010. “Bacterial Community Shifts in Taxa and Diversity in Response to Localized Organic Loading in the Deep Sea.” *Environmental Microbiology* 12(2):344–63.

Gong, Jun, Fei Shi, Bin Ma, Jun Dong, Maria Pachiadaki, Xiaoli Zhang, and Virginia P. Edgcomb. 2015. "Depth Shapes α- and β-Diversities of Microbial Eukaryotes in Surficial Sediments of Coastal Ecosystems." *Environmental Microbiology* 17(10):3722–37.

Green-Saxena, A., A. E. Dekas, N. F. Dalleska, and V. J. Orphan. 2014. "Nitrate-Based Niche Differentiation by Distinct Sulfate-Reducing Bacteria Involved in the Anaerobic Oxidation of Methane." *The ISME Journal* 8:150–63.

Grote, Jana, J. Cameron Thrash, Megan J. Huggett, Zachary C. Landry, Paul Carini, Stephen J. Giovannoni, and Michael S. Rappé. 2012. "Streamlining and Core Genome Conservation among Highly Divergent Members of the SAR11 Clade." *MBio* 3(5):1–13.

Guindon, Stéphane, Jean Franois Dufayard, Vincent Lefort, Maria Anisimova, Wim Hordijk, and Olivier Gascuel. 2010. "New Algorithms and Methods to Estimate Maximum-Likelihood Phylogenies: Assessing the Performance of PhyML 3.0." *Systematic Biology* 59(3):307–21.

Hamady, Micah, Jeffrey J. Walker, J. Kirk Harris, Nicholas J. Gold, and Rob Knight. 2008. "Error-Correcting Barcoded Primers Allow Hundreds of Samples to Be Pyrosequenced in Multiplex." *Nat Methods* 5(3):235–37.

Haroon, Mohamed F., Luke R. Thompson, and Ulrich Stingl. 2016. "Draft Genome Sequence of Uncultured SAR324 Bacterium Lautmerah10, Binned from a Red Sea Metagenome." *Genome Announcements* 4(1):e01711-15.

Hewson, Ian, Myrna E. Jacobson-Meyers, and Jed A. Fuhrman. 2007. "Diversity and Biogeography of Bacterial Assemblages in Surface Sediments across the San Pedro Basin, Southern California Borderlands." *Environmental Microbiology* 9(4):923–33.

Hondt, Steven D., Bo Barker Jørgensen, D. Jay Miller, Anja Batzke, Ruth Blake, Barry A. Cragg, Heribert Cypionka, Gerald R. Dickens, Timothy Ferdelman, Kai-uwe Hinrichs, Nils G. Holm, Richard Mitterer, Arthur Spivack, Guizhi Wang, Barbara Bekins, Bert Engelen, Kathryn Ford, Glen Gettemy, Scott D. Rutherford, Henrik Sass, C. Gregory Skilbeck, Christopher H. House, Ivano W. Aiello, Gilles Gue, Fumio Inagaki, Patrick Meister, Thomas Naehr, Sachiko Niitsuma, R. John Parkes, Axel Schippers, David C. Smith, Andreas Teske, Juergen Wiegel, Christian Naranjo Padilla, Juana Luz, and Solis Acosta. 2004. "Distributions of Microbial Activities in Deep Subseafloor Sediments." *Science* 306:2216–22.

Hug, Laura A., Brett J. Baker, Karthik Anantharaman, Christopher T. Brown, Alexander J. Probst, Cindy J. Castelle, Cristina N. Butterfield, Alex W. Hernsdorf, Yuki Amano, Kotaro Ise, Yohey Suzuki, Natasha Dudek, David A. Relman, Kari M. Finstad, Ronald Amundson, Brian C. Thomas, and Jillian F.

Banfield. 2016. “A New View of the Tree of Life.” *Nature Microbiology* 1(5):16048.

Jimenez-Infante, Francy, David Kamanda Ngugi, Manikandan Vinu, Jochen Blom, Intikhab Alam, Vladimir B. Bajic, and Ulrich Stingl. 2017. “Genomic Characterization of Two Novel SAR11 Isolates from the Red Sea, Including the First Strain of the SAR11 Ib Clade.” *FEMS Microbiology Ecology* 93(7):1–10.

Jing, Hongmei, Xiaomin Xia, Koji Suzuki, and Hongbin Liu. 2013. “Vertical Profiles of Bacteria in the Tropical and Subarctic Oceans Revealed by Pyrosequencing” edited by H. Smidt. *PLoS ONE* 8(11):e79423.

Jørgensen, B. B. 1982. “Mineralization of Organic Matter in the Sea Bed - the Role of Sulphate Reduction.” *Nature* 296:643–45.

Jørgensen, Bo Barker. 2000. *Marine Geochemistry*. edited by H. D. Schulz and M. Zabel. Berlin Heidelberg: Springer-Verlag.

Jørgensen, Bo Barker, Alyssa J. Findlay, and André Pellerin. 2019. “The Biogeochemical Sulfur Cycle of Marine Sediments.” *Frontiers in Microbiology* 10:849.

Karl, David M., George A. Knauer, and John H. Martin. 1988. “Downward Flux of Particulate Organic Matter in the Ocean: A Particle Decomposition Paradox.” *Nature* 332(6163):438–41.

Katija, Kakani, Rob E. Sherlock, Alana D. Sherman, and Bruce H. Robison. 2017. “New Technology Reveals the Role of Giant Larvaceans in Oceanic Carbon Cycling.” *Science Advances* 3:1–8.

Katoh, Kazutaka and Daron M. Standley. 2013. “MAFFT Multiple Sequence Alignment Software Version 7: Improvements in Performance and Usability.” *Molecular Biology and Evolution* 30(4):772–80.

Keith, S. M. and R. A. Herbert. 1983. “Dissimilatory Nitrate Reduction by a Strain of Desulfovibrio Desulfuricans.” *FEMS Microbiology Letters* 18:55–59.

Kembel, Steven W., Jonathan A. Eisen, Katherine S. Pollard, and Jessica L. Green. 2011. “The Phylogenetic Diversity of Metagenomes.” *PLoS ONE* 6(8).

Kuever, Jan. 2014. “The Family Desulfobulbaceae.” Pp. 1–413 in *The Prokaryotes: Deltaproteobacteria and Epsilonproteobacteria*. Vol. 9783642390, edited by E. Rosenberg, E. De Long, F. S. Loy, E. Stackebrandt, and F. Thompson. Berlin Heidelberg: Springer-Verlag.

Kuever, Jan, Fred A. Rainey, and Friedrich Widdel. 2015. “ Desulfobulbus .” *Bergey’s Manual of Systematics of Archaea and Bacteria* 1–6.

Lebrato, Mario, Pedro De Jesus Mendes, Deborah K. Steinberg, Joan E. Cartes,

Bethan M. Jones, Laura M. Birsa, Roberto Benavides, and Andreas Oschlies. 2013. “Jelly Biomass Sinking Speed Reveals a Fast Carbon Export Mechanism.” *Limnology and Oceanography* 58(3):1113–22.

Lennon, Jay T. and Stuart E. Jones. 2011. “Microbial Seed Banks : The Ecological and Evolutionary Implications of Dormancy.” *Nature Reviews Microbiology* 9:119–30.

De Leo, Fabio C., Craig R. Smith, Ashley A. Rowden, David A. Bowden, and Malcolm R. Clark. 2010. “Submarine Canyons: Hotspots of Benthic Biomass and Productivity in the Deep Sea.” *Proceedings of the Royal Society B: Biological Sciences* 277:2783–92.

De Leo, Fabio C., Eric W. Vetter, Craig R. Smith, Ashley A. Rowden, and Matthew McGranaghan. 2014. “Spatial Scale-Dependent Habitat Heterogeneity Influences Submarine Canyon Macrofaunal Abundance and Diversity off the Main and Northwest Hawaiian Islands.” *Deep-Sea Research Part II: Topical Studies in Oceanography* 104:267–90.

Li, Meng, Brett J. Baker, Karthik Anantharaman, Sunit Jain, John A. Breier, and Gregory J. Dick. 2015. “Genomic and Transcriptomic Evidence for Scavenging of Diverse Organic Compounds by Widespread Deep-Sea Archaea.” *Nature Communications* 6(May):1–6.

Li, Meng, Sunit Jain, Brett J. Baker, Chris Taylor, and Gregory J. Dick. 2014. “Novel Hydrocarbon Monooxygenase Genes in the Metatranscriptome of a Natural Deep-Sea Hydrocarbon Plume.” *Environmental Microbiology* 16(1):60–71.

Lima, I. D., P. J. Lam, and S. C. Doney. 2014. “Dynamics of Particulate Organic Carbon Flux in a Global Ocean Model.” *Biogeosciences* 11(4):1177–98.

Lindh, Markus V., Robert Lefébure, Rickard Degerman, Daniel Lundin, Agneta Andersson, and Jarone Pinhassi. 2015. “Consequences of Increased Terrestrial Dissolved Organic Matter and Temperature on Bacterioplankton Community Composition during a Baltic Sea Mesocosm Experiment.” *Ambio* 44(Suppl. 3):S402-412.

Love, Michael I., Wolfgang Huber, and Simon Anders. 2014. “Moderated Estimation of Fold Change and Dispersion for RNA-Seq Data with DESeq2.” *Genome Biology* 15(12):550.

Lundsten, Lonny, Kyra L. Schlining, Kaitlin Frasier, Shannon B. Johnson, Linda A. Kuhnz, Julio B. J. Harvey, Gillian Clague, and Robert C. Vrijenhoek. 2010. “Time-Series Analysis of Six Whale-Fall Communities in Monterey Canyon, California, USA.” *Deep-Sea Research Part I: Oceanographic Research Papers* 57(12):1573–84.

Marie, Dominique, Frédéric Partensky, Daniel Vaulot, and Corina Brussaard. 2001.

"Enumeration of Phytoplankton, Bacteria, and Viruses in Marine Samples." P. Chapter 11:Unit 11.11 in *Current Protocols in Cytometry*.

Martin, Marcel. 2011. "Cutadapt Removes Adapter Sequences from High-Throughput Sequencing Reads." *EMBnet Journal* 17:10–12.

Martínez-Espinosa, Rosa M., Frutos C. Marhuenda-Egea, and María José Bonete. 2001. "Assimilatory Nitrate Reductase from the Haloarchaeon Haloferax Mediterranei: Purification and Characterisation." *FEMS Microbiology Letters* 204:381–85.

Matsen, Frederick A., Robin B. Kodner, and E. Virginia Armbrust. 2010. "Pplacer: Linear Time Maximum-Likelihood and Bayesian Phylogenetic Placement of Sequences onto a Fixed Reference Tree." *BMC Bioinformatics* 11(1):538.

McCarren, J., J. W. Becker, D. J. Repeta, Y. Shi, C. R. Young, R. R. Malmstrom, S. W. Chisholm, and E. F. DeLong. 2010. "Microbial Community Transcriptomes Reveal Microbes and Metabolic Pathways Associated with Dissolved Organic Matter Turnover in the Sea." *Proceedings of the National Academy of Sciences* 107(38):16420–27.

McCready, R. G. L., W. D. Gould, and F. D. Cook. 1983. "Respiratory Nitrate Reduction by Desulfovibrio Sp." *Archives of Microbiology* 135:182–85.

Medina-Silva, Renata, Rafael R. de Oliveira, Maria A. G. Pivel, Luiz G. A. Borges, Taiz L. L. Simão, Leandro M. Pereira, Fernanda J. Trindade, Adolpho H. Augustin, Fernanda P. Valdez, Eduardo Eizirik, Laura R. P. Utz, Claudia Groposo, Dennis J. Miller, Adriano R. Viana, João M. M. Ketzer, and Adriana Giongo. 2018. "Microbial Diversity from Chlorophyll Maximum, Oxygen Minimum and Bottom Zones in the Southwestern Atlantic Ocean." *Journal of Marine Systems* 178:52–61.

Mestre, Mireia, Clara Ruiz-gonzález, Ramiro Logares, Carlos M. Duarte, and Josep M. Gasol. 2018. "Sinking Particles Promote Vertical Connectivity in the Ocean Microbiome." *PNAS* 1–9.

Mitchell, Garry J., J. Gwynfryn Jones, and Jeffrey A. Cole. 1986. "Distribution and Regulation of Nitrate and Nitrite Reduction by Desulfovibrio and Desulfotomaculum Species." *Archives of Microbiology* 144:35–40.

Morris, R. M., M. S. Rappé, E. Urbach, S. A. Connon, and S. J. Giovannoni. 2004. "Prevalence of the Chloroflexi-Related SAR202 Bacterioplankton Cluster throughout the Mesopelagic Zone and Deep Ocean." *Applied and Environmental Microbiology* 70(5):2836–42.

Morris, Robert M., Michael S. Rappé, Stephanie A. Connon, Kevin L. Vergin, William A. Siebold, Craig A. Carlson, and Stephen J. Giovannoni. 2002. "SAR11 Clade Dominates Ocean Surface Bacterioplankton Communities."

Nature 420:806–10.

Morris, Robert M., Kevin L. Vergin, Jang-Cheon Cho, Michael S. Rappé, Craig A. Carlson, and Stephen J. Giovannoni. 2005. "Temporal and Spatial Response of Bacterioplankton Lineages to Annual Convective Overturn at the Bermuda Atlantic Time-Series Study Site." *Limnology and Oceanography* 50(5):1687–96.

Moura, Isabel, Sergey Bursakov, Cristina Costa, and José J. .. Moura. 1997. "Nitrate and Nitrite Utilization in Sulfate-Reducing Bacteria." *Anaerobe* 3:279–90.

Mußmann, Marc, Petra Pjevac, Karen Krüger, and Stefan Dyksma. 2017. "Genomic Repertoire of the Woeseiaceae/JTB255, Cosmopolitan and Abundant Core Members of Microbial Communities in Marine Sediments." *The ISME Journal* 11:1276–81.

Needham, David M., Rohan Sachdeva, and Jed A. Fuhrman. 2017. "Ecological Dynamics and Co-Occurrence among Marine Phytoplankton, Bacteria and Myoviruses Shows Microdiversity Matters." *The ISME Journal* 11(7):1614–29.

Ngugi, David Kamanda and Ulrich Stingl. 2012. "Combined Analyses of the ITS Loci and the Corresponding 16S RRNA Genes Reveal High Micro- and Macrodiversity of SAR11 Populations in the Red Sea." *PLoS ONE* 7(11).

Nunoura, Takuro, Yoshihiro Takaki, Miho Hirai, Shigeru Shimamura, Akiko Makabe, Osamu Koide, Tohru Kikuchi, Junichi Miyazaki, Keisuke Koba, Naohiro Yoshida, Michinari Sunamura, and Ken Takai. 2015. "Hadal Biosphere: Insight into the Microbial Ecosystem in the Deepest Ocean on Earth." *Proceedings of the National Academy of Sciences of the United States of America* 112(11):E1230-6.

Oksanen, Jari, F. Guillaume Blanchet, Michael Friendly, Roeland Kindt, Pierre Legendre, Dan Mcglinn, Peter R. Minchin, R. B. O 'hara, Gavin L. Simpson, Peter Solymos, M. Henry, H. Stevens, Eduard Szoecs, and Helene Wagner. 2017. "Vegan: Community Ecology Package." *R Package Version 2.4-4* https://CRAN.R-project.org/package=vegan.

Omand, Melissa M., Eric A. D'Asaro, Craig M. Lee, Mary Jane Perry, Nathan Briggs, Ivona Cetinic, and Amala Mahadevan. 2015. "Eddy-Driven Subduction Exports Particulate Organic Carbon from the Spring Bloom." *Science* 348(March):1–35.

Pachiadaki, Maria G., Craig Taylor, Andreas Oikonomou, Michail M. Yakimov, Thorsten Stoeck, and Virginia Edgcomb. 2016. "In Situ Grazing Experiments Apply New Technology to Gain Insights into Deep-Sea Microbial Food Webs." *Deep Sea Research Part II: Topical Studies in Oceanography* 129:223–31.

Pasqual, Catalina, Cindy Lee, Miguel Goñi, Tommaso Tesi, Anna Sanchez-Vidal, Antoni Calafat, Miquel Canals, and Serge Heussner. 2011. "Use of Organic

Biomarkers to Trace the Transport of Marine and Terrigenous Organic Matter through the Southwestern Canyons of the Gulf of Lion." *Marine Chemistry* 126(1–4):1–12.

Peltzer, ET and NA Hayward. 1996. "Spatial and Temporal Variability of Total Organic Carbon along 14O°W in the Equatorial Pacific Ocean in 1992." *Deep-Sea Research Part II: Topical Studies in Oceanography* 43(4–6):1155–80.

Pennington, J. Timothy and Francisco P. Chavez. 2000. "Seasonal Fluctuations of Temperature, Salinity, Nitrate, Chlorophyll and Primary Production at Station H3 / M1 over 1989- 1996 in Monterey Bay, California." *Deep-Sea Research II* 47:947–73.

Peoples, Logan M., Eleanna Grammatopoulou, Michelle Pombrol, Xiaoxiong Xu, Oladayo Osuntokun, Jessica Blanton, Eric E. Allen, Clifton C. Nunnally, Jeffrey C. Drazen, Daniel J. Mayor, and Douglas H. Bartlett. 2019. "Microbial Community Diversity Within Sediments from Two Geographically Separated Hadal Trenches." *Frontiers in Microbiology* 10(March).

Pham, Vinh D., Konstantinos T. Konstantinidis, Tsultrim Palden, and Edward F. DeLong. 2008. "Phylogenetic Analyses of Ribosomal DNA-Containing Bacterioplankton Genome Fragments from a 4000 m Vertical Profile in the North Pacific Subtropical Gyre." *Environmental Microbiology* 10(9):2313–30.

Polymenakou, Paraskevi N., Nikolaos Lampadariou, and Anastasios Tselepides. 2008. "Exo-Enzymatic Activities and Organic Matter Properties in Deep-Sea Canyon and Slope Systems off the Southern Cretan Margin." *Deep-Sea Research Part I: Oceanographic Research Papers* 55(10):1318–29.

Pomeroy, Lawrence R., P. J. leB. Williams, F. Azam, and J. E. Hobbie. 2007. "The Microbial Loop." *Oceanography* 20(2):28–33.

Pommier, Thomas, P. R. Neal, Josep M. Gasol, Montserrat Coll, Silvia G. Acinas, and Carlos Pedrós-Alió. 2010. "Spatial Patterns of Bacterial Richness and Evenness in the NW Mediterranean Sea Explored by Pyrosequencing of the 16S RRNA." *Aquatic Microbial Ecology* 61(3):221–33.

Probandt, D., K. Knittel, H. E. Tegetmeyer, S. Ahmerkamp, M. Holtappels, and R. Amann. 2017. "Permeability Shapes Bacterial Communities in Sublittoral Surface Sediments." *Environmental Microbiology* 19(4):1584–99.

Pruesse, Elmar, Christian Quast, Katrin Knittel, Bernhard M. Fuchs, Wolfgang Ludwig, Jörg Peplies, and Frank Oliver Glöckner. 2007. "SILVA: A Comprehensive Online Resource for Quality Checked and Aligned Ribosomal RNA Sequence Data Compatible with ARB." *Nucleic Acids Research* 35(21):7188–96.

Rabus, Ralf, Dörte Gade, Roger Helbig, Margarete Bauer, Frank Oliver Glöckner,

Michael Kube, Heinz Schlesner, Richard Reinhardt, and Rudolf Amann. 2002. "Analysis of N-Acetylglucosamine Metabolism in the Marine Bacterium Pirellula Sp. Strain 1 by a Proteomic Approach." *Proteomics* 2:649–55.

Reeburgh, W. S. 1967. "An Improved Interstitial Water Sampler." *Limnol. Oceanogr* 12:163–65.

Rich, Virginia I., Vinh D. Pham, John Eppley, Yanmei Shi, and Edward F. DeLong. 2011. "Time-Series Analyses of Monterey Bay Coastal Microbial Picoplankton Using a 'genome Proxy' Microarray." *Environmental Microbiology* 13(1):116–34.

Robison, Bruce H., Kim R. Reisenbichler, and Rob E. Sherlock. 2005. "Giant Larvacean Houses: Rapid Carbon Transport to the Deep Sea Floor." *Science* 308(5728):1609–11.

Ronquist, Fredrik, Maxim Teslenko, Paul Van Der Mark, Daniel L. Ayres, Aaron Darling, Sebastian Höhna, Bret Larget, Liang Liu, Marc A. Suchard, and John P. Huelsenbeck. 2012. "Mrbayes 3.2: Efficient Bayesian Phylogenetic Inference and Model Choice across a Large Model Space." *Systematic Biology* 61(3):539–42.

Salazar, Guillem, Francisco M. Cornejo-Castillo, Verónica Benítez-Barrios, Eugenio Fraile-Nuez, X. Antón Álvarez-Salgado, Carlos M. Duarte, Josep M. Gasol, and Silvia G. Acinas. 2016. "Global Diversity and Biogeography of Deep-Sea Pelagic Prokaryotes." *The ISME Journal* 10(3):596–608.

Schäfer, Hendrik, Pierre Servais, and Gerard Muyzer. 2000. "Successional Changes in the Genetic Diversity of a Marine Bacterial Assemblage during Confinement." *Archives of Microbiology* 173:138–45.

Schwalbach, M. S., H. J. Tripp, L. Steindler, D. P. Smith, and S. J. Giovannoni. 2010. "The Presence of the Glycolysis Operon in SAR11 Genomes Is Positively Correlated with Ocean Productivity." *Environmental Microbiology* 12(2):490–500.

Sebastián, Marta, Jean Christophe Auguet, Claudia Ximena Restrepo-Ortiz, María Montserrat Sala, Celia Marrasé, and Josep M. Gasol. 2018. "Deep Ocean Prokaryotic Communities Are Remarkably Malleable When Facing Long-Term Starvation." *Environmental Microbiology* 20(2):713–23.

Seitz, Hans-jiirgen and Heribert Cypionka. 1986. "Chemolithotrophic Growth of Desulfovibrio Desulfuricans with Hudrogen Coupled to Ammonification of Nitrate or Nitrite." *Archives of Microbiology* 146:63–67.

Shade, Ashley, Stuart E. Jones, J. Gregory Caporaso, Jo Handelsman, Rob Knight, Noah Fierer, and Jack A. Gilbert. 2014. "Conditionally Rare Taxa Disproportionately Contribute to Temporal Changes in Microbial Diversity."

MBio 5(4):e01371.

Sheik, Cody S., Sunit Jain, and Gregory J. Dick. 2014. "Metabolic Flexibility of Enigmatic SAR324 Revealed through Metagenomics and Metatranscriptomics." *Environmental Microbiology* 16(1):304–17.

Signori, Camila N., François Thomas, Alex Enrich-Prast, Ricardo C. G. Pollery, and Stefan M. Sievert. 2014. "Microbial Diversity and Community Structure across Environmental Gradients in Bransfield Strait, Western Antarctic Peninsula." *Frontiers in Microbiology* 5(DEC):1–12.

Šimek, Karel, Karel Horňák, Jan Jezbera, Michal Mašín, Jiří Nedoma, Josep M. Gasol, and Michael Schauer. 2005. "Influence of Top-down and Bottom-up Manipulations on the R-BT065 Subcluster of β-Proteobacteria, an Abundant Group in Bacterioplankton of a Freshwater Reservoir." *Applied and Environmental Microbiology* 71(5):2381–90.

Smith, CR and AR Baco. 2003. "Ecology of Whale Falls at the Deep-Sea Floor." Pp. 311–54 in *Oceanography and marine biology: an Annual Review, volume 41*, edited by R. Gibson and R. Atkinson. Taylor and Francis.

Smith Jr, K. L., H. A. Ruhl, M. Kahru, C. L. Huffard, and A. D. Sherman. 2013. "Deep Ocean Communities Impacted by Changing Climate over 24 y in the Abyssal Northeast Pacific Ocean." *Proceedings of the National Academy of Sciences of the United States of America* 110(49):19838–41.

Sørensen, J. 1978. "Capacity for Denitrification and Reduction of Nitrate to Ammonia in a Coastal Marine Sediment." *Applied and Environmental Microbiology* 35(2):301–5.

Sowell, Sarah M., Larry J. Wilhelm, Angela D. Norbeck, Mary S. Lipton, Carrie D. Nicora, Douglas F. Barofsky, Craig A. Carlson, Richard D. Smith, and Stephen J. Giovanonni. 2009. "Transport Functions Dominate the SAR11 Metaproteome at Low-Nutrient Extremes in the Sargasso Sea." *ISME Journal* 3(1):93–105.

Stamatakis, Alexandros. 2014. "RAxML Version 8: A Tool for Phylogenetic Analysis and Post-Analysis of Large Phylogenies." *Bioinformatics* 30(9):1312–13.

Steele, Joshua A., Peter D. Countway, Li Xia, Patrick D. Vigil, J. Michael Beman, Diane Y. Kim, Cheryl Emiliane T. Chow, Rohan Sachdeva, Adriane C. Jones, Michael S. Schwalbach, Julie M. Rose, Ian Hewson, Anand Patel, Fengzhu Sun, David A. Caron, and Jed A. Fuhrman. 2011. "Marine Bacterial, Archaeal and Protistan Association Networks Reveal Ecological Linkages." *The ISME Journal* 5(9):1414–25.

Steinberg, Deborah K., Benjamin A. S. Van Mooy, Ken O. Buesseler, Philip W. Boyd, Toru Kobari, and David M. Karl. 2008. "Bacterial vs. Zooplankton

Control of Sinking Particle Flux in the Ocean's Twilight Zone." *Limnology and Oceanography* 53(4):1327–38.

Stingl, Ulrich, Harry James Tripp, and Stephen J. Giovannoni. 2007. "Improvements of High-Throughput Culturing Yielded Novel SAR11 Strains and Other Abundant Marine Bacteria from the Oregon Coast and the Bermuda Atlantic Time Series Study Site." *The ISME Journal* 1(4):361–71.

Sun, Jing, Laura Steindler, J. Cameron Thrash, Kimberly H. Halsey, Daniel P. Smith, Amy E. Carter, Zachary C. Landry, and Stephen J. Giovannoni. 2011. "One Carbon Metabolism in SAR11 Pelagic Marine Bacteria." *PLoS ONE* 6(8).

Sunagawa, Shinichi, Luis Pedro Coelho, Samuel Chaffron, Jens Roat Kultima, Karine Labadie, Guillem Salazar, Bardya Djahanschiri, Georg Zeller, Daniel R. Mende, Adriana Alberti, Francisco M. Cornejo-Castillo, Paul I. Costea, Corinne Cruaud, Francesco D'Ovidio, Stefan Engelen, Isabel Ferrera, Josep M. Gasol, Lionel Guidi, Falk Hildebrand, Florian Kokoszka, Cyrille Lepoivre, Gipsi Lima-Mendez, Julie Poulain, Bonnie T. Poulos, Marta Royo-Llonch, Hugo Sarmento, Sara Vieira-Silva, Céline Dimier, Marc Picheral, Sarah Searson, Stefanie Kandels-Lewis, Chris Bowler, Colomban de Vargas, Gabriel Gorsky, Nigel Grimsley, Pascal Hingamp, Daniele Iudicone, Olivier Jaillon, Fabrice Not, Hiroyuki Ogata, Stephane Pesant, Sabrina Speich, Lars Stemmann, Matthew B. Sullivan, Jean Weissenbach, Patrick Wincker, Eric Karsenti, Jeroen Raes, Silvia G. Acinas, and Peer Bork. 2015. "Structure and Function of the Global Ocean Microbiome." *Science* 348(6237):1261359.

Swan, Brandon K., Manuel Martinez-Garcia, Christina M. Preston, Alexander Sczyrba, Tanja Woyke, Dominique Lamy, Thomas Reinthaler, Nicole J. Poulton, E. Dashiell P. Masland, Monica Lluesma Gomez, Michael E. Sieracki, Edward F. DeLong, Gerhard J. Herndl, and Ramunas Stepanauskas. 2011. "Potential for Chemolithoautotrophy Among Ubiquious Bacteria Lineages in the Dark Ocean." *Science* 333:1296–1300.

Szewzyk, R. and N. Pfennig. 1987. "Complete Oxidation of Catechol by the Strictly Anaerobic Sulfate-Reducing Desulfobacterium Catecholicum Sp. Nov.*." *Archives of Microbiology* 147:163–68.

Takai, Ken, Barbara J. Campbell, S. Craig Cary, Masae Suzuki, Hanako Oida, Takuro Nunoura, Hisako Hirayama, Satoshi Nakagawa, Yohey Suzuki, Fumio Inagaki, and Koki Horikoshi. 2005. "Enzymatic and Genetic Characterization of Carbon and Energy Metabolisms by Deep-Sea Hydrothermal Chemolithoautotrophic Isolates of Epsilonproteobacteria." *Applied and Environmental Microbiology* 71(11):7310–20.

Teeling, Hanno, Bernhard M. Fuchs, Dörte Becher, Christine Klockow, Antje Gardebrecht, Christin M. Bennke, Mariette Kassabgy, Sixing Huang, Alexander J. Mann, Jost Waldmann, Marc Weber, Anna Klindworth, Andreas Otto, Jana

Lange, Jörg Bernhardt, Christine Reinsch, Michael Hecker, Jörg Peplies, Frank D. Bockelmann, Ulrich Callies, Gunnar Gerdts, Antje Wichels, Karen H. Wiltshire, Frank Oliver Glöckner, Thomas Schweder, and Rudolf Amann. 2012. "Substrate-Controlled Succession of Marinee Bacterioplankton Populations Induced by a Phytoplankton Bloom." *Science* 336(6081):608–12.

Tesi, T., L. Langone, M. A. Goñi, M. Turchetto, S. Miserocchi, and A. Boldrin. 2008. "Source and Composition of Organic Matter in the Bari Canyon (Italy): Dense Water Cascading versus Particulate Export from the Upper Ocean." *Deep-Sea Research Part I: Oceanographic Research Papers* 55(7):813–31.

Thrash, J. Cameron, Ben Temperton, Brandon K. Swan, Zachary C. Landry, Tanja Woyke, Edward F. DeLong, Ramunas Stepanauskas, and Stephan J. Giovannoni. 2014. "Single-Cell Enabled Comparative Genomics of a Deep Ocean SAR11 Bathytype." *The ISME Journal* 8(7):1440–51.

Treusch, Alexander H., Kevin L. Vergin, Liam A. Finlay, Michael G. Donatz, Robert M. Burton, Craig A. Carlson, and Stephen J. Giovannoni. 2009. "Seasonality and Vertical Structure of Microbial Communities in an Ocean Gyre." *The ISME Journal* 3:1148–63.

Tripp, H. James, Joshua B. Kitner, Michael S. Schwalbach, John W. H. Dacey, Larry J. Wilhelm, and Stephen J. Giovannoni. 2008. "SAR11 Marine Bacteria Require Exogenous Reduced Sulphur for Growth." *Nature* 452(7188):741–44.

Tripp, H. James, Michael S. Schwalbach, Michelle M. Meyer, Joshua B. Kitner, Ronald R. Breaker, and Stephen J. Giovannoni. 2009. "Unique Glycine-Activated Riboswitch Linked to Glycine-Serine Auxotrophy in SAR11." *Environmental Microbiology* 11(1):230–38.

Tsementzi, Despina, Jieying Wu, Samuel Deutsch, Sangeeta Nath, Luis M. Rodriguez-R, Andrew S. Burns, Piyush Ranjan, Neha Sarode, Rex R. Malmstrom, Cory C. Padilla, Benjamin K. Stone, Laura A. Bristow, Morten Larsen, Jennifer B. Glass, Bo Thamdrup, Tanja Woyke, Konstantinos T. Konstantinidis, and Frank J. Stewart. 2016. "SAR11 Bacteria Linked to Ocean Anoxia and Nitrogen Loss." *Nature* 536(7615):179–83.

Tseng, Ching Hung, Pei Wen Chiang, Hung Chun Lai, Fuh Kwo Shiah, Ting Chang Hsu, Yi Lung Chen, Liang Saw Wen, Chun Mao Tseng, Wung Yang Shieh, Isaam Saeed, Saman Halgamuge, and Sen Lin Tang. 2015. "Prokaryotic Assemblages and Metagenomes in Pelagic Zones of the South China Sea." *BMC Genomics* 16(1):1–16.

Vergin, Kevin L., Bánk Beszteri, Adam Monier, J. Cameron Thrash, Ben Temperton, Alexander H. Treusch, Fabian Kilpert, Alexandra Z. Worden, and Stephen J. Giovannoni. 2013. "High-Resolution SAR11 Ecotype Dynamics at the Bermuda Atlantic Time-Series Study Site by Phylogenetic Placement of Pyrosequences."

The ISME Journal 7(7):1322–32.

Vetter, E. W. and P. K. Dayton. 1998. "Macrofaunal Communities within and Adjacent to a Detritus-Rich Submarine Canyon System." *Deep-Sea Research Part II: Topical Studies in Oceanography* 45:25–54.

Walsh, Emily A., John B. Kirkpatrick, Scott D. Rutherford, David C. Smith, Mitchell Sogin, and Steven D. Hondt. 2016. "Bacterial Diversity and Community Composition from Seasurface to Subseafloor." *The ISME Journal* 10:979–89.

Wear, Emma K., Elizabeth G. Wilbanks, Craig E. Nelson, and Craig A. Carlson. 2018. "Primer Selection Impacts Specific Population Abundances but Not Community Dynamics in a Monthly Time-Series 16S RRNA Gene Amplicon Analysis of Coastal Marine Bacterioplankton." *Environmental Microbiology* 20(8):2709–26.

Wickham, H. 2016. *Ggplot2: Elegant Graphics for Data Analysis*. New York: Springer-Verlag.

Widdel, Friedrich and Norbet Pfennig. 1982. "Studies on Dissimilatory Sulfate-Reducing Bacteria That Decompose Fatty Acids II. Incomplete Oxidation of Propionate by Desulfobulbus Propionicus Gen. Nov., Sp. Nov." *Archives of Microbiology* 131:360–65.

Williams, Timothy J., Emilie Long, Flavia Evans, Mathew Z. Demaere, Federico M. Lauro, Mark J. Raftery, Hugh Ducklow, Joseph J. Grzymski, Alison E. Murray, and Ricardo Cavicchioli. 2012. "A Metaproteomic Assessment of Winter and Summer Bacterioplankton from Antarctic Peninsula Coastal Surface Waters." *ISME Journal* 6(10):1883–1900.

Wilson, Stephanie E., Ha Ruhl, and Kl Smith Jr. 2013. "Zooplankton Fecal Pellet Flux in the Abyssal Northeast Pacific: A 15 Year Time-Series Study." *Limnol. Oceanogr* 58(3):881–92.

Woese, C. R. 1987. "Bacterial Evolution." *Microbiological Reviews* 51(2):221–71.

Worden, Alexandra Z., Michael J. Follows, Stephen J. Giovannoni, Susanne Wilken, Amy E. Zimmerman, and Patrick J. Keeling. 2015. "Rethinking the Marine Carbon Cycle: Factoring in the Multifarious Lifestyles of Microbes." *Science* 347(6223):1257594.

Wright, Jody J., Kishori M. Konwar, and Steven J. Hallam. 2012. "Microbial Ecology of Expanding Oxygen Minimum Zones." *Nature Reviews Microbiology* 10(6):381–94.

Xing, Peng, Richard L. Hahnke, Frank Unfried, Stephanie Markert, Sixing Huang, Tristan Barbeyron, Jens Harder, Dörte Becher, Thomas Schweder, Frank Oliver Glöckner, Rudolf I. Amann, and Hanno Teeling. 2015. "Niches of Two

Polysaccharide-Degrading Polaribacter Isolates from the North Sea during a Spring Diatom Bloom." *The ISME Journal* 9(6):1410–22.

Zehr, Jonathan P. and Raphael M. Kudela. 2010. "Nitrogen Cycle of the Open Ocean: From Genes to Ecosystems." *Annual Review of Marine Science* 3:197–225.

Zhu, Anqi, Joseph G. Ibrahim, and Michael I. Love. 2018. "Heavy-Tailed Prior Distributions for Sequence Count Data: Removing the Noise and Preserving Large Differences." *Bioinformatics* 35(12):2084–92.

Zinger, Lucie, Linda A. Amaral-Zettler, Jed A. Fuhrman, M. Claire Horner-Devine, Susan M. Huse, David B. Mark Welch, Jennifer B. H. Martiny, Mitchell Sogin, Antje Boetius, and Alban Ramette. 2011. "Global Patterns of Bacterial Beta-Diversity in Seafloor and Seawater Ecosystems" edited by J. A. Gilbert. *PLoS ONE* 6(9):e24570.

Zinke, Laura A., Megan M. Mullis, Jordan T. Bird, Ian P. G. Marshall, Bo Barker Jørgensen, Karen G. Lloyd, Jan P. Amend, and Brandi Kiel Reese. 2017. "Thriving or Surviving? Evaluating Active Microbial Guilds in Baltic Sea Sediment." *Environmental Microbiology Reports* 9(5):528–36.